Title
Integration of signaling pathways during the unfolded protein response

Author
Bernales, Sebastian

Publication Date
2006

Peer reviewed|Thesis/dissertation

Integration of Signaling Pathways during the Unfolded Protein Response

by

Sebastián Bernales

DISSERTATION

Submitted in partial satisfaction of the requirements for the degree of

DOCTOR OF PHILOSOPHY

in

Cell Biology

in the

GRADUATE DIVISION

of the

UNIVERSITY OF CALIFORNIA, SAN FRANCISCO

I dedicate this dissertation to my wife, Paula,

my son, Lucas, and my daughter, Alicia,

and to my parents, Carmen and Sergio,

for making all of this possible, special, and worthy.

Acknowledgments

These years at UCSF have been extraordinary and I am very thankful for all the help and opportunities I have had here.

I am most grateful to Peter Walter, who taught me how to be a good scientist in the lab and a caring person in society. He was crucial in helping me mature and follow my dreams of contributing to science in Chile. Not only did he allow me to skip "a few" bench working days while I was organizing or participating in some extracurricular activities but he was also pivotal in the development and realization of most of the ideas.

I also wish to express my gratitude to the Walter lab family who unconditionally contributed to the discussion and growth of my research projects and to make the everyday work so enjoyable. In particular, I would like to thank the former members of the lab Gustavo Pesce for his friendship and for being my first scientific mentor at UCSF; Max Heiman for his critical thinking; Jason Brickner for all of the time he spent answering my questions; Jess Leber for giving me a place in his research; Chris Patil for his help with my research; Feroz Papa for interesting discussions; and Tobias Walther for showing me how to work as a team. I am also obliged to the current members of the lab including Pablo Aguilar, Tomas Aragon and Alex Engel for their exceptional comradeship both in and outside the lab; Shannon Behrman and Claudia Rubio for making the lab a happy place; Maria Paz Ramos for her courage and hard work; Niels Bradshaw for his considerate and thoughtful attitude; Marcy Diaz and Karen Moreira for their cheerfulness; Silke Nocke for being so caring and making the lab functional; Jonathan Lin for his translational insights on the UPR; Eelco van Anken, Saskia Neher, and Alexei Korennykh for their new friendship; Maria Victoria Dinglasan and Oya Unal

for maintaining our lab up and running; Sebastian Schuck for his new friendship and for continuing the project; Bob Farese for his time in the lab and his accurate diagnostic skills; Marc Shuman for his unconditional closeness, exceptional guidance, and extraordinary support; Patricia Caldera for her kindness and for encouragement to start a Chile-SEP; and Teresa Donovan for making all of the above possible. In addition, I would like to thank to all the excellent friends I made outside the lab at UCSF, especially to Greg Tully for an enduring and valuble friendship.

A crucial part of my graduate life at UCSF involved a close and fantastic relationship with Pablo Valenzuela and Bernardita Méndez at the Chilean Fundación Ciencia para la Vida. I am very thankful to them for all the time we spent together, for their valuable comments and advice, for their mentorship, and the many opportunities they gave me to co-organize scientific activities in Chile to establish and maintain a connection between UCSF and their non-profit organization. I am grateful to all of the people who were able to participate in our programs in Chile: Pablo Aguilar, Bruce Alberts, Raúl Andino, Patricia Caldera, Adam Carroll, Alejandro Colman-Lerner, Joe DeRisi, David Hung, Reg Kelly, Manuel Llinás, Marc Shuman, Peter Walter, Tobias Walther, David Wang, Keith Yamamoto, and the 44 UCSF graduate students.

I also would like to thank the Bay Area Chilean community for sharing their life and experiences and for helping me during many years. In particular, I am grateful to Pablo Garcia for his friendship and for being the one that introduced me to Peter; Angélica Medina and Mark Selby for a great relationship; Isabel Zaror, María Amelia Escobedo, and Jaime Escobedo for their closeness, Carlos George-Nascimento and Cecilia Collados for being an adoptive family.

I would also like to gratefully acknowledge my thesis committee members, Carol Gross and Hiten Madhani, for their great suggestions and assistance; and the terrific support given by Sue Adams and Danny Dam in the Tetrad Graduate Program.

ANNUAL REVIEWS
A NONPROFIT SCIENTIFIC PUBLISHER
www.annualreviews.org
4139 El Camino Way, P.O. Box 10139
Palo Alto, California 94303-0139
USA

Laura Folkner
Permissions Dept.
Lfolkner@annualreviews.org
650-843-6636
ARI Federal ID No. 94-1156476
ARI California Corp. No. 161041

November 29, 2006

To: Dr. Sebastian Bernales
Department of Biochemistry and Biophysics
University of San Francisco – MC 2200
600 16th Street, Genentech Hall N316
San Francisco, CA 94158-2517

From: Laura Folkner, Permissions Department

Thank you for your request for permission to reprint your article from the *Annual Review of Cell and Developmental Biology:*

"Intracellular Signaling by the Unfolded Protein Response"
***Annual Review of Cell and Developmental Biology*, Vol. 22: 487-508**

As author of the material which you wish to use, we are happy to grant you permission to use it in your thesis. Please use the following acknowledgment:

"Reprinted, with permission, from the *Annual Review of Cell and Developmental Biology*, Volume 22 ©2006 by Annual Reviews www.annualreviews.org"

Best wishes for continued success.

Integration of Signaling Pathways during the Unfolded Protein Response

by

Sebastián Bernales

Abstract

The unfolded protein response (UPR) is an intracellular signaling pathway that is activated by the accumulation of unfolded proteins in the endoplasmic reticulum (ER). UPR activation triggers an extensive transcriptional response, which adjusts the ER protein folding capacity according to need. As such, the UPR constitutes a paradigm of an intracellular control mechanism that adjusts organelle abundance in response to environmental or developmental clues. The pathway involves activation of ER unfolded protein sensors that operate in parallel circuitries to transmit information across the ER membrane, activating a set of downstream transcription factors by mechanisms that are unusual yet rudimentarily conserved in all eukaryotes.

Our research has identified a heretofore unrecognized pathway in yeast *Saccharomyces cerevisiae* that regulates the transcription of the gene that encodes the main UPR transcription factor, *HAC1*. The resulting increase in Hac1p production, combined with the production or activation of a putative UPR modulatory factor, is necessary to qualitatively modify the cellular response in order to survive the inducing conditions. This parallel ER–to–nucleus signaling pathway thereby serves to modify the UPR-driven transcriptional program. The results suggest a surprising conservation among all eukaryotes of the ways by which the elements of the UPR signaling circuit are connected. Our studies have shown that by adding an additional signaling element to the

basic UPR circuit, a simple switch is transformed into a complex response.

We also found that yeast cells expand their ER volume at least 5-fold under UPR-inducing conditions. Surprisingly, we discovered that ER proliferation is accompanied by the formation of autophagosome-like structures that are densely and selectively packed with membrane stacks derived from the UPR-expanded ER. This ER-specific autophagic described utilizes several autophagy genes that are induced by the UPR and are essential for the survival of cells subjected to severe ER stress. Intriguingly, cell survival does not require vacuolar proteases, indicating that ER sequestration into autophagosome-like structures, rather than their degradation, is the important step. Selective ER sequestration may help cells to maintain a new steady-state level of ER abundance even in the face of continuously accumulating unfolded proteins.

Peter Walter

Jan 2, 2004

Table of Contents

Chapter 1

Introduction: Intracellular Signaling by the Unfolded Protein Response.....1

Chapter 2

IRE1-independent Gain Control of the Unfolded Protein Response.....48

Chapter 3

Autophagy Counterbalances Endoplasmic Reticulum Expansion during the Unfolded Protein Response.....96

Appendix A

Transcriptional control of the *HAC1* mRNA during the S-UPR.....150

Appendix B

Viability during UPR-inducing conditions.....159

Appendix C

ATG8 transcriptional regulation.....163

Appendix D

Yeast Electron Microscopy.....168

List of Figures and Tables

Chapter 1

Figure 1-1: The three branches of the metazoan unfolded protein response.....40

Figure 1-2: Mechanism of Ire1-mediated mRNA splicing in yeast.....42

Figure 1-3: Evolutionary relationship of UPR components.....44

Figure 1-4: Structure of the Ire1 unfolded protein–sensing domain.....46

Chapter 2

Figure 2-1: ER-Distal Secretory Stress Boosts *HAC1* mRNA Abundance.....83

Figure 2-2: *HAC1* mRNA Induction Requires a Bipartite Signal and Is IRE1-Independent.....85

Figure 2-3: Activation of the *HAC1* Promoter Controls Increase in *HAC1* mRNA Abundance.....87

Figure 2-4: *HAC1* Promoter Regulation Is Required to Survive Stress.....89

Figure 2-5: Differential UPR Target Gene Induction by Elevated Hac1p Levels.....91

Figure 2-6: A Schematic of the Circuitry of the UPR.....94

Chapter 3

Figure 3-1: ER Proliferation under UPR-Inducing Conditions.....133

Figure 3-2: The ER Morphologically Changes during the UPR.....135

Figure 3-3: Characterization of ER-Containing Autophagosomes (ERAs) during the UPR.....137

Figure 3-4: Fluorescence Visualization of an ER Marker after UPR Induction.....139

Figure 3-5: Immunogold Labeling of ERAs with an Antibody Directed against an ER Membrane Marker.....141

Figure 3-6: UPR-Induction of the Autophagy Marker GFP-Atg8.....144

Figure 3-7: Localization of GFP-Atg8 during UPR Induction.....146

Figure 3-8: Atg8 and Other ATG Genes Are Necessary during UPR Induction.....148

Appendix A

Figure A-1: Analyses of the *HAC1* promoter.....155

Figure A-2: Motif I and II affect viability in S-UPR inducing plates.....157

Appendix B

Table B-1: Viability of yeast deletion strains during UPR-inducing conditions.....161

Appendix C

Figure C-1: FACS analyses of *ATG8*-inducing genes.....166

Appendix D

Figure D-1: Yeast electron micrographs.....170

Chapter 1

Introduction:

Intracellular Signaling by the Unfolded Protein Response

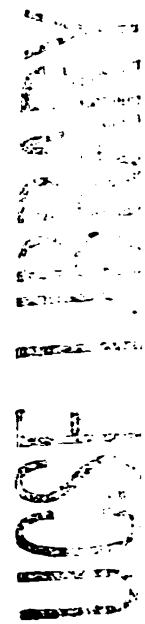

Intracellular Signaling by the Unfolded Protein Response

Sebastián Bernales[1], Feroz R. Papa[2], and Peter Walter[1]

[1]Howard Hughes Medical Institute, Departments of [1]Biochemistry and Biophysics and [2]Medicine, University of California, San Francisco, California 94143;

email: sebastian.bernales@ucsf.edu, frpapa@medicine.ucsf.edu, pwalter@biochem.ucsf.edu

INTRODUCTION AND OVERVIEW

All newly synthesized proteins need to fold properly and localize to their appropriate compartments within the cell. In eukaryotic cells, most secreted and plasma membrane proteins first enter the secretory pathway by translocation into the endoplasmic reticulum (ER). Proteins or membrane protein domains enter the ER through the translocon as unfolded polypeptide chains and fold within the lumen of this organelle (Wickner & Schekman 2005). Protein folding in the ER is facilitated by ER-resident chaperones, which prevent the nascent proteins from aggregating and instead steer them down productive folding pathways. Asparagine-linked carbohydrate moieties are added to many proteins entering the ER, and selective processing of the carbohydrate serves as a signal of the protein's folding state (Trombetta & Parodi 2003). Relative to the cytosol, the ER is an oxidizing environment, which facilitates formation of disulfide bonds in maturing proteins, further stabilizing the proteins' structure.

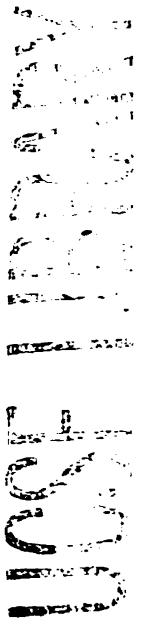

For secreted and membrane proteins to transit through the secretory pathway, they must first complete folding in the ER. The ER therefore constitutes a protein folding factory that imposes exquisite quality control on its products, ensuring that only properly assembled and functional proteins are delivered to their ultimate destinations (Ellgaard & Helenius 2003). Because many cell surface proteins relay important signals that ultimately determine cell fate—i.e., whether a cell is to differentiate, divide, migrate, or die—it is easy to appreciate why the fidelity of assembly of these components is vital for the health of an organism.

The load of proteins deposited into the ER varies between cell types and during the life of a cell. Developmental processes, cell cycle progression, and changes in the surrounding environment all can affect the amount and types of proteins that need to be folded in the ER. Thus, during their life, cells frequently encounter situations that cause the protein folding demand to overwhelm the ER's folding capacity, resulting in ER stress. ER stress can arise transiently as a cell's gene expression program is altered in response to changes in extracellular signals, or can be more permanent in cells bearing mutations that interfere with proper maturation of secretory or membrane proteins.

In some human genetic disorders, mutations in genes encoding important membrane and secretory proteins reduce the levels of these proteins because improper folding in the ER prevents their exit from this compartment. For example, the Z variant of α 1 antitrypsin is a folding mutant that is retained in the ER of the hepatocyte, reducing its levels in the lung, where it normally functions (Qu et al. 1996). ER stress can also be caused by environmental perturbations encountered commonly by cells. These include starvation for nutrients; anoxia and ischemia; infection by viruses; and heat, which denatures proteins (Ma & Hendershot 2004, Feldman et al. 2005, Wu & Kaufman 2006). In all these cases, the folding capacity of the organelle is perturbed, and the entire cell needs to adapt to the new condition.

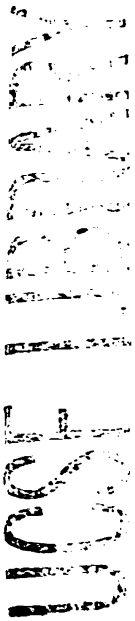

To cope with and adapt to ER stress, an intracellular ER-to-nucleus signal transduction pathway evolved to match dynamically the ER's protein folding capacity to need. This pathway, termed the unfolded protein response (UPR), increases the amount of ER membrane and its components, including chaperones and protein-modifying enzymes needed to fold proteins. The UPR also decreases translation and loading of

proteins into the ER and enhances the targeting of unfolded proteins in the ER for degradation. To this end, unsalvageable unfolded polypeptides are returned to the cytosol to be degraded by the proteasome via ER-associated degradation (ERAD) (Hiller et al. 1996, Wiertz et al. 1996, Meusser et al. 2005, Römisch 2005). If a homeostatic balance is not reestablished after inducing the UPR, i.e., if an acute UPR remains induced for a prolonged time, the cell commits apoptosis. Thus, cells at risk of displaying malfunctioning proteins on their surface are actively eliminated from an organism.

The signaling components that mediate the UPR were first discovered in the yeast Saccharomyces cerevisiae more than a decade ago. The two principal components of the pathway are an unfolded protein sensor in the ER membrane, the transmembrane signaling protein Ire1 (Cox et al. 1993, Mori et al. 1993), and a downstream effector, the transcription activator Hac1 (Cox & Walter 1996, Mori et al. 1996). The transcriptional targets of Hac1 ameliorate ER stress by expanding the ER (Sriburi et al. 2004) and with it the protein folding capacity of the cell. The initial understanding of the UPR was that of a simple feedback pathway: increased unfolded proteins activation of Ire1 production of Hac1 activation of UPR target genes decrease of unfolded proteins. Later, as the salient features of the yeast UPR were confirmed in metazoan cells, it became clear that the UPR in higher eukaryotes contains parallel and cross-wired circuitry, suggesting that the UPR is more accurately described as a signaling network that integrates information transmitted through multiple unfolded protein sensors and their downstream effectors. Recent studies in yeast indicate that the UPR in yeast also possesses the molecular roots for this complexity, upon which mammalian cells have built to adapt and enrich

processing of the information flow through the pathway according to their unique requirements (Leber et al. 2004, Patil et al. 2004).

In this review we examine the remarkably conserved ensemble of UPR effectors and their mechanistic interconnections, injecting an evolutionary perspective as we trace the course of the unfolded protein signal between the compartments of the cell. We begin by describing the general circuitry of the different branches of the UPR and the transcriptional programs that they execute. We then follow the signal backward through the cytosol to the ER and close with a description of recent advances in our understanding of how unfolded proteins are recognized in the ER lumen.

UPR SIGNALING NETWORK AND TRANSCRIPTIONAL CONTROL

The UPR operates as a homeostatic control circuit that regulates the protein folding and secretion capacity of the cell according to need. At its core, the circuitry features a collection of transcriptional programs, whose targets expand the size and capacity of the entire secretory apparatus of the cell. UPR transcriptional control is exerted by the combinatorial action of a set of transcription factors whose qualitative makeup and concentration regimes are finely controlled by the conditions within the ER.

To date, three primary branches of the UPR have been characterized; each contributes via unique transcription factors to the execution of the transcriptional response (Figure 1). Most centrally, the central logic of transcriptional control by the Ire1 branch is highly conserved. In yeast, the accumulation of unfolded proteins in the ER activates Ire1, which transmits the information across the ER membrane and excises an

intron from *HAC1* mRNA in the cytosol (Cox & Walter 1996, Shamu & Walter 1996, Welihinda & Kaufman 1996, Kawahara et al. 1997, Sidrauski & Walter 1997), which in yeast is Ire1's unique target RNA (Niwa et al. 2005). Fusion of the resulting exons by tRNA ligase (Sidrauski et al. 1996) leads to a spliced mRNA that is efficiently translated to produce the Hac1 transcription factor responsible for activating UPR target genes. Analogously, Ire1-dependent mRNA splicing in higher eukaryotes removes an intron from *XBP1* mRNA, encoding the metazoan Hac1 ortholog (Shen et al. 2001, Yoshida et al. 2001, Calfon et al. 2002). Thus, the key regulatory step in the Ire1-branch of UPR signaling is the nonconventional splicing of the mRNA encoding the transcription activator.

It is likely that the UPR controls a similar basic set of target genes in all eukaryotic cells. A comprehensive study defined the transcriptional scope of the Ire1/Hac1-mediated UPR in yeast to comprise some 400 genes (5% of the yeast genome), using stringent criteria based on bioinformatics and mutational analyses for inclusion of genes in the set (Travers et al. 2000). Thus, the extent of UPR transcriptional control mediated through the Ire1 branch alone is much larger than anticipated, including genes encoding proteins involved in ER protein folding and modification, phospholipid biosynthesis, ERAD, and vesicular transport in the secretory pathway downstream of the ER. Consequently, the UPR transcriptional program not only increases the capacity of the ER folding machinery but also promotes clearance of proteins from the ER. At present, the inventory of metozoan UPR target genes is still incomplete. Nonetheless, as in yeast, it has been shown that ER folding factors, lipid biosynthetic enzymes, and ERAD components are coregulated during the response (Harding et al. 2003, Lee et al. 2003,

Shaffer et al. 2004, Sriburi et al. 2004). Recent gene expression profiling in *Caenorhabditis elegans* classified some 500 UPR target genes according to the UPR branch that controls their activation and their developmental roles (X. Shen et al. 2005).

In yeast, the best-understood upstream activation sequence to which Hac1 binds, the unfolded protein response element 1 (UPRE-1), was identified in the promoter of the UPR target *KAR2* (Mori et al. 1992, Kohno et al. 1993). It came as a surprise that less than a fifth of the yeast UPR target genes contained this sequence element within their promoters. A bioinformatics approach revealed overrepresented motifs in promoters of other UPR target genes that define two additional UPREs (UPRE-2 and UPRE-3), which—although they share no recognizable sequence similarity—also bind Hac1 (Patil et al. 2004). This result suggests that Hac1 binds DNA differently depending on the UPREs present in a given promoter, possibly in combination with other transcription factors. Indeed, a genetic screen identified an additional activator, Gcn4, which, together with Hac1, binds to these two newly identified elements (Patil et al. 2004). Surprisingly, Gcn4 is also required to activate transcription of UPRE-1-driven promoters. Whether utilization of the three types of UPREs affords additional control of the UPR remains unknown. Moreover, the UPREs identified to date still explain the activation of only approximately half the UPR target genes, indicating that, even at the level of yeast target gene promoters, the full extent of regulatory complexity has not yet been revealed.

Gcn4 participates in several stress responses, including amino acid starvation, glucose limitation, and UV irradiation. Gcn4 is conditionally translated under such conditions (Yang et al. 2000, Natarajan et al. 2001, Stitzel et al. 2001). To work as Hac1's partner in activating transcription at the UPREs, however, Gcn4 does not require

induction of its translation as in the other responses. Rather, its basal expression level is necessary and sufficient. Intriguingly, ATF4, the metazoan ortholog of Gcn4, likewise is a transcription activator of the UPR (Harding et al. 2000, Novoa et al. 2003). By contrast to Gcn4, ATF4 translation is under control of the ER-proximal signal transducer PERK, which defines the second, but metazoan-specific, branch of the UPR (Figure 1).

During UPR induction conditions, the level of *HAC1* mRNA does not change. Synthesis of Hac1 is under tight translation control: Only spliced *HAC1* mRNA from which the intron has been removed is translated. When cells suffer from particularly harsh stress conditions, such as ER stress in combination with temperature increase, the transcription of *HAC1* mRNA is upregulated three- to fourfold (Leber et al. 2004). Increasing the cellular *HAC1* mRNA concentration alone has no effect on the production of Hac1 until induction of splicing removes the translational block, leading to higher levels of Hac1. During this enhanced response, termed super-UPR (S-UPR), the transcription of UPR target genes is modified by the higher Hac1 concentrations, eliciting a qualitatively different transcriptional response to adjust to the stress conditions. Under S-UPR conditions, *HAC1* mRNA transcription is upregulated independently of Ire1 and Hac1 activity. Thus, in yeast a second pathway must operate in parallel to the Ire1-dependent branch of the UPR, sensing the conditions inside the ER and affecting a transcriptional response. The molecular components that carry out ER-to-nucleus signaling under S-UPR conditions remain to be identified.

A third branch of the metazoan UPR is mediated by ATF6 (Figure 1). ATF6 is a bZIP transcription factor, but it is initially synthesized as an ER-resident transmembrane protein. Upon UPR induction, it migrates to the Golgi apparatus, where a cytosolic

fragment (ATF6f) bearing the transcription factor function is severed proteolytically from the membrane (Ye et al. 2000). ATF6f activates transcription from promoters containing ER stress response elements (ERSE-I and ERSE-II) (Yoshida et al. 1998, Li et al. 2000, Kokame et al. 2001, Okada et al. 2002). In mammals, a family of ATF6-like proteins includes at least four members, ATF6α, ATF6β, OASIS, and CREBH, that are regulated in a similar fashion during the UPR. Their expression varies among cell types—OASIS and CREBH, for example, have particularly important roles in astrocytes and liver cells, respectively (Omori et al. 2001, Kondo et al. 2005, Zhang et al. 2006). One of the transcriptional targets of ATF6 is *XBP1* mRNA (Yoshida et al. 2000). The concentration of XBP1 is therefore responsive to the conditions in the ER lumen, conceptually parallel to the control of Hac1 concentration afforded by the S-UPR in yeast.

In the yeast UPR signaling network, the Gcn4 and S-UPR branches modulate the basic Ire1/Hac1-dependent ON/OFF switch. The S-UPR acts as a gain control, setting the final Hac1 concentration, and both Gcn4 and the postulated S-UPR-mediating transcription factor combinatorially collaborate with Hac1. All UPR transcription factors identified to date are bZIP proteins, which in principle could form, through their leucine zipper domains, hetero- and/or homodimers, and in doing so they could modulate the response combinatorially. In yeast, for example, Hac1 and Gcn4 bind to the same UPREs, presumably as a heterodimer, to activate these genes (Patil et al. 2004). Thus, it is likely that the promoters of different target genes are tuned to respond to the combination of transcription factors in the cell and that the selective utilization of different UPREs contributes to control. One of the most challenging questions in the field

is how varying conditions in the ER are integrated with information about general cell physiology and lead to appropriate stress- and cell-type-specific transcriptional responses.

A still more complex type of transcriptional control is exhibited by a subset of UPR target genes, including the genes encoding phospholipid biosynthesis enzymes, such as *INO1*. These genes are controlled through an upstream activation sequence (UASino) element in their promoters (Greenberg et al. 1982, Cox et al. 1997) and in the off state are repressed by Opi1. Upon UPR induction, Hac1 relieves Opi1-mediated repression by an unknown mechanism. Intriguingly, the activation of *INO1* depends on the intranuclear localization of the *INO1* locus: The integral membrane protein Scs2 and recruitment of the *INO1* locus to the nuclear periphery are required for activation (Brickner & Walter 2004).

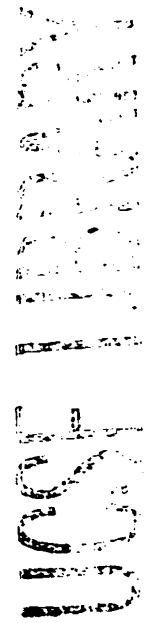

Depending on the particular state of the cell and what type of ER stress is encountered, these outputs of the UPR can dynamically proliferate the ER, degrade unfolded proteins, or initiate apoptotic programs. Through these outputs, cells increase ER folding capacity and expand the organelle. A remarkable demonstration of the role of the UPR in development is seen during terminal differentiation of B cells into plasma cells as they prepare to convert their secretory system into antibodies factories (Gass et al. 2002). This differentiation process is XBP1 dependent (Reimold et al. 2001, Iwakoshi et al. 2003). The ER proliferates many fold, and nearly all known ER-resident proteins increase accordingly, allowing plasma cells to produce and secrete huge concentrations of immunoglobulins.

If subjected to continuous ER stress such that homeostasis is not regained, cells commit to apoptosis. Apoptotic programs are activated by a combination of signals from

each of the three UPR branches as well as Ca2+ release from the ER (Scorrano et al. 2003, Zong et al. 2003). In particular, the PERK and ATF6 branches of the UPR both contribute to transcriptional upregulation of proapoptotic genes, such as *CHOP*, which is under transcriptional control by ATF4 (Harding et al. 2000) and ATF6f (Yoshida et al. 2000). CHOP downregulates the expression of Bcl-2 (McCullough et al. 2001, Ma et al. 2002), and hence one of its downstream effects is to promote mitochondrial cytochrome *c* release, apoptosome formation, and activation of caspases that lead to cell demise. In parallel, Ire1 activation and binding to TRAF2 are thought to turn on the JNK cascade (Urano et al. 2000) and contribute to proteolytic activation of caspases, including the ER-localized caspase-12 and caspase-4 (Nakagawa et al. 2000, Hitomi et al. 2004). One of the initial proteases believed to trigger the proteolytic cascade is calpain (Yoneda et al. 2001), which responds to Ca2+ release from the ER. It is unknown how unfolded protein accumulation leads to Ca2+ release, and the molecular details of how cells integrate the various proapoptotic signals to ultimately make a binary life/death decision are not yet understood. The choice to commit to cell death rather than display potentially malformed and improperly functioning protein receptors on the cell surface can be thought of as the ultimate solution to protect the organism from cells that may no longer respond properly to signals from their environment and hence may exhibit uncontrolled growth or differentiation. Thus, cytoprotective and cytotoxic pathways compete to determine whether the cell will survive ER stress.

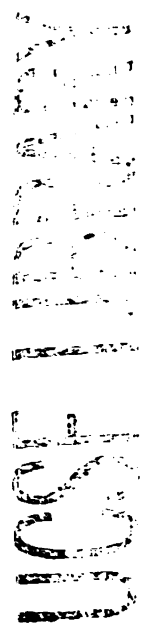

CONTROL OF SYNTHESIS OF THE UPR TRANSCRIPTION ACTIVATORS

As expected for homeostatic regulation, the initiation and shutoff of the UPR are tightly controlled, and UPR regulation is exerted at many steps of the pathway. The key regulatory step in the Ire1-dependent branch of the UPR is the removal of an intron from *HAC1* and *XBP1* mRNA in yeast and mammalian cells, respectively. Yeasts and metazoan cells appear to differ in the details of regulation afforded by this splicing event. In metazoan cells, the intron in *XBP1* mRNA is very short (23 or 26 nucleotides, depending on the species) and contained centrally in the open reading frame of the transcription factor. Its removal leads to a frame shift, resulting in production of a spliced mRNA that encodes a qualitatively different protein (the active transcription factor XBP1s) from that encoded on the unspliced mRNA (*XBP1u*). The role of XBP1u may be to downregulate XBP1s by binding and targeting it into a degradative pathway (Yoshida et al. 2006).

By contrast, the yeast intron in *HAC1* mRNA is 252 nucleotides long, and its presence controls the translation of *HAC1* mRNA (Figure 2). Unspliced *HAC1* mRNA is localized to the cytoplasm and engaged with functional polyribosomes, but the ribosomes are stalled on the mRNA owing to the presence of the intron, and no Hac1 is produced (Cox & Walter 1996, Chapman & Walter 1997). The translational attenuation afforded by the intron involves a direct, 16-nucleotide-long base-pairing interaction between the *HAC1* 5' untranslated region (UTR) and the intron (Ruegsegger et al. 2001). The mechanism by which the base-pairing interaction leads to stalling of the ribosomes is unknown, but it conceptually resembles translational control by microRNAs (miRNAs).

In *C. elegans*, for example, the small developmentally controlled miRNA lin-4 binds to *LIN-14* mRNA, inhibiting its translation on polyribosomes (Lee et al. 1993, Wightman et al. 1993, Bartel 2004). Thus, it is intriguing to speculate that the mechanism of translational control mediated by miRNAs in trans may be similar to that mediated by the *HAC1* intron in cis. By contrast, *XBP1* intron is too short and does not contain sequences that allow pairing to the 5' UTR. The details of the translational control described for *HAC1* mRNA are therefore yeast-specific. Still, the possibility of translational control of *XBP1* mRNA has been suggested (Calfon et al. 2002) and deserves further investigation.

A different type of translational control is mediated by the phosphorylation of the α subunit of translation initiation factor 2 (eIF2α) via the PERK branch of the mammalian UPR (Shi et al. 1998, Harding et al. 1999) and Gcn2 in yeast (Patil et al. 2004). Like Ire1, PERK is a single-pass ER transmembrane kinase. Upon activation by the accumulation of unfolded proteins in the ER lumen, it phosphorylates eIF2α, which blocks the formation of ribosomal preinitiation complexes and causes general translation attenuation, thereby decreasing the load of proteins translocated into the ER. A direct consequence of this reduction in translation is a rapid decrease in the concentration of cellular cyclin D1 and a concomitant G1 cell cycle arrest (Brewer et al. 1999, Brewer & Diehl 2000, Niwa & Walter 2000). Although translation of most mRNA is attenuated under conditions of limiting eIF2α, a subset of mRNAs that contain small upstream open reading frames (Miller & Hinnebusch 1990, Harding et al. 2000) or internal ribosome entry sites (Fernandez et al. 2002) is preferentially translated under these conditions (Lu et al. 2004). In this way, PERK activation leads to the production of the

UPR transcription factor ATF4 (Harding et al. 2000, Scheuner et al. 2001). *XBP1* mRNA as well as some other mRNAs are enriched on the ER surface, where they may be preferentially translated when eIF2 α is limiting (Stephens et al. 2005).

ER STRESS SENSORS: TRANSDUCTION OF THE UNFOLDED PROTEIN SIGNAL ACROSS THE MEMBRANE

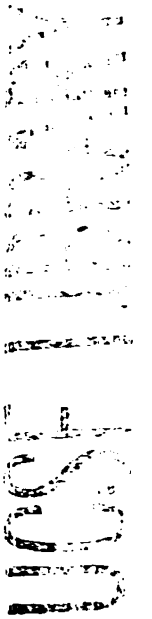

Each of the three classes of ER stress sensors—Ire1, PERK, and ATF6—independently transduces the unfolded protein signal across the ER membrane. The Ire1-dependent UPR branch is evolutionarily conserved in all eukaryotic cells and is the most ancient, whereas PERK and ATF6 first evolved in metazoans (Figure 3). In mammals, the IRE1 gene became duplicated, giving rise to Ire1 α and Ire β. Whereas Ire1 α is expressed in all mammalian cells, Ire β is expressed primarily in intestinal epithelial cells (Tirasophon et al. 1998, Wang et al. 1998, Bertolotti et al. 2001). It is not known whether Ire α and Ire β have different activities; the two isoforms appear to have the same in vitro activities, subcellular localizations, and downstream target (*XBP1* mRNA). However, whereas IRE1 α is essential for mammalian development (Zhang et al. 2005), IRE1 β deletion does not lead to significant developmental defects (Bertolotti et al. 2001).

PERK evolved from Ire1 by grafting its ER-lumenal unfolded protein–sensing domain and transmembrane region onto an eIF2 α kinase domain. This evolutionarily chimeric protein introduces a new function in metazoans: attenuation of translation under

ER stress. In mammals this function becomes pivotal, especially for professional secretory cells, as demonstrated by its absence in PERK-deficient homozygous patients with Wolcott-Rallison syndrome (Zhang et al. 2002). Affected individuals have vastly shortened lifespans of their endocrine and exocrine pancreatic cells as well as osteoblasts, all cell types specialized to secrete proteins.

Studies in yeast have shown that the yeast ER-lumenal domain (LD) of Ire1 is functionally interchangeable with the LD of PERK from *C. elegans* (Liu et al. 2000), underscoring their common evolutionary origin and suggesting a similar mode of unfolded protein recognition. In both proteins, oligomerization of the LDs is thought to lead to clustering of the cytosolic kinase domains, which then become activated by transautophosphorylation. In this sense, Ire1 and PERK resemble a plethora of membrane receptor kinases that dimerize/oligomerize in the plasma membrane upon binding of cognate ligands, facilitating their activation.

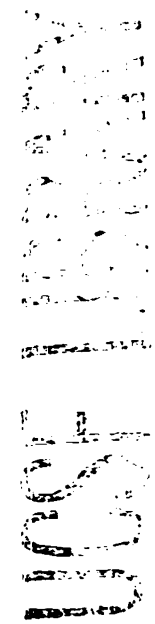

By contrast, no sequence similarity is apparent between the LDs of Ire1 and PERK and the LD of ATF6, which is activated through an entirely different process: It is cleaved through regulated intramembrane proteolysis by Site 1 and Site 2 Proteases under conditions of unfolded protein accumulation, resulting in liberation of soluble ATF6f (Ye et al. 2000). Activation of ATF6 resembles activation of SREBP (Sterol Regulatory Element–Binding Protein), a transcription factor involved in cholesterol sensing and biosynthesis. In the presence of sufficient cholesterol, SREBP is retained in the ER by association with an anchor protein (Insig-1) together with its cholesterol-sensing partner protein Scap. When cholesterol levels become limiting, SREBP is released from the anchor and travels to the Golgi apparatus, where it is proteolyzed to release a functional

transcription factor (Gong et al. 2006). By contrast to this well-established paradigm, it is not known how the intracellular localization of ATF6 is modulated in response to unfolded protein accumulation. BiP binding may retain ATF6 in the ER (Shen et al. 2002, J. Shen et al. 2005)

Evolution has spawned another Ire1 descendant, RNaseL, which is a component in the innate immune response (Zhou et al. 1993). RNaseL resembles Ire1 in its gross architecture (Figure 3) yet yields a radically different function. It is a soluble, cytosolic protein, with a kinase-like domain and an RNase related to Ire1. Like Ire1, RNaseL contains an N-terminal activation domain (in this case comprised of a series of ankyrin repeats) that drives dimerization upon ligand binding (Dong & Silverman 1995, Cole et al. 1996, Nakanishi et al. 2005). The ligands are 2'-5' oligoadenylates that are produced in response to interferon signaling when viruses infect mammalian cells (Player & Torrence 1998). Dimerization activates the C-terminal RNase domain, which, in contrast to Ire1's site-specific RNase activity, nonspecifically degrades bulk ribosomal and other RNAs, thereby containing viral infection. It is unknown how the respective RNases of Ire1 and RNaseL discriminate their corresponding substrates.

For Ire1, the kinase is a necessary component of the circuitry that allows transfer of an unfolded protein signal by this sensor. Mutations of catalytically essential kinase active site residues—or residues known to become phosphorylated—demonstrate that Ire1's kinase phosphotransfer function is essential for RNase activation (Shamu & Walter 1996). By contrast, RNaseL has lost phosphotransfer function during the course of evolution, yet its (pseudo)kinase domain is still necessary for activation of its RNase. It is

thought that the kinases of Ire1 and RNaseL are dimerization modules and conformational switches that position the attached RNases to control their activation.

Adenosine nucleotide binding to the active kinase of Ire1 and to the pseudokinase of RNaseL stimulates the attached RNase activities. Interestingly, the requirement for both the kinase activity and phosphorylation of Ire1 is alleviated if a small ATP mimic, 1NM-PP1, is provided to a mutant Ire1 enzyme that has an expanded active site designed to accommodate 1NM-PP1. Thus, mere binding of a ligand in the active site of Ire1 is sufficient to propagate the unfolded protein signal through the kinase domain, and phosphotransfer can be bypassed (Papa et al. 2003). In response to adenosine nucleotide binding, the kinase domain may switch conformation and/or change its oligomeric state such that the RNase now becomes active. By analogy, the adenosine nucleotide ligand-occupied kinase domain of RNaseL may serve as a module that participates in activation and regulation of the RNase function. The elucidation of the roles of the kinase domains of Ire1 and RNaseL as conformational switches may shed light on the functions of other multidomain proteins containing kinase or enzymatically inactive pseudokinase domains.

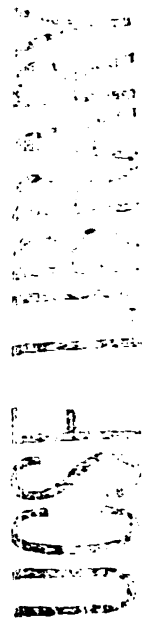

The biological role of ligand occupancy is unknown. For Ire1, the in vitro adenosine nucleotide stimulatory effect is most pronounced when ADP is used. If ADP is the natural stimulatory ligand of Ire1's kinase domain in vivo, it may be providing some information about the cell's nutritional state. For instance, ADP levels rise temporarily in proportion to nutritional stress in many professional secretory cells, such as the β-cells of the endocrine pancreas. ATP levels also fluctuate but not as much as ADP levels (because ADP is normally maintained at low concentrations). Thus, ADP is poised to serve as a cofactor—or second messenger—that could signal a starvation state. ADP-

mediated conformational changes may increase the dwell time of activated Ire1, serving as complementary input for activation of Ire1 (the other input is unfolded proteins). Protein folding becomes inefficient as the nutritional status of cells declines, triggering the UPR. Through this mechanism, information about nutritional stress may be relayed to the UPR in the face of energy depletion. As such, Ire1 may have evolved this regulatory mechanism to monitor the energy balance of the cell and to couple this information to activation of the UPR. Indeed, one proposed role of the UPR is that of a nutrition-sensing device, matching protein synthetic activity to energy supply (Kaufman et al. 2002).

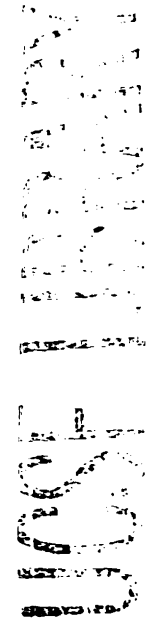

THE MECHANISM OF SENSING UNFOLDED PROTEINS IN THE ER

The recent crystal structure of yeast Ire1 LD and structure-guided functional analyses of this domain provide a first glimpse at the mechanism by which unfolded proteins may be recognized in the ER lumen (Credle et al. 2005) (Figure 4). The structure revealed an ordered conserved core region (cLD), flanked on either side by disordered and functionally dispensable sequences. Whereas the cLD is a monomer in solution, two cLD monomers associate in an almost perfectly twofold symmetric head-to-head arrangement in the crystal lattice, burying a large interface. The most remarkable feature of the cLD dimer is a deep central groove formed by a β-sheet floor and walls composed of α-helices. In its architecture and dimensions, the groove resembles that of the peptide-binding pocket of major histocompatibility complexes (MHCs) (Bjorkman et al. 1987), suggesting that unfolded polypeptide chains bind there directly.

Mutational analyses suggest that cLD dimers form higher-order oligomers necessary for UPR activation across both head-to-head and tail-to-tail interfaces seen in the crystal lattice (Credle et al. 2005). Experimental dimerization of Ire1 mutants with engineered leucine zippers yielded partial activation of the RNase (Liu et al. 2000), perhaps indicating that the activation state of Ire1 is regulated in a continuum depending on the extent of oligomerization. According to this notion, unfolded proteins may tether cLD dimers into higher-order oligomers. In turn, such an event may change the quaternary association of Ire1 in the plane of the ER membrane to position the kinase domains in the cytoplasm optimally for autophosphorylation and RNase activation. Indeed, Ire1 aggregates into higher-order structures (with a stoichiometry greater than dimeric) upon UPR activation (Shamu & Walter 1996), resembling the activation mechanism of other membrane-localized sensing proteins (e.g., aspartate chemoreceptors of eubacteria).

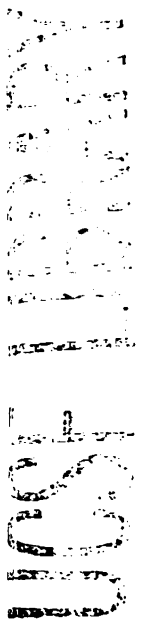

The topic of the mechanism by which unfolded proteins are recognized in the ER lumen has generated lively debate. Previous models ascribed a negative regulatory role to the ER chaperone BiP (Bertolotti et al. 2000, Okamura et al. 2000). It was proposed that, as BiP binds to the LD of Ire1, it acts as a negative regulator, thus preventing Ire1 activation. This notion derives from the observation that Ire1 activation is temporally linked to reversible dissociation from BiP. In this view, free BiP levels fall as BiP engages unfolded proteins, and Ire1 becomes free to self-associate and activate. However, genetic and structural evidence supporting the idea that BiP dissociation causes, rather than simply being correlated with, Ire1 activation has not been readily forthcoming. Furthermore, this previous model was fraught with inconsistencies. First, BiP is present

in the ER lumen at very high concentrations (in the millimolar range). Therefore, the UPR would not become activated unless and until large concentrations of unfolded proteins accumulated to provide a sufficiently large sink for free BiP. However, the UPR seems to respond to small fluctuations in the ER protein folding state, as would seem appropriate for a sensor that adjusts the ER protein folding capacity homeostatically. Second, recent studies identified the BiP-binding site in Ire1 to lie outside the cLD and showed that deletion of this region did not impair Ire1 regulation by the presence or absence of unfolded protein (Kimata et al. 2004, Oikawa et al. 2005).

Structure-guided analyses of LD provoke a new model wherein BiP binding and release in Ire1 activation are irrelevant or possibly only important under extreme activation conditions when the pool of free BiP becomes severely depleted. Such situations may arise under nonphysiological experimental conditions or upon prolonged UPR induction. BiP release under such conditions may serve to enter a different activation state, perhaps signaling that the UPR is not able to reestablish homeostasis in the ER and leading the cell down an apoptotic pathway. Conversely, BiP binding may dampen activation of Ire1 under conditions of mild unfolded protein accumulation (i.e., during conditions that may be dealt with through existing concentrations of ER chaperones). In this view, BiP binding would buffer Ire1 against normal fluctuations of ER unfolded proteins, thereby reducing "noise" in UPR signaling.

The gross resemblance of Ire1 cLD to the peptide binding domain of MHC-I suggests that unfolded proteins bind in the groove (Figure 4). Indeed, the groove is lined with a phylogenetically conserved patchwork of hydrophobic and polar amino acid side chains. Their substitution to alanine reduces UPR signaling (Credle et al. 2005). Thus,

unfolded polypeptide chains and/or possibly partially folded proteins with exposed loops on their surface may bind to Ire1 directly in this groove, providing the primary signal mediating its activation.

If the groove in cLD indeed serves to bind portions of unfolded polypeptides, a variety of different—yet not mutually exclusive—mechanisms may provide the means for recognition. Hsp70-type chaperones such as BiP recognize a signature motif on unfolded proteins, which consists of hydrophobic amino acids in every other position (Flynn et al. 1991, Blond-Elguindi et al. 1993). Such a sequence resembles a β-strand, one side of which is destined to pack onto the hydrophobic core of a folded protein but has not yet been properly accommodated in the protein fold. Indeed, the groove in cLD contains a patchwork of conserved hydrophobic and hydrophilic residues. Thus, recognition of specific side chains or classes of side chains in preferred positions may play an important part in unfolded protein recognition by cLD.

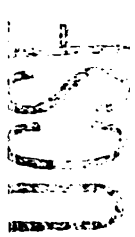

Although sequence specificity may influence binding of particular polypeptides to cLD, the simple property of accessibility by itself may allow discrimination between the folded and unfolded states. By analogy, unfolding of ER proteins exposes interior regions to UDP-Glc glycoprotein glucosyltransferase, a quality-control activity of the ER. The enzyme recognizes innermost sugars in the oligosaccharide moiety and hydrophobic polypeptide cores that become accessible only in misfolded glycoproteins (Trombetta & Parodi 2005). Given the depth of the cLD groove, it is inaccessible to surface residues on compactly folded proteins. In the extreme, interactions in the groove may be limited to backbone contacts only, paying little or no attention to the amino acid sequence of the polypeptide. On the other hand, these mechanisms need not be mutually exclusive, and

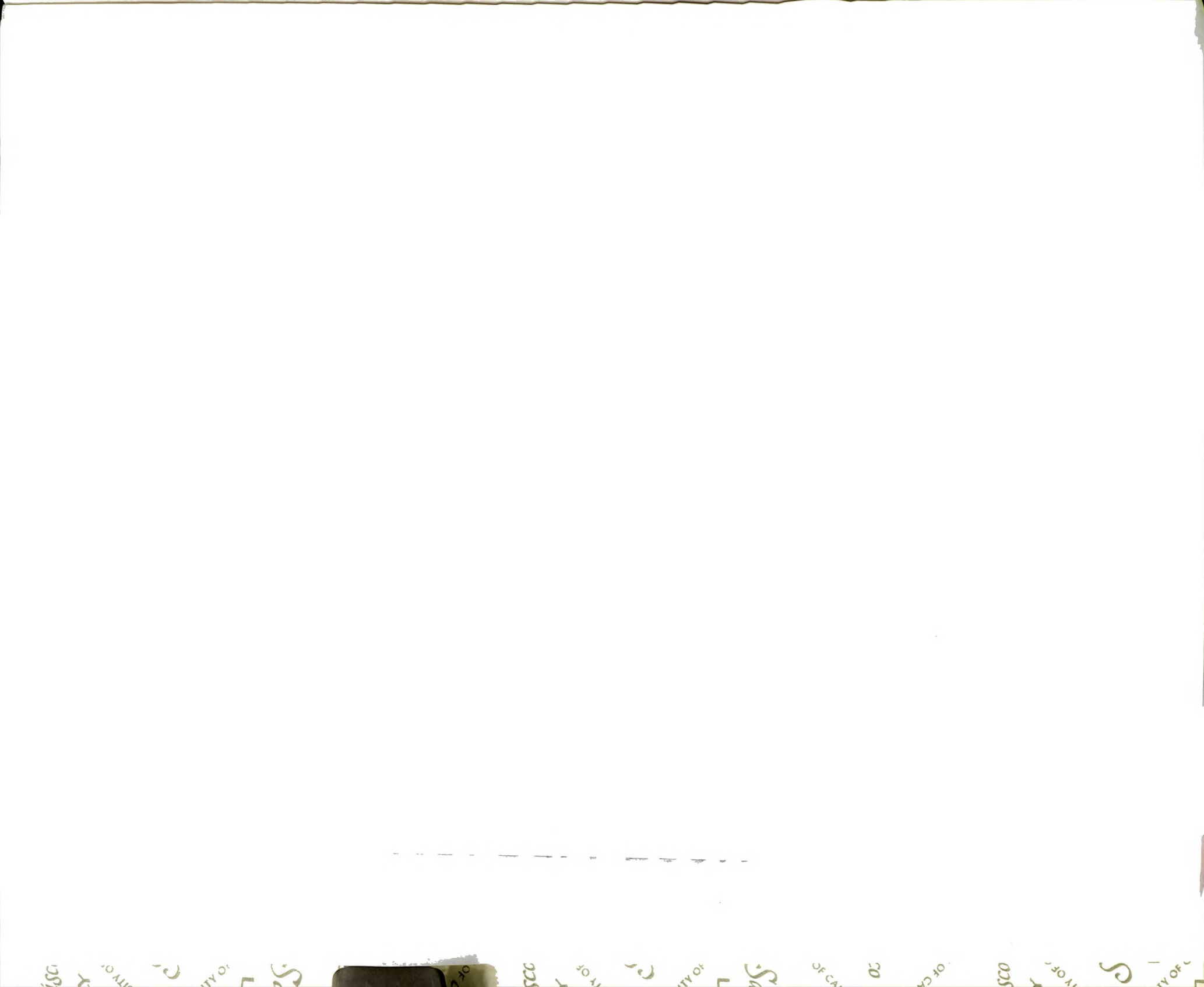

both accessibility and sequence specificity may be important parameters in recognition of the unfolded protein by cLD. The next challenge in the field is to ascertain whether cLD binds unfolded proteins through these or yet other means.

Ultimately, it will be important to compare and contrast the mechanistic details of unfolded protein recognition by each of the different sensor proteins in the ER. PERK and Ire share a basic molecular architecture of the cLD but may differ in unfolded protein binding strength or kinetics. Similarly, the ATF6-like sensors may recognize unfolded proteins with distinct binding characteristics. Thus, the individual branches of the UPR may be activated differentially (Yoshida et al. 2003), perhaps by fine-tuning the response to a particular signature of the inducing signal or causing a particular temporal sequence to engage the UPR transcriptional effectors. Without question, much of the physiological importance of the UPR circuitry remains to be discovered.

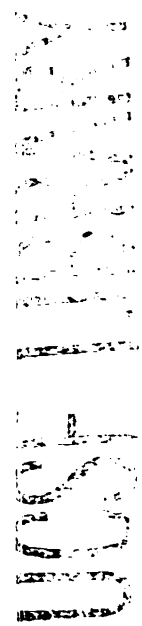

SUMMARY POINTS

1. The unfolded protein response (UPR) is a homeostatic signaling pathway that adjusts ER protein folding capacity according to need.
2. The UPR employs three types of sensors that recognize unfolded proteins in the ER lumen and activate separate branches of the signaling network. Structural modules and mechanistic concepts are phylogenetically conserved; some have been duplicated and rearranged in evolution to generate higher complexity.

3. The UPR employs a variety of mechanisms in signal transduction, including regulated splicing, translational control, and regulated proteolysis.

4. The transcriptional output of the UPR is determined by the combinatorial action of the transcription factors activated through its signaling branches.

5. Structural and mutational analyses of the Ire1 unfolded protein-sensing domain suggest that unfolded proteins are recognized in the ER lumen by binding to Ire1 directly.

FUTURE ISSUES

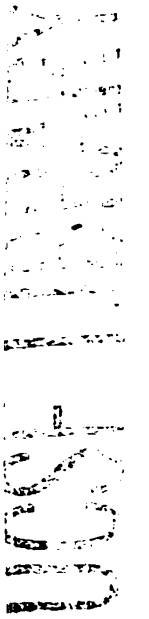

1. If the UPR cannot reestablish ER homeostasis, cells commit to apoptosis. It is unknown how, mechanistically, this important binary life/death decision is made.

2. The three branches of the UPR use different unfolded protein sensors. It is unknown whether they recognize unfolded proteins differently and thus allow for differentiated responses that are tailored to specific needs. We have only incomplete information regarding the scope of the UPR transcriptional programs and how they relate to cell type or ER-stress-specific needs.

3. Many exciting mechanistic details of the signal transduction devices in the UPR remain to be explored. How are unfolded proteins recognized? How does the Ire1 kinase domain activate the RNase function? How is the ER Golgi movement of ATF6 regulated? How is translation regulated by the *HAC1* mRNA intron? How does Ire1 recognize the splice site with such high specificity?

ACKNOWLEDGMENTS

The authors wish to thank Tomás Aragón, Jason Brickner, Alex Engel, Scott Oakes, and Tobias Walther for their valuable comments on the manuscript. This work was supported by an American Heart Predoctoral Fellowship for S.B. and by grants from the National Institutes of Health to F.R.P. and P.W. P.W. is an Investigator of the Howard Hughes Medical Institute.

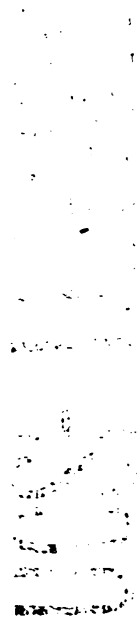

LITERATURE CITED

Bartel DP. 2004. MicroRNAs: genomics, biogenesis, mechanism, and function. Cell 116(2):281–97

Bertolotti A, Wang X, Novoa I, Jungreis R, Schlessinger K, et al. 2001. Increased sensitivity to dextran sodium sulfate colitis in IRE1 β-deficient mice. J. Clin. Invest. 107(5):585–93

Bertolotti A, Zhang Y, Hendershot LM, Harding HP, Ron D. 2000. Dynamic interaction of BiP and ER stress transducers in the unfolded-protein response. Nat. Cell Biol. 2(6):326–32

Bjorkman PJ, Saper MA, Samraoui B, Bennett WS, Strominger JL, Wiley DC. 1987. Structure of the human class I histocompatibility antigen, HLA-A2. Nature 329(6139):506–12

Brewer JW, Diehl JA. 2000. PERK mediates cell-cycle exit during the mammalian unfolded protein response. Proc. Natl. Acad. Sci. USA 97(23):12625–30

Brewer JW, Hendershot LM, Sherr CJ, Diehl JA. 1999. Mammalian unfolded protein response inhibits cyclin D1 translation and cell-cycle progression. Proc. Natl. Acad. Sci. USA 96(15):8505–10

Blond-Elguindi S, Cwirla SE, Dower WJ, Lipshutz RJ, Sprang SR, et al. 1993. Affinity panning of a library of peptides displayed on bacteriophages reveals the binding specificity of BiP. Cell 75(4):717–28

Brickner JH, Walter P. 2004. Gene recruitment of the activated INO1 locus to the nuclear membrane. PLoS Biol. 2(11):e342

Calfon M, Zeng H, Urano F, Till JH, Hubbard SR, et al. 2002. IRE1 couples endoplasmic reticulum load to secretory capacity by processing the XBP-1 mRNA. Nature 415(6867):92–96

Chapman RE, Walter P. 1997. Translational attenuation mediated by an mRNA intron. Curr. Biol. 7(11):850–59

Cole JL, Carroll SS, Kuo LC. 1996. Stoichiometry of 2',5'-oligoadenylate-induced dimerization of ribonuclease L. A sedimentation equilibrium study. J. Biol. Chem. 271(8):3979–81

Cox JS, Chapman RE, Walter P. 1997. The unfolded protein response coordinates the production of endoplasmic reticulum protein and endoplasmic reticulum membrane. Mol. Biol. Cell 8(9):1805–14

Cox JS, Shamu CE, Walter P. 1993. Transcriptional induction of genes encoding endoplasmic reticulum resident proteins requires a transmembrane protein kinase. Cell 73(6):1197–206

Cox JS, Walter P. 1996. A novel mechanism for regulating activity of a transcription factor that controls the unfolded protein response. Cell 87(3):391–404

Credle JJ, Finer-Moore JS, Papa FR, Stroud RM, Walter P. 2005. On the mechanism of sensing unfolded protein in the endoplasmic reticulum. Proc. Natl. Acad. Sci. USA 102(52):18773–84

DenBoer LM, Hardy-Smith PW, Hogan MR, Cockram GP, Audas TE, Lu R. 2005. Luman is capable of binding and activating transcription from the unfolded protein response element. Biochem. Biophys. Res. Commun. 331(1):113–19

Dong B, Silverman RH. 1995. 2-5A-dependent RNase molecules dimerize during activation by 2-5A. J. Biol. Chem. 270(8):4133–37

Ellgaard L, Helenius A. 2003. Quality control in the endoplasmic reticulum. Nat. Rev. Mol. Cell. Biol. 4(3):181–91

Feldman DE, Chauhan V, Koong AC. 2005. The unfolded protein response: a novel component of the hypoxic stress response in tumors. Mol. Cancer Res. 3(11):597–605

Fernandez J, Bode B, Koromilas A, Diehl JA, Krukovets I, et al. 2002. Translation mediated by the internal ribosome entry site of the cat-1 mRNA is regulated by glucose availability in a PERK kinase-dependent manner. J. Biol. Chem. 277(14):11780–87

Flynn GC, Pohl J, Flocco MT, Rothman JE. 1991. Peptide-binding specificity of the molecular chaperone BiP. Nature 353(6346):726–30

Gass JN, Gifford NM, Brewer JW. 2002. Activation of an unfolded protein response during differentiation of antibody-secreting B cells. J. Biol. Chem. 277(50):49047–54

Gong Y, Lee JN, Lee PC, Goldstein JL, Brown MS, Ye J. 2006. Sterol-regulated ubiquitination and degradation of Insig-1 creates a convergent mechanism for feedback control of cholesterol synthesis and uptake. Cell Metab. 3(1):15–24

Greenberg ML, Goldwasser P, Henry SA. 1982. Characterization of a yeast regulatory mutant constitutive for synthesis of inositol-1-phosphate synthase. Mol. Gen. Genet. 186(2):157–63

Harding HP, Novoa I, Zhang Y, Zeng H, Wek R, et al. 2000. Regulated translation initiation controls stress-induced gene expression in mammalian cells. Mol. Cell 6(5):1099–108

Harding HP, Zhang Y, Ron D. 1999. Protein translation and folding are coupled by an endoplasmic-reticulum-resident kinase. Nature 397(6716):271–74

Harding HP, Zhang Y, Zeng H, Novoa I, Lu PD, et al. 2003. An integrated stress response regulates amino acid metabolism and resistance to oxidative stress. Mol. Cell 11(3):619–33

Hiller MM, Finger A, Schweiger M, Wolf DH. 1996. ER degradation of a misfolded luminal protein by the cytosolic ubiquitin-proteasome pathway. Science 273(5282):1725–28

Hitomi J, Katayama T, Eguchi Y, Kudo T, Taniguchi M, et al. 2004. Involvement of caspase-4 in endoplasmic reticulum stress-induced apoptosis and Aβ-induced cell death. J. Cell Biol. 165(3):347–56

Iwakoshi NN, Lee AH, Vallabhajosyula P, Otipoby KL, Rajewsky K, Glimcher LH. 2003. Plasma cell differentiation and the unfolded protein response intersect at the transcription factor XBP-1. Nat. Immunol. 4(4):321–29

Kaufman RJ, Scheuner D, Schroder M, Shen X, Lee K, et al. 2002. The unfolded protein response in nutrient sensing and differentiation. Nat. Rev. Mol. Cell Biol. 3(6):411–21

Kawahara T, Yanagi H, Yura T, Mori K. 1997. Endoplasmic reticulum stress-induced mRNA splicing permits synthesis of transcription factor Hac1p/Ern4p that activates the unfolded protein response. Mol. Biol. Cell 8(10):1845–62

Kimata Y, Oikawa D, Shimizu Y, Ishiwata-Kimata Y, Kohno K. 2004. A role for BiP as an adjustor for the endoplasmic reticulum stress-sensing protein Ire1. J. Cell Biol. 167(3):445–56

Kohno K, Normington K, Sambrook J, Gething MJ, Mori K. 1993. The promoter region of the yeast KAR2 (BiP) gene contains a regulatory domain that responds to the presence of unfolded proteins in the endoplasmic reticulum. Mol. Cell Biol. 13(2):877–90

Kokame K, Kato H, Miyata T. 2001. Identification of ERSE-II, a new cis-acting element responsible for the ATF6-dependent mammalian unfolded protein response. J. Biol. Chem. 276(12):9199–205

Kondo S, Murakami T, Tatsumi K, Ogata M, Kanemoto S, et al. 2005. OASIS, a CREB/ATF-family member, modulates UPR signaling in astrocytes. Nat. Cell. Biol. 7(2):186–94

Leber JH, Bernales S, Walter P. 2004. IRE1-independent gain control of the unfolded protein response. PLoS Biol. 2(8):E235

Lee AH, Iwakoshi NN, Glimcher LH. 2003. XBP-1 regulates a subset of endoplasmic reticulum resident chaperone genes in the unfolded protein response. Mol. Cell Biol. 23(21):7448–59

Lee RC, Feinbaum RL, Ambros V. 1993. The *C. elegans* heterochronic gene lin-4 encodes small RNAs with antisense complementarity to lin-14. Cell 75(5):843–54

Li M, Baumeister P, Roy B, Phan T, Foti D, et al. 2000. ATF6 as a transcription activator of the endoplasmic reticulum stress element: thapsigargin stress-induced changes and synergistic interactions with NF-Y and YY1. Mol. Cell Biol. 20(14):5096–106

Liu CY, Schroder M, Kaufman RJ. 2000. Ligand-independent dimerization activates the stress response kinases IRE1 and PERK in the lumen of the endoplasmic reticulum. J. Biol. Chem. 275(32):24881–85

Lu PD, Harding HP, Ron D. 2004. Translation reinitiation at alternative open reading frames regulates gene expression in an integrated stress response. J. Cell Biol. 167(1):27–33

Ma Y, Brewer JW, Diehl JA, Hendershot LM. 2002. Two distinct stress signaling pathways converge upon the CHOP promoter during the mammalian unfolded protein response. J. Mol. Biol. 318(5):1351–65

Ma Y, Hendershot LM. 2004. The role of the unfolded protein response in tumor development: friend or foe? Nat. Rev. Cancer 4(12):966–77

McCullough KD, Martindale JL, Klotz LO, Aw TY, Holbrook NJ. 2001. Gadd153 sensitizes cells to endoplasmic reticulum stress by down-regulating Bcl2 and perturbing the cellular redox state. Mol. Cell Biol. 21(4):1249–59

Meusser B, Hirsch C, Jarosch E, Sommer T. 2005. ERAD: the long road to destruction. Nat. Cell. Biol. 7(8):766–72

Miller PF, Hinnebusch AG. 1990. cis-acting sequences involved in the translational control of GCN4 expression. Biochim. Biophys. Acta 1050(1–3):151–54

Mori K, Kawahara T, Yoshida H, Yanagi H, Yura T. 1996. Signalling from endoplasmic reticulum to nucleus: transcription factor with a basic-leucine zipper motif is required for the unfolded protein-response pathway. Genes Cells 1(9):803–17

Mori K, Ma W, Gething MJ, Sambrook J. 1993. A transmembrane protein with a cdc2+/CDC28-related kinase activity is required for signaling from the ER to the nucleus. Cell 74(4):743–56

Mori K, Sant A, Kohno K, Normington K, Gething MJ, Sambrook JF. 1992. A 22 bp cis-acting element is necessary and sufficient for the induction of the yeast KAR2 (BiP) gene by unfolded proteins. EMBO J. 11(7):2583–93

Nakagawa T, Zhu H, Morishima N, Li E, Xu J, et al. 2000. Caspase-12 mediates endoplasmic-reticulum-specific apoptosis and cytotoxicity by amyloid-β. Nature 403(6765):98–103

Nakanishi M, Tanaka N, Mizutani Y, Mochizuki M, Ueno Y, et al. 2005. Functional characterization of 2',5'-linked oligoadenylate binding determinant of human RNase L. J. Biol. Chem. 280(50):41694–99

Natarajan K, Meyer MR, Jackson BM, Slade D, Roberts C, et al. 2001. Transcriptional profiling shows that Gcn4p is a master regulator of gene expression during amino acid starvation in yeast. Mol. Cell Biol. 21(13):4347–68

Niwa M, Patil CK, DeRisi J, Walter P. 2005. Genome-scale approaches for discovering novel nonconventional splicing substrates of the Ire1 nuclease. Genome Biol. 6(1):R3

Niwa M, Walter P. 2000. Pausing to decide. Proc. Natl. Acad. Sci. USA 97(23):12396–97

Novoa I, Zhang Y, Zeng H, Jungreis R, Harding HP, Ron D. 2003. Stress-induced gene expression requires programmed recovery from translational repression. EMBO J. 22(5):1180–87

Oikawa D, Kimata Y, Takeuchi M, Kohno K. 2005. An essential dimer-forming subregion of the endoplasmic reticulum stress sensor Ire1. Biochem. J. 391(Pt. 1):135–42

Okada T, Yoshida H, Akazawa R, Negishi M, Mori K. 2002. Distinct roles of activating transcription factor 6 (ATF6) and double-stranded RNA-activated protein kinase-like endoplasmic reticulum kinase (PERK) in transcription during the mammalian unfolded protein response. Biochem. J. 366(Pt. 2):585–94

Okamura K, Kimata Y, Higashio H, Tsuru A, Kohno K. 2000. Dissociation of Kar2p/BiP from an ER sensory molecule, Ire1p, triggers the unfolded protein response in yeast. Biochem. Biophys. Res. Commun. 279(2):445–50

Omori Y, Imai J, Watanabe M, Komatsu T, Suzuki Y, et al. 2001. CREB-H: a novel mammalian transcription factor belonging to the CREB/ATF family and functioning via the box-B element with a liver-specific expression. Nucleic Acids Res. 29(10):2154–62

Papa FR, Zhang C, Shokat K, Walter P. 2003. Bypassing a kinase activity with an ATP-competitive drug. Science 302(5650):1533–37

Patil CK, Li H, Walter P. 2004. Gcn4p and novel upstream activating sequences regulate targets of the unfolded protein response. PLoS Biol. 2(8):E246

Player MR, Torrence PF. 1998. The 2-5A system: modulation of viral and cellular processes through acceleration of RNA degradation. Pharmacol. Ther. 78(2):55–113

Qu D, Teckman JH, Omura S, Perlmutter DH. 1996. Degradation of a mutant secretory protein, α 1-antitrypsin Z, in the endoplasmic reticulum requires proteasome activity. J. Biol. Chem. 271(37):22791–95

Reimold AM, Iwakoshi NN, Manis J, Vallabhajosyula P, Szomolanyi-Tsuda E, et al. 2001. Plasma cell differentiation requires the transcription factor XBP-1. Nature 412(6844):300–37

Römisch K. 2005. Endoplasmic reticulum-associated degradation. Annu. Rev. Cell Dev. Biol. 21:435–56 [Abstract]

Ruegsegger U, Leber JH, Walter P. 2001. Block of *HAC1* mRNA translation by long-range base pairing is released by cytoplasmic splicing upon induction of the unfolded protein response. Cell 107(1):103–14

Scheuner D, Song B, McEwen E, Liu C, Laybutt R, et al. 2001. Translational control is required for the unfolded protein response and in vivo glucose homeostasis. Mol. Cell 7(6):1165–76

Scorrano L, Oakes SA, Opferman JT, Cheng EH, Sorcinelli MD, et al. 2003. BAX and BAK regulation of endoplasmic reticulum Ca2+: a control point for apoptosis. Science 300(5616):135–39

Shaffer AL, Shapiro-Shelef M, Iwakoshi NN, Lee AH, Qian SB, et al. 2004. XBP1, downstream of Blimp-1, expands the secretory apparatus and other organelles, and increases protein synthesis in plasma cell differentiation. Immunity 21(1):81–93

Shamu CE, Walter P. 1996. Oligomerization and phosphorylation of the Ire1p kinase during intracellular signaling from the endoplasmic reticulum to the nucleus. EMBO J. 15(12):3028–39

Shen J, Chen X, Hendershot L, Prywes R. 2002. ER stress regulation of ATF6 localization by dissociation of BiP/GRP78 binding and unmasking of Golgi localization signals. Dev. Cell 3(1):99–111

Shen X, Ellis RE, Lee K, Liu CY, Yang K, et al. 2001. Complementary signaling pathways regulate the unfolded protein response and are required for *C. elegans* development. Cell 107(7):893–03

Shen X, Ellis RE, Sakaki K, Kaufman RJ. 2005. Genetic interactions due to constitutive and inducible gene regulation mediated by the unfolded protein response in *C. elegans*. PLoS Genet. 1(3):e37

Shen J, Snapp EL, Lippincott-Schwartz J, Prywes R. 2005. Stable binding of ATF6 to BiP in the endoplasmic reticulum stress response. Mol. Cell Biol. 25(3):921–32

Shi Y, Vattem KM, Sood R, An J, Liang J, et al. 1998. Identification and characterization of pancreatic eukaryotic initiation factor 2 α-subunit kinase, PEK, involved in translational control. Mol. Cell Biol. 18(12):7499–509

Sidrauski C, Cox JS, Walter P. 1996. tRNA ligase is required for regulated mRNA splicing in the unfolded protein response. Cell 87(3):405–13

Sidrauski C, Walter P. 1997. The transmembrane kinase Ire1p is a site-specific endonuclease that initiates mRNA splicing in the unfolded protein response. Cell 90(6):1031–39

Sriburi R, Jackowski S, Mori K, Brewer JW. 2004. XBP1: a link between the unfolded protein response, lipid biosynthesis, and biogenesis of the endoplasmic reticulum. J. Cell Biol. 167(1):35–41

Stephens SB, Dodd RD, Brewer JW, Lager PJ, Keene JD, Nicchitta CV. 2005. Stable ribosome binding to the endoplasmic reticulum enables compartment-specific regulation of mRNA translation. Mol. Biol. Cell 16(12):5819–31

Stirling J, O'Hare P. 2006. CREB4, a transmembrane bZip transcription factor and potential new substrate for regulation and cleavage by S1P. Mol. Biol. Cell 17(1):413–26

Stitzel ML, Durso R, Reese JC. 2001. The proteasome regulates the UV-induced activation of the AP-1-like transcription factor Gcn4. Genes Dev. 15(2):128–33

Tirasophon W, Welihinda AA, Kaufman RJ. 1998. A stress response pathway from the endoplasmic reticulum to the nucleus requires a novel bifunctional protein kinase/endoribonuclease (Ire1p) in mammalian cells. Genes Dev. 12(12):1812–24

Travers KJ, Patil CK, Wodicka L, Lockhart DJ, Weissman JS, Walter P. 2000. Functional and genomic analyses reveal an essential coordination between the unfolded protein response and ER-associated degradation. Cell 101(3):249–58

Trombetta ES, Parodi AJ. 2003. Quality control and protein folding in the secretory pathway. Annu. Rev. Cell. Dev. Biol. 19:649–76 [Abstract]

Trombetta ES, Parodi AJ. 2005. Glycoprotein reglucosylation. Methods 35(4):328–37

Urano F, Wang X, Bertolotti A, Zhang Y, Chung P, et al. 2000. Coupling of stress in the ER to activation of JNK protein kinases by transmembrane protein kinase IRE1. Science 287(5453):664–66

van Anken E, Romijn EP, Maggioni C, Mezghrani A, Sitia R, et al. 2003. Sequential waves of functionally related proteins are expressed when B cells prepare for antibody secretion. Immunity 18(2):243–53

Wang XZ, Harding HP, Zhang Y, Jolicoeur EM, Kuroda M, Ron D. 1998. Cloning of mammalian Ire1 reveals diversity in the ER stress responses. EMBO J. 17(19):5708–17

Welihinda AA, Kaufman RJ. 1996. The unfolded protein response pathway in Saccharomyces cerevisiae. Oligomerization and trans-phosphorylation of Ire1p (Ern1p) are required for kinase activation. J. Biol. Chem. 271(30):18181–87

Wickner W, Schekman R. 2005. Protein translocation across biological membranes. Science 310(5753):1452–56

Wiertz EJ, Tortorella D, Bogyo M, Yu J, Mothes W, et al. 1996. Sec61-mediated transfer of a membrane protein from the endoplasmic reticulum to the proteasome for destruction. Nature 384(6608):432–38

Wightman B, Ha I, Ruvkun G. 1993. Posttranscriptional regulation of the heterochronic gene lin-14 by lin-4 mediates temporal pattern formation in *C. elegans*. Cell 75(5):855–62

Wu J, Kaufman RJ. 2006. From acute ER stress to physiological roles of the Unfolded Protein Response. Cell Death Differ. 13(3):374–84

Yang R, Wek SA, Wek RC. 2000. Glucose limitation induces GCN4 translation by activation of Gcn2 protein kinase. Mol. Cell Biol. 20(8):2706–17

Ye J, Rawson RB, Komuro R, Chen X, Dave UP, et al. 2000. ER stress induces cleavage of membrane-bound ATF6 by the same proteases that process SREBPs. Mol. Cell. 6(6):1355–64

Yoneda T, Imaizumi K, Oono K, Yui D, Gomi F, et al. 2001. Activation of caspase-12, an endoplastic reticulum (ER) resident caspase, through tumor necrosis factor receptor-associated factor 2-dependent mechanism in response to the ER stress. J. Biol. Chem. 276(17):13935–40

Yoshida H, Haze K, Yanagi H, Yura T, Mori K. 1998. Identification of the cis-acting endoplasmic reticulum stress response element responsible for transcriptional induction of mammalian glucose-regulated proteins. Involvement of basic leucine zipper transcription factors. J. Biol. Chem. 273(50):33741–49

Yoshida H, Matsui T, Hosokawa N, Kaufman RJ, Nagata K, Mori K. 2003. A time-dependent phase shift in the mammalian unfolded protein response. Dev. Cell 4(2):265–71

Yoshida H, Matsui T, Yamamoto A, Okada T, Mori K. 2001. XBP1 mRNA is induced by ATF6 and spliced by IRE1 in response to ER stress to produce a highly active transcription factor. Cell 107(7):881–91

Yoshida H, Okada T, Haze K, Yanagi H, Yura T, et al. 2000. ATF6 activated by proteolysis binds in the presence of NF-Y (CBF) directly to the cis-acting element responsible for the mammalian unfolded protein response. Mol. Cell Biol. 20(18):6755–67

Yoshida H, Oku M, Suzuki M, Mori K. 2006. pXBP1(U) encoded in XBP1 pre-mRNA negatively regulates unfolded protein response activator pXBP1(S) in mammalian ER stress response. J. Cell. Biol. 172(4):565–75

Zhan K, Narasimhan J, Wek RC. 2004. Differential activation of eIF2 kinases in response to cellular stresses in Schizosaccharomyces pombe. Genetics 168(4):1867–75

Zhang P, McGrath B, Li S, Frank A, Zambito F, et al. 2002. The PERK eukaryotic initiation factor 2 α kinase is required for the development of the skeletal system, postnatal growth, and the function and viability of the pancreas. Mol. Cell Biol. 22(11):3864–74

Zhang K, Shen X, Wu J, Sakaki K, Saunders T, et al. 2006. Endoplasmic reticulum stress activates cleavage of CREBH to induce a systemic inflammatory response. Cell 124(3):587–99

Zhang K, Wong HN, Song B, Miller CN, Scheuner D, Kaufman RJ. 2005. The unfolded protein response sensor IRE1 α is required at 2 distinct steps in B cell lymphopoiesis. J. Clin. Invest. 115(2):268–81

Zhou A, Hassel BA, Silverman RH. 1993. Expression cloning of 2–5A-dependent RNAase: a uniquely regulated mediator of interferon action. Cell 72(5):753–65

Zong WX, Li C, Hatzivassiliou G, Lindsten T, Yu QC, et al. 2003. Bax and Bak can localize to the endoplasmic reticulum to initiate apoptosis. J. Cell Biol. 162(1):59–69

RELATED RESOURCES

Orengo CA, Thornton JM. 2005. Protein families and their evolution—a structural perspective. Annu. Rev. Biochem. 74:867–900

Schröder M, Kaufman RJ. 2005. The mammalian unfolded protein response. Annu. Rev. Biochem. 74:739–89

Figure 1-1: The three branches of the metazoan unfolded protein response (UPR). The three types of endoplasmic reticulum (ER) stress transducers—PERK, ATF6, and Ire1—sense the levels of unfolded protein in the lumen of the ER and communicate this information across the membrane to activate cognate bZip transcription factor via regulation of translational control, regulated proteolysis, and regulated mRNA splicing, respectively. In mammalian cells, ATF6f upregulates expression of *XBP1* mRNA (indicated by plus sign). The output of the transcription factors is integrated through their combinatorial action on UPR target genes, whose products increase the protein folding capacity of the cell and hence help the system reestablish homeostasis. PERK also reduces general translation in cells, thereby reducing the protein influx into the ER. If homeostasis in ER protein folding cannot be reached, cells undergo apoptosis. K, kinase domain; R, ribonuclease domain.

Figure 1-1 *Bernales et al. (2006)*

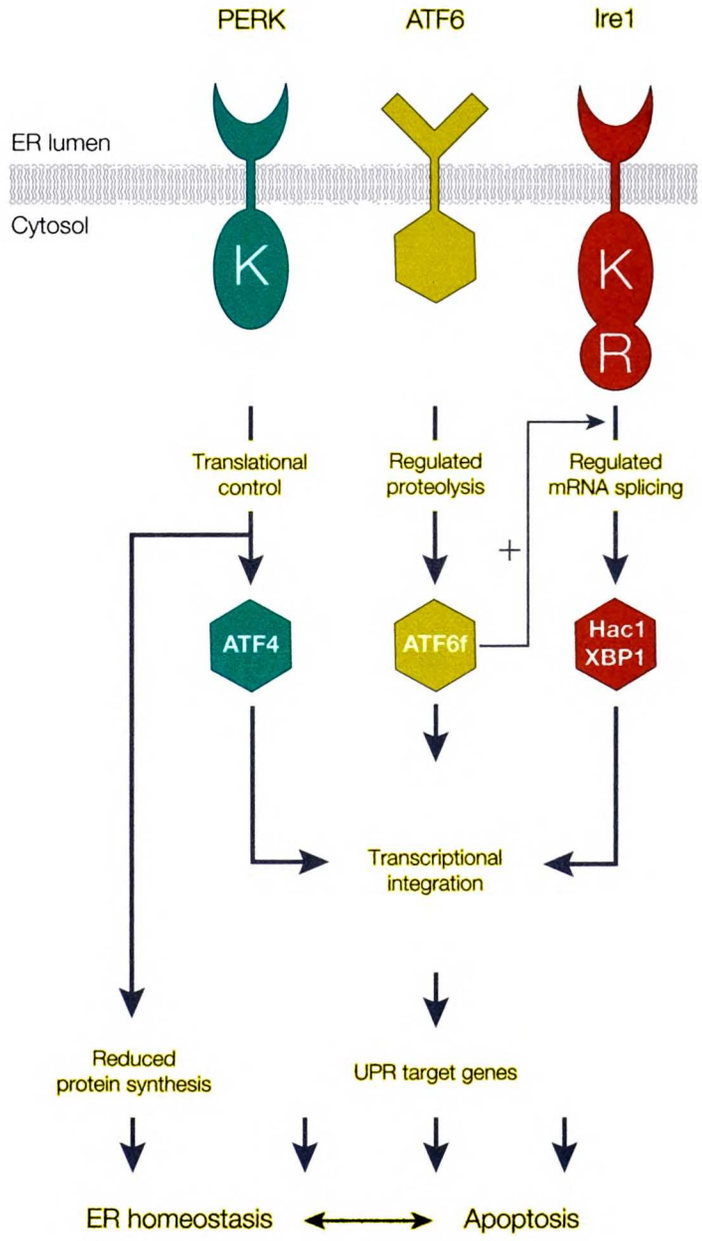

Figure 1-2: Mechanism of Ire1-mediated mRNA splicing in yeast.

Unfolded proteins are recognized by the ER-lumenal domain of Ire1, leading to clustering of this stress sensor in the ER membranes. The Ire1 cytosolic domains become juxtaposed, in turn promoting transautophosphorylation by the kinase domain (K) and concomitant activation of the endoribonuclease domain (R). Base-pairing between the 5' UTR and the intron of *HAC1* mRNA inhibits its translation; ribosomes are already loaded on the translationally inhibited mRNA. Ire1 excises the *HAC1* mRNA intron, and the resulting exons are ligated by tRNA ligase. Spliced *HAC1* mRNA is efficiently translated, producing the transcription factor Hac1, which travels to the nucleus and activates its target genes.

Figure 1-2 *Bernales et al. (2006)*

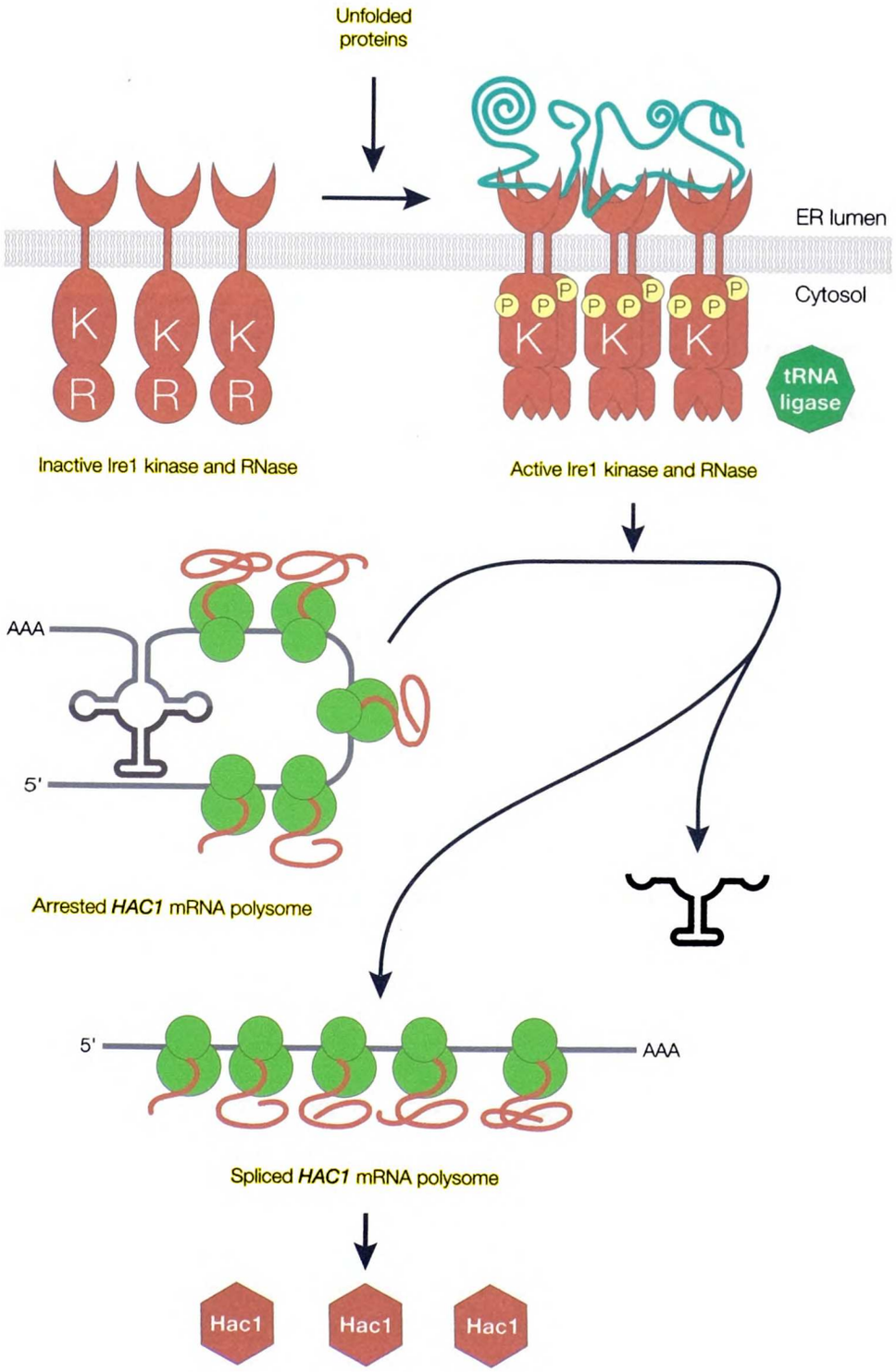

Figure 1-3: Evolutionary relationship of UPR components.

The main components of the UPR are conserved through evolution, and many of the protein domains used by the UPR have been duplicated and adapted in higher metazoans, increasing the level of complexity of the response in these organisms. The Gcn2 kinase domain (K) is present in a single gene in yeast; in two genes, *GCN2* and *PEK* (*PERK*), in *C. elegans*; and in four genes—*GCN2*, *PKR*, *HRI*, and *PERK*—in mammalian cells. As such, mammalian cells respond by eIF2 phosphorylation through Gcn2 kinases to four different signals: starvation, double-stranded RNAs, heme, and unfolded proteins in the ER. Yeast S. cerevisiae has only Gcn2, but *Schizosaccharomyces pombe* has Gcn2 and two HRIs (Zhan et al. 2004). The PEK/PERK's ER-lumenal domain likely originated from *IRE1*, and both proteins are likely to sense unfolded proteins by similar mechanisms. *IRE1* also gave rise to RNaseL, which inherited the kinase/RNase module (denoted by K and R, respectively). The kinase/endoribonuclease domain of Ire1 can also be found in RNaseL, but the phosphotransfer activity of RNaseL's kinase domain has been lost in evolution. Two ATF6-like unfolded protein sensors in *C. elegans* gave rise to at least four [and possibly more (DenBoer et al. 2005, Stirling & O'Hare 2006)] family members in mammalian cells (ATF6 α, ATF6 β, OASIS, and CREBH). There is at least one additional way of transducing the unfolded protein signal in yeast (denoted by the question mark and defined phenotypically by the S-UPR), but the protein(s) mediating this branch remains to be identified.

Figure 1-3 *Bernales et al. (2006)*

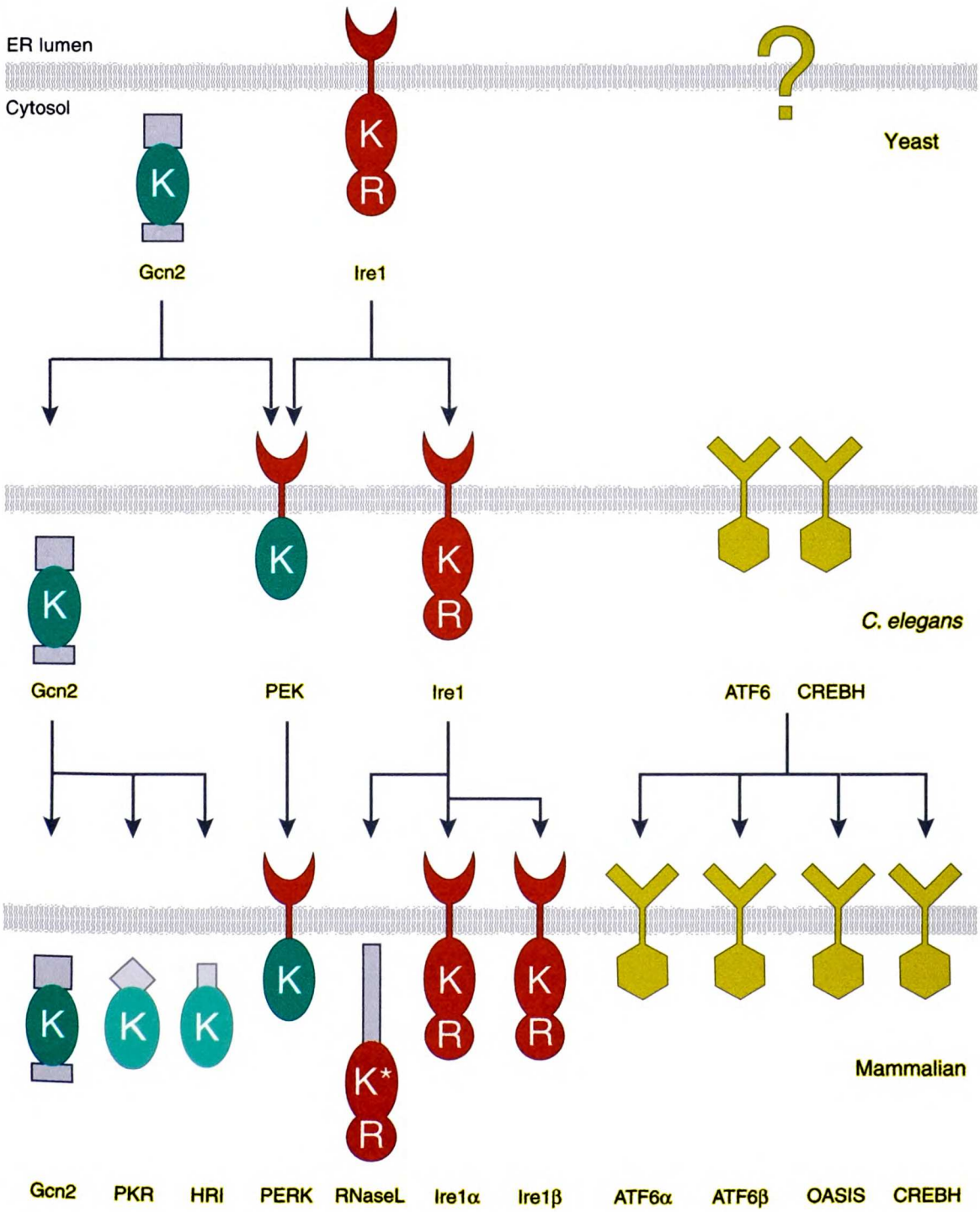

Figure 1-4: Structure of the Ire1 unfolded protein–sensing domain.

(Top row) Ribbon diagrams of the cLD dimer (left) and MHC-1 (right) shown in the same scale for comparison. These two proteins have convergently evolved toward similar architectures, each containing a β-sheet floor on which two α-helices form a deep central groove. Ire1 cLD is a homodimer; the red line demarcates the division between two cLD monomers. (Bottom row) A topographic map of cLD and MHC-I seen from the top. The map displays the grooves as deep canyons of roughly equivalent depths and widths in the two structures. The vertical spacing of the contour lines connecting points of equal depths is 2 Å, and different elevations are colored according to the scale provided. The red index line at depth 0 is set in both structures at the point where the rim becomes discontinuous. Relative to this contour, the grooves in both structures are 11-Å deep at their lowest point. The canyon of Ire1 is lined with conserved alternating hydrophobic and polar residues that may recognize unfolded proteins, which are proposed to bind there (modified from Credle et al. 2005).

Figure 1-4 *Bernales et al. (2006)*

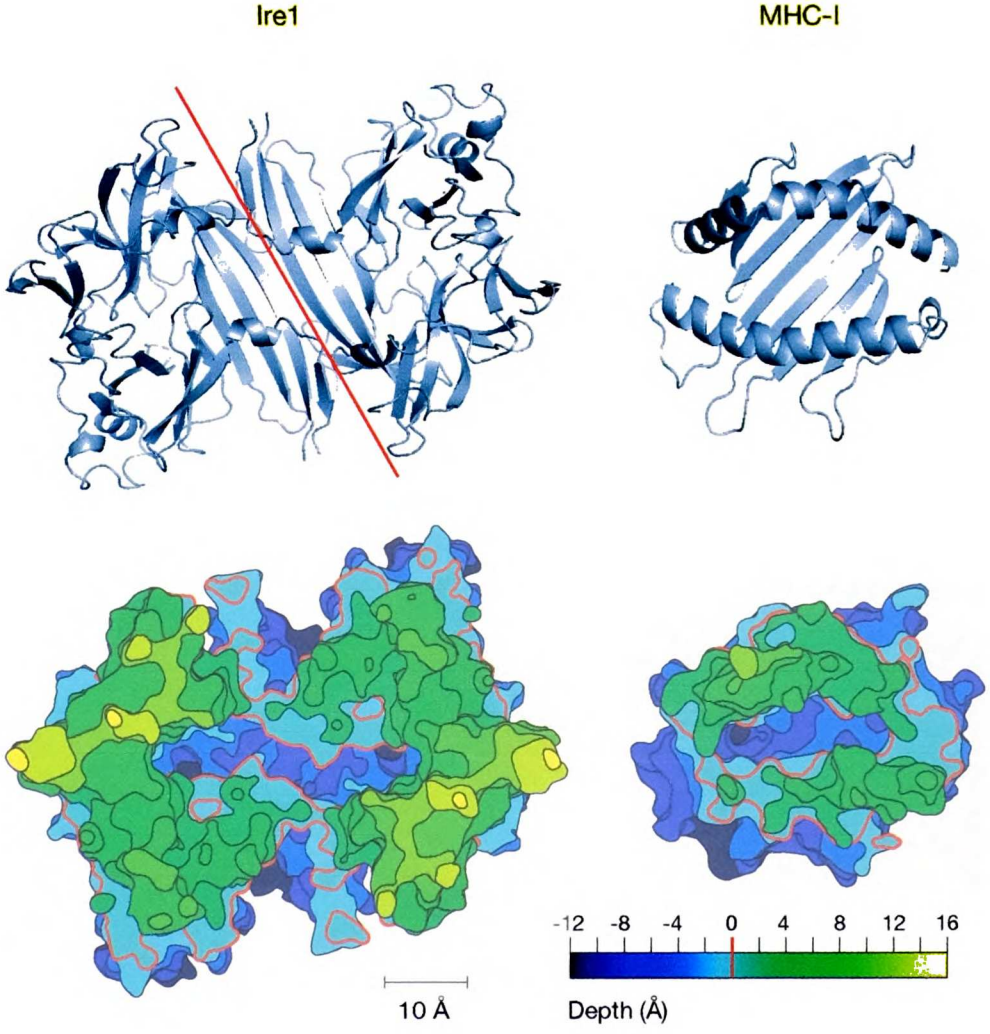

Chapter 2

IRE1-independent Gain Control of the Unfolded Protein Response

IRE1-Independent Gain Control of the Unfolded Protein Response

Jess H. Leber, Sebastián Bernales, Peter Walter*

Howard Hughes Medical Institute, and

Department of Biochemistry and Biophysics,

University of California, San Francisco,

California, United States of America

* Corresponding author

phone: (415) 476-5017

fax: (415) 476-5233

email: walter@cgl.ucsf.edu

SUMMARY

Nonconventional splicing of the gene encoding the Hac1p transcription activator regulates the unfolded protein response (UPR) in *Saccharomyces cerevisiae*. This simple on/off switch contrasts with a more complex circuitry in higher eukaryotes. Here we show that a heretofore unrecognized pathway operates in yeast to regulate the transcription of *HAC1*. The resulting increase in Hac1p production, combined with the production or activation of a putative UPR modulatory factor, is necessary to qualitatively modify the cellular response in order to survive the inducing conditions. This parallel endoplasmic reticulum–to–nucleus signaling pathway thereby serves to modify the UPR-driven transcriptional program. The results suggest a surprising conservation among all eukaryotes of the ways by which the elements of the UPR signaling circuit are connected. We show that by adding an additional signaling element to the basic UPR circuit, a simple switch is transformed into a complex response.

Running title: Transcriptional control of Hac1p expression

INTRODUCTION

In eukaryotes, the endoplasmic reticulum (ER) serves as the first station of the secretory pathway, through which all secreted and membrane proteins must pass. Within the ER, proteins are folded into their native structure and multisubunit protein complexes are assembled. The ER is a dynamic organelle, capable of sensing and adjusting its folding capacity in response to increased demand: when misfolded proteins accumulate in the ER, a signaling pathway, termed the unfolded protein response (UPR), is activated (reviewed in Ma and Hendershot 2001; Patil and Walter 2001; Kaufman 2002; Ron 2002). The UPR activates the expression of genes that enable the cell to adapt to and survive the stress, including those encoding ER-resident chaperones (Lee 1987; Kozutsumi et al. 1988), key enzymes in lipid biosynthesis (Cox et al. 1997), members of the ER-associated degradation (ERAD) machinery, and other components of the secretory system (Ng et al. 2000; Travers et al. 2000; Urano et al. 2000).

In yeast, the UPR is controlled by a binary switch imposed by a nonconventional splicing reaction that governs the production of the Hac1p transcription factor responsible for the activation of UPR target genes (Cox et al. 1993; Kohno et al. 1993; Cox and Walter 1996; Mori et al. 1992, 1996). In uninduced cells, direct base pairing between the 5′ untranslated region (UTR) and an intron at the 3′ end of the mRNA prevents *HAC1* mRNA translation (Chapman and Walter 1997; Ruegsegger et al. 2001). Accumulation of unfolded proteins activates the ER-resident transmembrane kinase/endoribonuclease Ire1p, which then cleaves the *HAC1* mRNA at two precise splice junctions, excising the intron (Cox et al. 1993; Mori et al. 1993; Sidrauski and Walter 1997). The two *HAC1*

exons are then joined by tRNA ligase, allowing translation of Hac1p (Sidrauski et al. 1996).

To date, Ire1-dependent *HAC1* mRNA splicing is the only identified way by which signals from the ER lumen affect transcription in yeast. By contrast, in metazoan cells three mechanistically distinct pathways are known that operate in parallel, although their relative importance in different tissues remains to be determined (reviewed in Ma and Hendershot 2001). Hints that further complexity also exists in yeast comes from data presented in the accompanying paper (Patil et al. 2004): these data demonstrate that Hac1p activity is modulated by interaction with Gcn4p, a transcription factor central to regulation of amino acid biosynthesis. The UPR, therefore, may integrate signals from more than one source to compute a transcriptional output appropriate for the physiological conditions of the cell.

In this paper, we show that *HAC1* mRNA transcription is regulated, resulting in control of Hac1p abundance. Thus the on/off switch provided by IRE1-dependent splicing is not the only regulatory step of the UPR. This regulation responds to a bipartite signal that emanates from the ER and is communicated by an Ire1p-independent pathway. As a consequence, an alternate transcriptional program is triggered, with specific alterations to the normal UPR allowing the cell to survive. Thus, quantitative modulation of Hac1p imposes gain control on a binary switch in the UPR circuitry and, in collaboration with an additional signaling input, transforms a discrete transcriptional response into a more complex signaling function.

RESULTS

Secretory Stress Boosts *HAC1* mRNA Abundance

To define the basic circuitry of signal transduction in the UPR, we evaluated the *HAC1* mRNA processing step in a quantitative manner. To this end, we induced the UPR with either dithiothreitol (DTT) or tunicamycin (both agents that cause protein misfolding selectively in the ER) and monitored *HAC1* mRNA by Northern blot analysis (Figure 1A). In agreement with previous results, we observed rapid and efficient splicing of *HAC1* mRNA, as apparent from the conversion of unspliced *HAC1u* mRNA (u for UPR-uninduced) to spliced *HAC1i* mRNA (i for UPR-induced). Quantitation of the results shows that the relative abundance of *HAC1* mRNA (the sum of *HAC1u* and *HAC1i* mRNAs) remained unchanged over at least 12 h (Figure 1A; unpublished data). These data demonstrate that acute induction of unfolded proteins triggers a simple on/off switch that controls *HAC1* mRNA splicing.

In light of these observations, we were surprised to find that blocking the secretory pathway distal to the ER resulted in a pronounced increase in *HAC1* mRNA abundance. As shown in Figure 1B, *HAC1* mRNA levels increased 3- to 4-fold in mutant strains compromised at various steps in the secretory pathway when shifted to the nonpermissive temperature (*sec12–1*: ER → Golgi, lanes 5–8; *sec14–1*: intra-Golgi, lanes 9–12; and *sec1–1*: Golgi → plasma membrane, lanes 13–16) (Novick et al. 1980). Splicing was also induced, albeit to a lesser degree than was observed with DTT or tunicamycin treatment. The observed splicing suggests that blockages in ER-distal

compartments of the secretory pathway lead to activation of Ire1p in the ER. Temperature shift alone only transiently induced *HAC1* mRNA splicing and had no effect on *HAC1* mRNA abundance (Figure 1B, lanes 1–4). To determine if any disruption of the secretory pathway had similar consequences, we blocked earlier stages of protein traffic. Mutations that blocked protein entry into the ER had no effect (Figure 1C: *sec62–101*, lanes 13–16; *sec63–201*, lanes 17–20) or only a mild effect (*sec61–101*, lanes 9–12) on *HAC1* mRNA abundance.

Thus, a surveillance pathway operates to adjust *HAC1* mRNA levels in response to altered conditions in the secretory pathway. In the experiments described above, we observed *HAC1* mRNA induction only in sec mutants that block transport distal to the ER, not in those that block protein entry into the ER. One common consequence of blocking the secretory pathway at later stages is that proteins in transit will eventually back up into the ER (Rose et al. 1989; Chang et al. 2002). This condition results in protein folding defects, thereby activating Ire1p, as indicated by the observed *HAC1* mRNA splicing. From the data discussed above (Figure 1A), however, we know that an accumulation of unfolded proteins alone is insufficient to trigger an upregulation of *HAC1* mRNA, suggesting that an additional inducing signal is required.

HAC1 mRNA Induction Requires a Bipartite Signal

To determine the nature of this second signal, we sought conditions that induce *HAC1* mRNA when combined with ER protein misfolding drugs. Canvassing different conditions, we found two scenarios under which wild-type (WT) cells can be induced to upregulate *HAC1* mRNA: (1) ER protein misfolding combined with a temperature shift from 23 °C to 37 °C (Figure 2A) and (2) ER protein misfolding combined with inositol

starvation (Figure 2B). Intriguingly, while ER protein misfolding and inositol starvation each activated the UPR individually (as shown by the activation of *HAC1* mRNA splicing; Figure 2A, lanes 5–8; Figure 2B, lanes 1–4 and 5–8), neither stress alone was sufficient to cause *HAC1* mRNA upregulation. Similarly, the temperature shift reproducibly caused a transient UPR induction (see Figure 1B, lanes 1–4; Figure 2A, lanes 1–4) but by itself did not affect *HAC1* mRNA levels. Only the combination of ER stress with either temperature shift (Figure 2A, lanes 9–12) or inositol starvation (Figure 2B, lanes 9–12) led to an increase in *HAC1* mRNA abundance. Subjecting cells to both temperature shift and inositol deprivation had no additive effect, nor did treating cells with both DTT and tunicamycin (unpublished data). Thus, *HAC1* mRNA induction requires a bipartite signal, consisting of one input provided by unfolded proteins in the ER (UP signal), and the other input provided by inositol starvation or temperature shift (I/T signal).

The heat shock response is transiently induced by shifting cells from 23 °C to 37 °C. To determine whether the heat shock response is an important component of the I/T signal, we tested whether continued growth at 37 °C or expression of a constitutively active allele of the heat shock factor Hsf1p (Sorger 1991; Bulman et al. 2001) would substitute for the temperature shift described above. Constitutive expression of active Hsf1p (Figure 2C, lanes 5–8) led to upregulation of SSA1, a known target of the heat shock response (Slater and Craig 1989), but did not substitute for the I/T signal for *HAC1* upregulation. In contrast, continued growth at 37 °C (Figure 2C, lanes 9–12) allowed for modest induction of *HAC1* mRNA. Thus, elevated temperature elicits effects other than heat shock, which are important for *HAC1* mRNA upregulation.

HAC1 Induction Is IRE1-Independent

The UP signal was experimentally induced by DTT or tunicamycin treatment of the cells. As Ire1p is a sensor of folding conditions within the ER lumen, we tested next whether Ire1p was required to transmit this signal. Surprisingly, it was not. *HAC1* mRNA abundance was induced 2.6-fold in *Δire1* cells (Figure 2D, lanes 9–12), similar to the 3-fold induction observed in WT cells (Figure 2A, lanes 9–12). These results show that a previously unrecognized Ire1p-independent surveillance mechanism must exist that monitors protein folding in the ER.

HAC1 mRNA Abundance Is Regulated Transcriptionally

Increase of *HAC1* mRNA abundance could result from increased transcription, reduced degradation, or both. To distinguish between these possibilities, we constructed a reporter gene consisting of the *HAC1* promoter driving transcription of the open reading frame encoding the green fluorescent protein (GFP) flanked by *ACT1* untranslated regions (*HAC1*pro-*GFP*). The resulting heterologous GFP mRNA therefore contained no *HAC1* mRNA sequences. Under conditions providing both the UP and I/T signals, the change in abundance of the *GFP* mRNA (Figure 3A, lanes 5–8) mirrored that of the endogenous *HAC1* mRNA (Figure 3A, lanes 1–4), both in the kinetics and magnitude of the response. These data demonstrate that the observed increase in *HAC1* mRNA abundance was caused by increased transcriptional activity of the *HAC1* promoter.

To further test this notion, we compared the rate of decay of *HAC1* mRNA under both *HAC1*mRNA-inducing and noninducing conditions. To this end, we employed a strain bearing a temperature-sensitive allele of RNA polymerase II, which was subjected to either elevated temperature alone, or to both elevated temperature and DTT treatment. In both cases, polymerase II transcription ceased upon temperature shift, and mRNA decay was measured. As shown in Figure 3B, the rate of decay of *HAC1* mRNA was indistinguishable under the two conditions. Therefore, the increase in *HAC1* mRNA abundance in response to the combination of UP and I/T signals is due solely to activation of the *HAC1* promoter.

HAC1 Promoter Regulation Is Required to Survive Certain Stress Conditions

The results presented so far define a novel regulatory mechanism whereby cells adjust the amount of *HAC1* mRNA. This mRNA is the substrate for the Ire1p-mediated splicing reaction, which in turn produces *HAC1i* mRNA that is translated to produce Hac1p transcription factor. We therefore asked whether elevated levels of *HAC1* mRNA led to a proportional increase in the level of Hac1p. Quantitative Western blot analysis showed that this is indeed the case: when cells were treated with DTT and concomitantly shifted to 37 °C, the levels of Hac1p increased 3-fold (Figure 4A, lanes 5–8), relative to the Hac1p levels observed in cells subjected to DTT treatment alone (Figure 4A, lanes 1–4). Therefore, the transcriptional induction of *HAC1* mRNA combined with Ire1p-mediated splicing results in elevated Hac1p levels, characterizing a new physiological state. Henceforth, we refer to this state as the "Super-UPR" (S-UPR).

To assess the physiological role of the S-UPR, we sought conditions that would allow us to directly monitor the consequences of changes in *HAC1* mRNA levels under otherwise identical growth conditions. To this end, we engineered a yeast strain unable to transcriptionally upregulate *HAC1*. In these cells, *HAC1* mRNA expression was removed from the control of the *HAC1* promoter and was instead driven by the heterologous *ADH1* promoter (*ADH1*pro-*HAC1*), at levels closely approximating the uninduced *HAC1* state (Figure 4B, compare *ADH1*pro-*HAC1*, lanes 5–8, to *HAC1*pro-*HAC1*, lanes 1–4). Expression from the ADH1 promoter was constitutive, and the levels of *HAC1* mRNA did not change significantly under the various inducing conditions described above. As expected, induction of the UPR in these strains led to efficient *HAC1* mRNA splicing and Hac1p production. This strain therefore allowed us to fix the cellular Hac1p concentration to a level closely approximating the basal *HAC1* expression state observed during the UPR.

We next assessed whether we could identify physiological conditions under which elevated *HAC1* mRNA levels were required for cell growth. Therefore, we subjected WT cells and the engineered strain described above to the combinations of stresses described in Figure 2. Cells expressing *HAC1* from the endogenous or from the *ADH1* promoter grew equally well on plates lacking inositol (Figure 4C, left, first and third rows). This condition induces the UPR and requires the expression of at least a minimal amount of *HAC1* mRNA, as *Δhac1* cells fail to grow (Figure 4C, left, second row). In contrast, only WT cells, which are able to upregulate *HAC1* mRNA production, grew on plates lacking inositol and also containing tunicamycin. Cells expressing *HAC1* mRNA only at the basal levels from the *ADH1* promoter were nonviable on these plates (Figure 4C, right, third

row). As shown previously in Figure 2B, this combination of stresses induces the S-UPR. The data therefore reveal that regulation provided by the *HAC1* promoter is necessary for cells to survive certain stress conditions that otherwise are lethal.

Differential UPR Target Gene Induction by Elevated Hac1p Levels

To begin to characterize the cause for increased viability, we next determined differences in UPR target gene expression resulting from either UPR or S-UPR induction.

To this end, we used DNA microarray chip analysis to determine the complete mRNA profile of cells grown under UPR and S-UPR conditions. The results of this analysis are shown in Figure 5A. Each spot represents the fold induction of a UPR target under UPR conditions (x-axis) or S-UPR conditions (y-axis) (see Materials and Methods for definition of the UPR target set used in this analysis). UPR target genes for which the S-UPR has no additional effect should undergo equal induction under both conditions, and are expected to scatter around the diagonal, indicated by the dashed line. This was the case for many UPR targets. However, induction of a substantial number of genes was skewed to the top of the graph, indicating stronger induction under S-UPR conditions than under UPR conditions. These same data are displayed in Figure 5B to highlight and categorize these differences. In the histogram, the x-axis represents the ratio of the induction of a target gene during S-UPR and UPR conditions, and the y-axis shows the number of genes with a given ratio. We have operationally divided UPR target genes into three classes, based on their fold induction during the S-UPR compared to their fold induction during the UPR. (1) Class 1 targets (Figure 5, red bars) exhibit little if any difference in induction during the UPR and S-UPR (S-UPR induction / UPR induction < 2). Thus, the increased Hac1p during the S-UPR does not lead to enhanced transcription,

indicating that for these genes the response is already saturated at UPR Hac1p levels. Class 1 targets include many of the known genes encoding ER lumenal chaperones (including *KAR2, SCJ1, LHS1*, and *JEM1*) and redox proteins (including *PDI1, EUG1*, and *ERO1*). (2) Class 2 targets (Figure 5, blue bars) are induced to a 2- to 4-fold greater extent during S-UPR than during the UPR. Transcription of these genes is therefore roughly proportional to the Hac1p levels in the cell. Class 2 targets include *YIP3*, involved in ER-to-Golgi transport, *OPI3*, encoding a phospholipid methyltransferase, and the hexose transporters *HXT12, HXT15, HXT16*, and *HXT17*. (3) Class 3 targets (Figure 5, green bars) are induced by the S-UPR greater than 4-fold more than by the UPR. Class 3 contains the UPR targets *DER1*, involved in ER-associated degradation (Knop et al. 1996; Ng et al. 2000; Travers et al. 2000), and *INO1*, critical for membrane biogenesis (Hirsch and Henry 1986).

Role for a Putative UPR Modulatory Factor

The increased transcriptional output under S-UPR conditions could occur for two reasons. It could be due to increased Hac1p concentrations in the cell, or it could result because an additional S-UPR-specific transcription factor is produced or activated (perhaps the same that regulates *HAC1* transcription). It could also be due to a combination of these two scenarios. To distinguish among these possibilities, we determined the target gene induction profile in cells in which the *HAC1* mRNA concentration was artificially elevated to a similar level as that found after S-UPR induction. We took advantage of a specific 15-bp deletion in the *HAC1* promoter

(*HAC1*proHI), which increases basal expression by about 3-fold, as compared to the endogenous promoter (Figure 5C). In cells bearing a *HAC1*proHI-*HAC1* gene ("*HAC1*proHI cells"), splicing of *HAC1* mRNA was somewhat reduced upon UPR induction (47%, compared to 67% for WT); however, even with this reduction, *HAC1*proHI cells produced approximately 2.5-fold more spliced *HAC1i* mRNA than WT cells (Figure 5C, compare lanes 3 and 4 to lanes 1 and 2). The increased levels of *HAC1i* mRNA led to a corresponding increase in Hac1p (Figure 5D, compare lanes 3 and 4 to lanes 1 and 2). The amount of Hac1p produced by DTT induction of *HAC1*proHI cells is approximately the same as the amount of Hac1p produced during the S-UPR (compare Figure 5D, lanes 2 and 4 with Figure 4A, lanes 4 and 8).

The ability to set *HAC1* mRNA levels to S-UPR levels allowed us to compare directly UPR target gene induction with the cellular Hac1p concentration being the only variable. We induced the UPR in both WT and *HAC1*proHI cells with DTT and determined the mRNA expression profiles. For each class of UPR target defined above, the expression analysis of UPR-induced WT and *HAC1*proHI cells is shown in Figure 5E. In the histograms, the x-axis shows the ratio of target gene induction during the UPR driven by a high level of Hac1p from *HAC1*proHI cells compared to induction during the UPR in WT cells. The y-axis shows the number of genes at any given ratio. As expected, Class 1 targets (Figure 5E, top panel) did not further respond to the higher levels of Hac1p produced in *HAC1*proHI cells. The majority of Class 2 and Class 3 targets (Figure 5E, middle and bottom panels) also did not respond to higher levels of Hac1p (ratio less than 2), indicating that only raising the Hac1p concentration in cells is not sufficient to account for their full increased induction during the S-UPR. By contrast, ten of the 32

Class 2 and Class 3 targets were significantly induced (ratio greater than 2) in cells expressing high levels of Hac1p. For the Class 3 target *DER1*, high levels of Hac1p were sufficient to elevate expression to S-UPR levels (compare 8-fold induction in DTT-treated *HAC1*proHI cells to 9-fold induction in WT cells during the S-UPR). Otherwise, however, high levels of Hac1p did not fully reconstitute the induction seen during the S-UPR. For example, while the Class 3 gene *INO1* was induced 7.5-fold more in the S-UPR than in the UPR, it was induced only 3-fold more by high levels of Hac1p, compared to normal levels. We conclude that elevated Hac1p levels are sufficient to selectively increase the induction of a few UPR targets, but that the full transcriptional program of the S-UPR predicts the production or activation of an additional transcriptional activator, which we term UPR modulatory factor (UMF).

To dissect further the UMF contribution during the S-UPR, we sought conditions under which UMF activity was the only variable. To this end, we induced the S-UPR in ADH1pro-*HAC1* cells, which are prevented from achieving high level Hac1p expression, and compared the mRNA expression profile against the UPR in WT cells. In this analysis, Hac1p levels were approximately equivalent in the two conditions, so variations from the normal UPR transcriptional program reflect the activity of UMF. The results are shown in Figure 5F, with the data displayed similarly to Figure 5E: the x-axis shows the ratio of target gene induction during the S-UPR in *ADH1*pro-*HAC1* cells, compared to induction during the UPR in WT cells, and the y-axis shows the number of genes at any given ratio. Not surprisingly, the induction of Class 1 targets (Figure 5F, top panel) was unaffected: these are targets that are fully induced by even low levels of Hac1p and are not more induced during the S-UPR. Two Class 3 targets, *YOR289W* and *YHR087W*

(both of unknown function) reach near WT S-UPR induction levels, without elevated levels of Hac1p; for these targets, UMF likely plays a leading role in their induction, with Hac1p having less influence. Most Class 2 and Class 3 targets (Figure 5F, middle and bottom panels), however, do not reach full S-UPR induction levels in the absence of elevated Hac1p levels. For example, the Class 3 target *INO1* is induced roughly 25-fold in *ADH1*pro-*HAC1* cells during S-UPR conditions; while this is roughly twice the induction observed during the UPR, it falls far short of the 75-fold S-UPR induction in WT cells.

These results reinforce the in vivo requirement for high levels of Hac1p to survive S-UPR stress, demonstrated in Figure 4C. Taken together with the data shown in Figure 5E, we conclude that the full S-UPR transcriptional program results from a collaboration between elevated Hac1p levels and UMF, with the relative contribution from each varying among different target genes.

DISCUSSION

The Circuitry of the UPR

In this paper, we describe a novel ER surveillance pathway in yeast that modulates the UPR, resulting in a new physiological state that we term the S-UPR. In response to a bipartite signal transmitted from the ER by an *IRE1*-independent pathway, the *HAC1* promoter is activated, resulting in increased *HAC1* mRNA levels that, upon splicing, yield more Hac1p. The increased Hac1p concentration, in conjunction with an additional postulated factor(s) produced or activated by the S-UPR (UMF), allows the cell to mount a modified transcriptional response to cope with the inducing stress conditions.

Figure 6 shows the UPR as a circuit diagram utilizing multiple logical operations to integrate various signals. In the "classical UPR" (in red), basal transcription of *HAC1* produces *HAC1u* mRNA, which is translationally inactive due to the presence of the inhibitory intron. In response to unfolded proteins, Ire1p performs an on/off operation, excising the intron from *HAC1u* mRNA to generate spliced *HAC1i* mRNA, which is translated to produce the Hac1p transcription activator. The S-UPR provides another layer of regulation superimposed on the UPR (in blue). If ER folding stress is combined with either a shift to elevated temperature or inositol starvation, an AND gate integrates this bipartite signal and boosts *HAC1* mRNA levels. In turn, this regulation causes increased Hac1p production. Together with UMF, Hac1p induces UPR target genes, with particular genes responding differentially to differences in Hac1p and UMF concentration. Thus the S-UPR can be seen as an adaptation of the classical (or basal)

UPR, fine-tuning the activation of select targets to produce a response suited to the challenge faced by the cell.

In the accompanying paper, Patil et al. (2004) describe a third signaling element, which additionally modifies the transcriptional program of the yeast UPR. The authors show that the transcriptional activator Gcn4p collaborates with Hac1p at the promoters of UPR targets, providing an additional opportunity for integration of information about the physiological state of the cell. Gcn4p is a highly regulated transcription regulator that responds to metabolic conditions, such as amino acid availability. Gcn4p is not UMF, as S-UPR induction of *HAC1* proceeds normally in *Δgcn4* cells (unpublished data). A recent report from Ogawa and coworkers (Ogawa and Mori 2004) demonstrates autoregulation of *HAC1* expression under conditions of extreme and prolonged ER stress, mediated by Hac1p binding to its own promoter. Because the S-UPR can be triggered in *Δire1* cells that do not produce Hac1p, autoregulation and the S-UPR are distinct pathways. The existence of multiple mechanisms of *HAC1* regulation reinforces the notion that multiple cellular stimuli become integrated to fine-tune an appropriate response.

Bipartite Signal Requirement for S-UPR Activation

Presently, the molecular details of the pathway by which the S-UPR signal exerts transcriptional control are not known. In particular, it will be of interest to determine where in the cell the two branches of the S-UPR signal are integrated, i.e., how the AND gate is constructed and where it resides. One possibility is that this signal integration

event occurs close to the source at the ER membrane. Both temperature shift and inositol starvation can equally induce the I/T signal pathway, and it is conceivable that both conditions affect ER membrane properties similarly. Inositol is an essential precursor for phosphatidylinositol, a major structural phospholipid in yeast that is required for proper functioning of the secretory system (White et al. 1991; Zinser and Daum 1995; Greenberg and Lopes 1996). Previous work has demonstrated an intimate link between inositol regulation and the UPR, presumably to coordinate the concentration of ER lumenal and membrane components (Cox et al. 1997). A similar sensing mechanism operates in cholesterol homeostasis, with sterol composition in ER membranes affecting the activity of SCAP, a membrane-bound regulator of SREBP intramembrane proteolysis (Espenshade et al. 2002). It is likely that elevated temperatures also affect ER membrane properties, such as fluidity (Laroche et al. 2001). If such a property were sensed, it would explain how the temperature effect contributing to the I/T signal is separate from the heat shock response. ER membranes distressed by either inositol deprivation or elevated temperature (the I/T signal) might then control the activity of a membrane-bound component of a signal transduction machine that also senses protein folding conditions (the UP signal) in the ER lumen.

Alternatively, the AND gate might be well removed from the ER membrane, with I/T and UP signals traveling separately through the cell and meeting possibly as late as at the promoters of the affected target genes. Components that map onto either signaling pathway need to be identified and placed into the circuit to distinguish between these possibilities.

The Transcriptional Output of the S-UPR

The transcriptional response elicited by the S-UPR reveals different classes of UPR targets. During the S-UPR, the further activation of UPR targets is not simply proportional to the increase in Hac1p concentration; rather, we observe a multitude of complex responses. Some targets are already maximally transcribed during UPR conditions and are not induced further during the S-UPR, while other targets become significantly more induced. For some targets (a minority), elevated Hac1p concentrations are sufficient to increase transcriptional induction, while for others, S-UPR-derived UMF is also required. We find evidence for both kinds of regulation. The promoters of target genes, therefore, display differential responsiveness to Hac1p concentration and UMF activity.

The production of different levels of Hac1p allowed us to isolate and directly assess the responsiveness of target genes to Hac1p concentration under otherwise identical conditions. Those target genes that undergo equivalent activation under both conditions likely have promoters that are saturated by the lower amount of Hac1p, and thus reach full activation more readily. For UPR targets at the other end of the spectrum, induction continues to increase as Hac1p levels increase; lower concentrations of Hac1p are inadequate for full stimulation of these genes, which may have lower affinity for Hac1p. Because genes respond differentially to Hac1p levels, regulation of *HAC1* mRNA abundance can be used as a gene-specific gain control for target activation. This control is similar to that observed in regulation of phosphate metabolism, where the differential

affinity of certain Pho4p phosphoforms for target promoters allows for the selective activation of a subset of phosphate-responsive genes (Springer et al. 2003).

For most target genes, however, the S-UPR further enhances the transcriptional activity even in the presence of high concentrations of Hac1p. For example, *INO1* is induced over 75-fold by the S-UPR in WT cells, compared to 33-fold during the UPR in *HAC1*proHI cells, while the amount of Hac1p produced in both cases is approximately the same. This added induction during the S-UPR is dependent on Hac1p, as *ADH1*pro-*HAC1* cells treated with DTT and shifted to elevated temperature show significantly reduced induction of *INO1*. The simplest interpretation of these findings is that S-UPR-induced UMF, which may or may not be identical to the transcription factor regulating *HAC1* mRNA, collaborates with Hac1p to further boost transcription of these genes.

The cis determinants that instruct genes to behave as Class 1, 2, or 3 targets are unknown. One attractive possibility is that target gene promoters have differential affinity for Hac1p and/or UMF. Promoters with stronger affinity for Hac1p would be maximally occupied and fully activated during a normal UPR and would not further respond to increased Hac1p levels (i.e., Class 1 targets). Promoters with lesser affinity for Hac1p would increase in occupancy, and hence transcriptional activation, as Hac1p levels rose during the S-UPR, and would possibly achieve full transcriptional activity only with the additional binding of UMF (i.e., Class 2 and 3 targets). Such a mechanism of promoter-encoded differential responsiveness to transcription factor concentration would explain the selective regulation of subsets of UPR target genes.

Links with the Metazoan UPR

Higher eukaryotes possess three separate pathways to sense ER stress and direct overlapping but distinct transcriptional outputs (reviewed in Ma and Hendershot 2001). In the first branch, Ire1p senses unfolded proteins in the ER lumen and directs the cleavage of an intron from the mRNA encoding the XBP-1 transcription factor, analogous to the splicing of *HAC1* in yeast (Yoshida et al. 2001; Calfon et al. 2002). In a second branch, the transmembrane kinase PERK phosphorylates and inactivates the eIF2-α translation initiation factor (Harding et al. 1999). This attenuates global protein synthesis, but selectively increases the translation of a small number of proteins including the ATF-4 transcriptional activator. Interestingly, ATF-4 is the metazoan ortholog of Gcn4p, the yeast transcription factor demonstrated by Patil et al. (2004) to collaborate with Hac1p. Finally, in a third branch, activation of the UPR in metazoans allows for the ER-to-Golgi transit of the membrane-tethered ATF-6 protein. In the Golgi apparatus, ATF-6 undergoes proteolytic cleavage within its membrane-spanning domain, and the soluble fragment subsequently travels to the nucleus as an active transcription factor (Haze et al. 1999; Ye et al. 2000). XBP-1, ATF-4, and ATF-6 all activate separate but overlapping transcriptional programs that enable the cell to respond to changing conditions in the ER. Notably, the *XBP-1* promoter is a target of ATF-6 activation (Yoshida et al. 2001), reminiscent of the circuitry described here for yeast. Conceptually, therefore, *HAC1* mRNA upregulation by the S-UPR pathway in yeast takes the place of *XBP-1* upregulation by the ATF-6 fragment in metazoans. Moreover, ATF-6 and XBP-1 can heterodimerize (Lee et al. 2002), reminiscent of the proposed collaboration of UMF

and Hac1p. Thus, intriguing parallels between yeast and metazoans in the wiring that connects the elements of the UPR signaling circuit are beginning to come to light.

These findings suggest a common strategy among all eukaryotic cells for responding to challenges to the secretory system. Maintaining separate ER surveillance pathways creates the potential for cells to integrate multiple signals that, in principle, could convey precise information regarding the nature of the imbalance to afford finely tailored corrective measures. In this view, the UPR operates as a homeostatic control circuit, in which such regulation ensures that components of the secretory apparatus are produced according to need. The challenge now at hand is to decipher the logic between the UPR inducing conditions and the transcriptional output to add physiological explanations to the complex regulation of the response that we observe experimentally.

MATERIALS AND METHODS

Yeast strains. The WT strain W303–1A, the *Δire1* strain CS165, and the *Δhac1* strain JC408 are as described previously (Cox et al. 1993; Cox and Walter 1996). All sec strains used in this study were provided by Robert Fuller (University of Michigan, Ann Arbor, Michigan, United States) and are otherwise genotypically identical to W303. The HSF1c strain was a kind gift of Hillary Nelson (University of Pennsylvania, Philadelphia, Pennsylvania, United States) and contains the R222A allele of HSF1 (Bulman et al. 2001) replacing the chromosomal locus in a W303 background. Strains used in the experiments described in Figure 3A were *Δhac1* transformed with pPW598 (*HAC1*pro-*HAC1*, HA-tagged *HAC1* [Cox and Walter 1996] under its own promoter and with native *HAC1* flanking sequences, in a pRS304 background) or with pPW599 (*HAC1*pro-*GFP*, the GFP ORF, driven by the *HAC1* promoter [defined as the region starting at the mapped start site of *HAC1* transcription (Ruegsegger et al. 2001) and extending 500 bp upstream] and flanked by 5′ UTR and 3′ UTR sequences from ACT1). Strains used in experiments described in Figure 4 were *HAC1*pro-*HAC1* and Δhac1 (described above) and Δhac1 transformed with pPW600 (ADH1pro-*HAC1*, HA-tagged *HAC1* with 5′ and 3′ UTR *HAC1* sequence subcloned into the p414 ADH expression vector [Mumberg et al. 1995] and transferred to a pRS304 backbone). In Figure 5, *HAC1*proHI (pPW601) was made by subjecting *HAC1*pro-*HAC1* to QuikChange mutagenesis (Stratagene, La Jolla, California, United States) following the manufacturer's protocol,

using oligonucleotides to remove the 15 bp at coordinates -338 to -323 (+1 representing the start site of transcription).

Cell culture and plates. Yeast cultures were grown in YPD medium (unless otherwise specified) at the indicated temperatures to midlog phase (OD600 ≈ 0.5). For temperature shift experiments, cultures were transferred to a preheated 37 °C water bath shaking incubator. DTT (Roche, Basel, Switzerland) was added to a final concentration of 6 mM, and tunicamycin (Boehringer Mannheim, Indianapolis, Indiana, United States) was added to a final concentration of 1 μg/ml. For experiments involving inositol deprivation in liquid medium, yeast cells were grown in liquid complete synthetic medium described by Sherman (1991), supplemented with myo-inositol (Sigma, St. Louis, Missouri, United States) to a final concentration of 100 μg/ml. Cells were then harvested by filtration, washed three times in prewarmed complete synthetic medium lacking inositol, and then filter-transferred to a flask containing prewarmed complete synthetic medium lacking inositol.

For the experiment described in Figure 4C, yeast strains were grown in YPD to midlog phase (OD600 ≈ 0.5), transferred to a 96-well microtiter plate, and serially 5-fold diluted in fresh YPD. Using a liquid transfer prong ("frogging") tool (Aladin Enterprises, San Francisco, California, United States), approximately 3 μl of all serial dilutions of all strains was simultaneously transferred to complete synthetic plates lacking inositol (described above), either in the absence or presence of 0.2 μg/ml tunicamycin. After approximately 2 d of incubation at 30 °C, plates were photographed using the Epi Chemi II Darkroom GelDoc system (UVP, Upland, California, United States).

RNA analysis. Isolation of total RNA from yeast cells was carried out with the modified hot-phenol extraction method described in Ruegsegger et al.(2001). For Northern blot analysis, 10 μg of total RNA was separated on a 1.5% w/v agarose gel and transferred to a Duralon-UV nylon membrane (Stratagene), which was incubated with a probe directed against the 5′ exon of *HAC1*. The mRNA abundance was quantitated using a PhosporImager (Molecular Dynamics, Sunnyvale, California, United States). The membranes were then stripped with two serial washes using 0.1% SDS at 65 °C for 60 min each and incubated with a probe directed against the 3′ exon of *ACT1*, and mRNA abundance was again quantitated. To control for the variable strength of Northern blot probes across multiple experiments, the relative *HAC1*/*ACT1* mRNA abundance ratio is always normalized to the untreated (t = 0) sample. For the detection of other mRNAs, membranes were incubated with the additional relevant probes (*GFP*, *SSA1*) concurrent with the *HAC1* probe. All data shown are an average of at least two independent experiments.

PolyA+ mRNA was isolated from total RNA using the PolyATract system (Promega, Madison, Wisconsin, United States) according to the manufacturer's instructions. Microarray analysis, using yeast ORF arrays printed at the University of California, San Francisco, Core Center for Genomics and Proteomics (http://derisilab.ucsf.edu/core/, was performed as in Carroll et al. (2001) using protocols and reagents described at http://microarrays.org/. All array data are the average of two independent experiments. For this study, we were obliged to evaluate UPR targets

differently than in Travers et al. (2000), as we considered *HAC1*-independent responses, whereas the former study specifically isolated genes induced by unfolded proteins via Hac1p (z-score $\geq 3.6\ \sigma$). Here, UPR targets were defined as those genes that met the following three criteria in a parallel set of microarray experiments using WT (W303) and *Δhac1* (JC408) strains. First, induction (log2 of the fold change in gene expression) in WT cells treated with DTT must be at least one standard deviation greater than the mean ([inductionWT,DTT - μ WT,DTT]/ σ WT,DTT ≥ 1). Second, induction in WT cells treated with tunicamycin must be at least one standard deviation greater than the mean ([inductionWT,tunicamycin - μ WT,tunicamycin]/ σ WT,tunicamycin ≥ 1). Third, induction in *Δhac1* cells treated with DTT must be at least one standard deviation less than the induction in WT cells treated with DTT (or, more awkwardly, [([(inductionWT,DTT - μ WT,DTT)/ σ WT,DTT] - [(induction *Δhac1*,DTT - μ *Δhac1*,DTT)/ σ *Δhac1*,DTT]) - μ WT,DTT - *Δhac1*,DTT]/ σ WT,DTT - *Δhac1*,DTT ≥ 1).

Isolation and detection of protein from yeast cells. Cells were collected by filtration, frozen in liquid nitrogen, and disrupted in 150 μl of 8 M urea/1% SDS by vortexing for 5 min at 4 °C in the presence of 150 μl of silica beads. The samples were then boiled for 5 min and the lysates cleared by centrifugation at 16,200g for 5 min at room temperature. SDS-PAGE was performed on 20 μg of protein separated on NuPAGE 10% w/v SDS-

polyacrylamide gels (Invitrogen, Carlsbad, California, United States), and Western blots were visualized using SuperSignal West Dura Extended Duration ECL Substrate (Pierce Biotechnology, Rockford, Illinois, United States) according to the instructions of the manufacturer. Hac1p was detected using a polyclonal antibody raised against the carboxy terminus (see Figure 4) or a monoclonal antibody raised against the HA epitope and directly coupled to horseradish peroxidase (see Figure 5) (Molecular Probes, Eugene, Oregon, United States), and Pgk1p was detected using a commercially available polyclonal antibody (Molecular Probes). Protein abundance was quantified using the Epi Chemi II Darkroom GelDoc system (UVP). Parallel experiments using serial protein dilutions were performed to confirm that the detected protein levels were within the linear range of the system.

Transcription shut-off. The yeast strain JC218 (Sidrauski et al. 1996; rbp1–1) was grown in YPD at 23 °C to OD600 ≈ 0.5 and then shifted to a 37 °C water bath, shaking at 250 RPM. To induce the UPR, DTT was added to a final concentration of 6 mM. Cells were harvested and total RNA isolated, at 20 min intervals, as described above.

SUPPORTING INFORMATION

Accession Numbers. The GenBank accession numbers of the sequences discussed in this paper are Hac1p (NP_ 116622), Ire1p (NP_011946), and tRNA ligase (NP_012448). Microarray data can be accessed at the Gene Expression Omnibus (GEO) at the National Center for Biotechnology Information (NCBI) database as platform number GPL999 and sample numbers GSM16978–GSM1984.

Acknowledgments. We thank Jason Brickner and other members of the Walter lab for helpful discussions and comments on the manuscript, Adam Carroll and Manuel Llinas for assistance with microarrays, Chris Patil and Hao Li for help with bioinformatic analyses, and Robert Fuller and Hillary Nelson for yeast strains. Also, we acknowledge Vladimir Denic for initial observations regarding *HAC1* mRNA transcriptional control. This work was supported by a University of California at San Francisco (UCSF) Chancellor's Fellowship to JL, by support from the UCSF Herbert H. Boyer Fund to SB, and by grants from the National Institutes of Health to PW. PW is an Investigator of the Howard Hughes Medical Institute.

Conflicts of interest. The authors have declared that no conflicts of interest exist.

Author contributions. JHL and PW conceived and designed the experiments. JHL and SB performed the experiments. JHL and PW analyzed the data and wrote the paper.

REFERENCES

1. Bulman AL, Hubl ST, Nelson HC (2001) The DNA-binding domain of yeast heat shock transcription factor independently regulates both the N- and C-terminal activation domains. J Biol Chem 276:40254–40262.

2. Calfon M, Zeng H, Urano F, Till JH, Hubbard SR, et al. (2002) IRE1 couples endoplasmic reticulum load to secretory capacity by processing the XBP-1 mRNA. Nature 415:92–96.

3. Carroll AS, Bishop AC, DeRisi JL, Shokat KM, O'Shea EK (2001) Chemical inhibition of the Pho85 cyclin-dependent kinase reveals a role in the environmental stress response. Proc Natl Acad Sci U S A 98:12578–12583.

4. Chang HJ, Jones EW, Henry SA (2002) Role of the unfolded protein response pathway in regulation of INO1 and in the sec14 bypass mechanism in Saccharomyces cerevisiae. Genetics 162:29–43.

5. Chapman RE, Walter P (1997) Translational attenuation mediated by an mRNA intron. Curr Biol 7:850–859.

6. Cox JS, Walter P (1996) A novel mechanism for regulating activity of a transcription factor that controls the unfolded protein response. Cell 87:391–404.

7. Cox JS, Shamu CE, Walter P (1993) Transcriptional induction of genes encoding endoplasmic reticulum resident proteins requires a transmembrane protein kinase. Cell 73:1197–1206.

8. Cox JS, Chapman RE, Walter P (1997) The unfolded protein response coordinates the production of endoplasmic reticulum protein and endoplasmic reticulum membrane. Mol Biol Cell 8:1805–1814.

9. Espenshade PJ, Li WP, Yabe D (2002) Sterols block binding of COPII proteins to SCAP, thereby controlling SCAP sorting in ER. Proc Natl Acad Sci U S A 99:11694–11699.

10. Greenberg ML, Lopes JM (1996) Genetic regulation of phospholipid biosynthesis in Saccharomyces cerevisiae. Microbiol Rev 60:1–20.

11. Harding HP, Zhang Y, Ron D (1999) Protein translation and folding are coupled by an endoplasmic-reticulum-resident kinase. Nature 397:271–274.

12. Haze K, Yoshida H, Yanagi H, Yura T, Mori K (1999) Mammalian transcription factor ATF6 is synthesized as a transmembrane protein and activated by proteolysis in response to endoplasmic reticulum stress. Mol Biol Cell 10:3787–3799.

13. Hirsch JP, Henry SA (1986) Expression of the Saccharomyces cerevisiae inositol-1-phosphate synthase (INO1) gene is regulated by factors that affect phospholipid synthesis. Mol Cell Biol 6:3320–3328.

14. Kaufman RJ (2002) Orchestrating the unfolded protein response in health and disease. J Clin Invest 110:1389–1398.

15. Knop M, Finger A, Braun T, Hellmuth K, Wolf DH (1996) Der1, a novel protein specifically required for endoplasmic reticulum degradation in yeast. EMBO J 15:753–763.

16. Kohno K, Normington K, Sambrook J, Gething MJ, Mori K (1993) The promoter region of the yeast KAR2 (BiP) gene contains a regulatory domain that responds to the presence of unfolded proteins in the endoplasmic reticulum. Mol Cell Biol 13:877–890.

17. Kozutsumi Y, Segal M, Normington K, Gething MJ, Sambrook J (1988) The presence of malfolded proteins in the endoplasmic reticulum signals the induction of glucose-regulated proteins. Nature 332:462–464.

18. Laroche C, Beney L, Marechal PA, Gervais P (2001) The effect of osmotic pressure on the membrane fluidity of Saccharomyces cerevisiae at different physiological temperatures. Appl Microbiol Biotechnol 56:249–254.

19. Lee AS (1987) Coordinated regulation of a set of genes by glucose and calcium ionophores in mammalian cells. Trends Biochem Sci 12:20–23.

20. Lee K, Tirasophon W, Shen X, Michalak M, Prywes R, et al. (2002) IRE1-mediated unconventional mRNA splicing and S2P-mediated ATF6 cleavage merge to regulate XBP1 in signaling the unfolded protein response. Genes Dev 16:452–466.

21. Ma Y, Hendershot LM (2001) The unfolding tale of the unfolded protein response. Cell 107:827–830.

22. Mori K, Sant A, Kohno K, Normington K, Gething MJ, et al. (1992) A 22 bp cis-acting element is necessary and sufficient for the induction of the yeast KAR2 (BiP) gene by unfolded proteins. EMBO J 11:2583–2593.

23. Mori K, Ma W, Gething MJ, Sambrook J (1993) A transmembrane protein with a cdc2+/CDC28-related kinase activity is required for signaling from the ER to the nucleus. Cell 74:743–756.

24. Mori K, Kawahara T, Yoshida H, Yanagi H, Yura T (1996) Signalling from endoplasmic reticulum to nucleus: Transcription factor with a basic-leucine zipper motif is required for the unfolded protein-response pathway. Genes Cells 1:803–817.

25. Mumberg D, Muller R, Funk M (1995) Yeast vectors for the controlled expression of heterologous proteins in different genetic backgrounds. Gene 156:119–122.

26. Ng DT, Spear ED, Walter P (2000) The unfolded protein response regulates multiple aspects of secretory and membrane protein biogenesis and endoplasmic reticulum quality control. J Cell Biol 150:77–88.

27. Novick P, Field C, Schekman R (1980) Identification of 23 complementation groups required for posttranslational events in the yeast secretory pathway. Cell 21:205–215.

28. Ogawa N, Mori K (2004) Autoregulation of the *HAC1* gene is required for sustained activation of the yeast unfolded protein response. Genes Cells 9:95–104.

29. Patil C, Walter P (2001) Intracellular signaling from the endoplasmic reticulum to the nucleus: The unfolded protein response in yeast and mammals. Curr Opin Cell Biol 13:349–355.

30. Patil C, Li H, Walter P (2004) Gcn4 and novel upstream activating sequences regulate targets of the unfolded protein response. PLoS Biol 2:e246 10.1371/journal.pbio.0020246.

31. Ron D (2002) Translational control in the endoplasmic reticulum stress response. J Clin Invest 110:1383–1388.

32. Rose MD, Misra LM, Vogel JP (1989) KAR2, a karyogamy gene, is the yeast homolog of the mammalian BiP/GRP78 gene. Cell 57:1211–1221.

33. Ruegsegger U, Leber JH, Walter P (2001) Block of *HAC1* mRNA translation by long-range base pairing is released by cytoplasmic splicing upon induction of the unfolded protein response. Cell 107:103–114.

34. Sherman F (1991) Getting started with yeast. Methods Enzymol 194:3–21.

35. Sidrauski C, Walter P (1997) The transmembrane kinase Ire1p is a site-specific endonuclease that initiates mRNA splicing in the unfolded protein response. Cell 90:1031–1039.

36. Sidrauski C, Cox JS, Walter P (1996) tRNA ligase is required for regulated mRNA splicing in the unfolded protein response. Cell 87:405–413.

37. Slater MR, Craig EA (1989) The SSA1 and SSA2 genes of the yeast Saccharomyces cerevisiae. Nucleic Acids Res 17:805–806.

38. Sorger PK (1991) Heat shock factor and the heat shock response. Cell 65:363–366.

39. Springer M, Wykoff DD, Miller N, O'Shea EK (2003) Partially phosphorylated Pho4 activates transcription of a subset of phosphate-responsive genes. PLoS Biol 1:E28 10.1371/journal.pbio.0010028.

40. Travers KJ, Patil CK, Wodicka L, Lockhart DJ, Weissman JS, et al. (2000) Functional and genomic analyses reveal an essential coordination between the unfolded protein response and ER-associated degradation. Cell 101:249–258.

41. Urano F, Wang X, Bertolotti A, Zhang Y, Chung P, et al. (2000) Coupling of stress in the ER to activation of JNK protein kinases by transmembrane protein kinase IRE1. Science 287:664–666.

42. White MJ, Lopes JM, Henry SA (1991) Inositol metabolism in yeast. Adv Microb Physiol 32:1–51.

43. Ye J, Rawson RB, Komuro R, Chen X, Davé UP, et al. (2000) ER stress induces cleavage of membrane-bound ATF6 by the same proteases that process SREBPs. Molecular Cell 6:1355–1364.

44. Yoshida H, Matsui T, Yamamoto A, Okada T, Mori K (2001) XBP1 mRNA is induced by ATF6 and spliced by IRE1 in response to ER stress to produce a highly active transcription factor. Cell 107:881–891.

45. Zinser E, Daum G (1995) Isolation and biochemical characterization of organelles from the yeast, Saccharomyces cerevisiae Yeast 11:493–536.

Figure 2-1: ER-Distal Secretory Stress Boosts *HAC1* mRNA Abundance.

(A) Determination of *HAC1* mRNA abundance during the UPR. The UPR was induced in WT cells by addition of either 6 mM DTT (lanes 1–4) or 1 μg/ml tunicamycin (lanes 5–8) for the times indicated. Total RNA was harvested at the indicated intervals, and the relative abundance of *HAC1* and *ACT1* mRNAs was analyzed by Northern blot analysis (see Materials and Methods). Splicing was calculated at the ratio of spliced (*HAC1i*) to total (*HAC1i* + *HAC1u*) mRNA.

(B) Determination of *HAC1* mRNA abundance during ER-distal secretory stress. WT, *sec12–1, sec14–3,* and *sec1–1* strains were grown at 23 °C and shifted to 37 °C.

(C) Determination of *HAC1* mRNA abundance during ER-proximal secretory stress. WT, *sec14–3, sec61–101, sec62–101*, and *sec63–201* strains were grown at 23 °C and shifted to 37 °C.

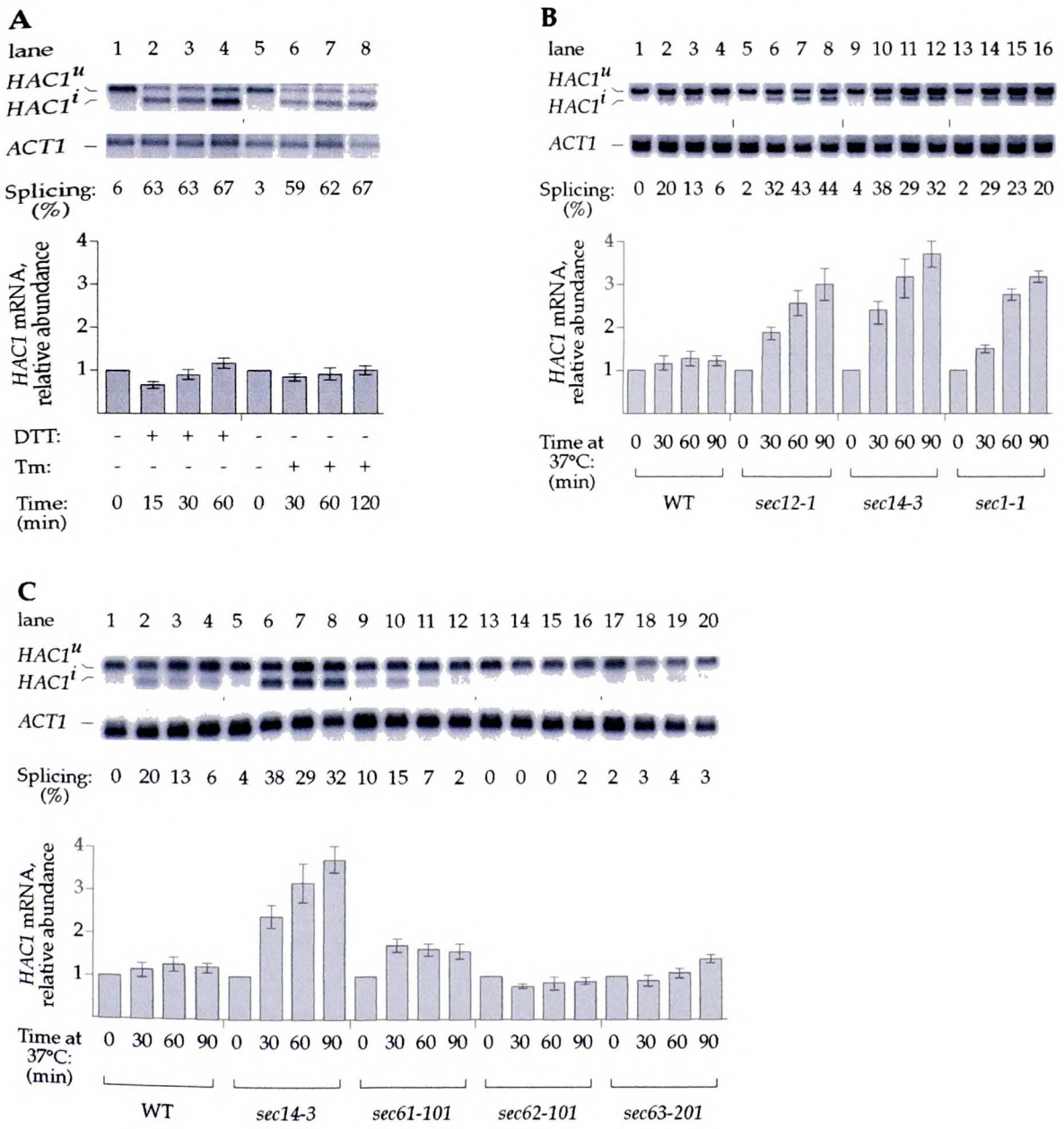
A
lane 1 2 3 4 5 6 7 8
HAC1u
HAC1i
ACT1
Splicing: (%) 6 63 63 67 3 59 62 67
HAC1 mRNA, relative abundance
DTT: - + + + - - - -
Tm: - - - - - + + +
Time: (min) 0 15 30 60 0 30 60 120
B
lane 1 2 3 4 5 6 7 8 9 10 11 12 13 14 15 16
HAC1u
HAC1i
ACT1
Splicing: (%) 0 20 13 6 2 32 43 44 4 38 29 32 2 29 23 20
HAC1 mRNA, relative abundance
Time at 37°C: (min) 0 30 60 90 0 30 60 90 0 30 60 90 0 30 60 90
WT sec12-1 sec14-3 sec1-1
C
lane 1 2 3 4 5 6 7 8 9 10 11 12 13 14 15 16 17 18 19 20
HAC1u
HAC1i
ACT1
Splicing: (%) 0 20 13 6 4 38 29 32 10 15 7 2 0 0 0 2 2 3 4 3
HAC1 mRNA, relative abundance
Time at 37°C: (min) 0 30 60 90 0 30 60 90 0 30 60 90 0 30 60 90 0 30 60 90
WT sec14-3 sec61-101 sec62-101 sec63-201

Figure 2-2: *HAC1* mRNA Induction Requires a Bipartite Signal and Is IRE1-Independent.

(A) Determination of *HAC1* mRNA abundance during ER stress and temperature shift. WT cells were grown at 23 °C and shifted to 37 °C (lanes 1–4 and 9–12) or kept constant at 30 °C (lanes 5–8). DTT was added as indicated (lanes 5–8 and 9–12).

(B) Determination of *HAC1* mRNA abundance during ER stress and inositol deprivation. WT cells were grown at 30 °C in synthetic medium supplemented with inositol and shifted to synthetic medium lacking inositol (lanes 1–4 and 9–12), or continuously grown in medium supplemented with inositol (lanes 5–8). Tunicamycin was added to a final concentration of 1 μg/ml as indicated (lanes 5–8 and 9–12).

(C) Distinction between heat shock response and *HAC1*-mRNA-inducing conditions. WT (lanes 1–4 and 9–12) and HSF1c (lanes 5–8) strains were grown at 23 °C and shifted to 37 °C (lanes 1–4 and 5–8) or continuously grown at 37 °C (lanes 9–12), and DTT added as indicated.

(D) Analysis of IRE1 pathway for a role in *HAC1* mRNA induction. Δ*ire1* cells were grown at 23 °C and shifted to 37 °C (lanes 1–4 and 9–12) or continuously grown at 30 °C (lanes 5–8), and DTT was added as indicated (lanes 5–8 and 9–12). Note that in Δ*ire1* cells, *HAC1* mRNA is modestly induced in response to DTT alone (lanes 5–8). This observation is indicative of feedback regulation, whereby a block in the UPR induces the I/T signal.

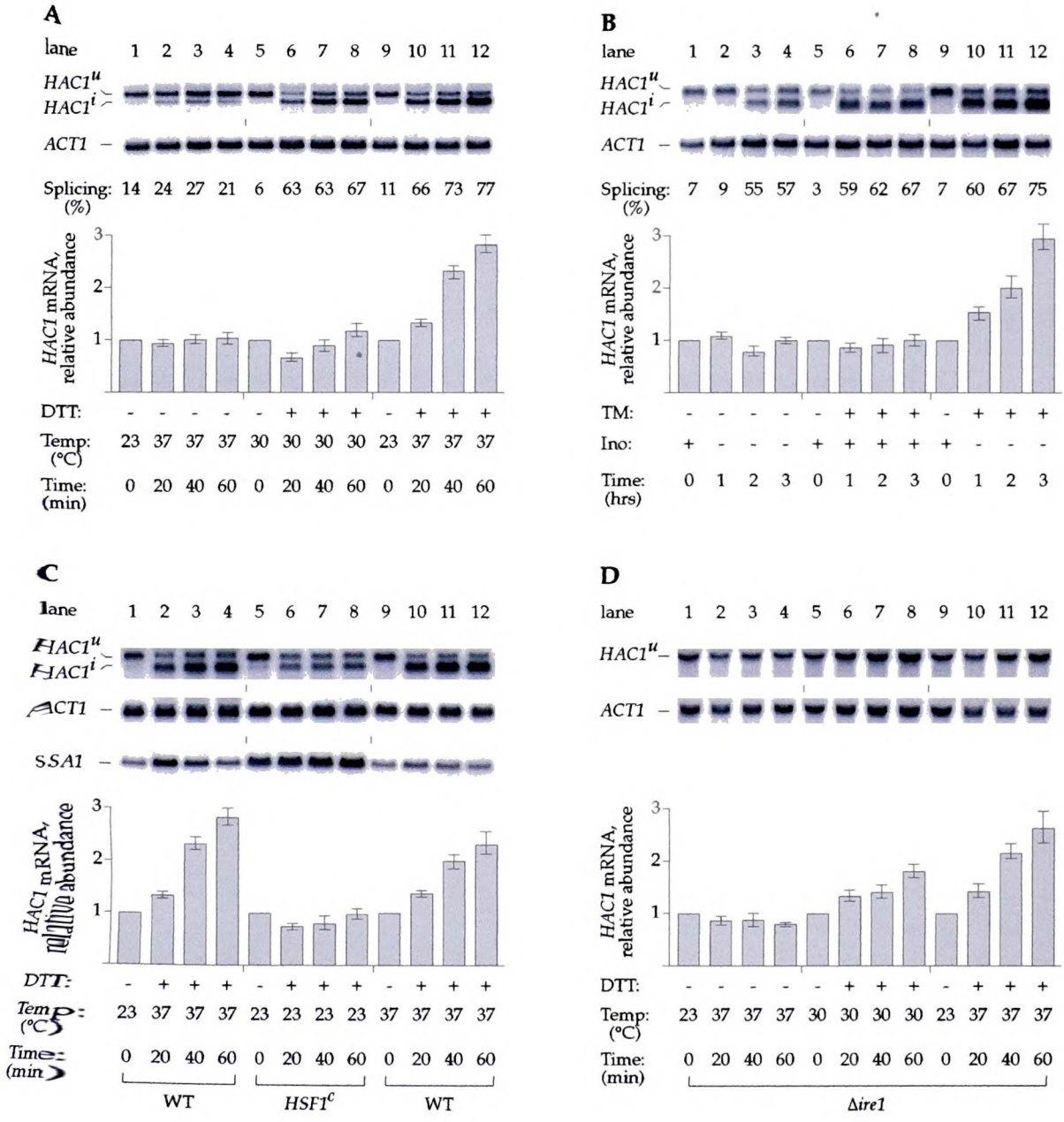
A
lane 1 2 3 4 5 6 7 8 9 10 11 12
HAC1u
HAC1i
ACT1
Splicing: (%) 14 24 27 21 6 63 63 67 11 66 73 77
HAC1 mRNA, relative abundance
DTT: - - - - - + + + - + + +
Temp: (°C) 23 37 37 37 30 30 30 30 23 37 37 37
Time: (min) 0 20 40 60 0 20 40 60 0 20 40 60
B
lane 1 2 3 4 5 6 7 8 9 10 11 12
HAC1u
HAC1i
ACT1
Splicing: (%) 7 9 55 57 3 59 62 67 7 60 67 75
HAC1 mRNA, relative abundance
TM: - - - - - + + + - + + +
Ino: + - - - + + + + + - - -
Time: (hrs) 0 1 2 3 0 1 2 3 0 1 2 3
C
lane 1 2 3 4 5 6 7 8 9 10 11 12
HAC1u
HAC1i
ACT1
SSA1
HAC1 mRNA, relative abundance
DTT: - + + + - + + + - + + +
Temp: (°C) 23 37 37 37 23 23 23 23 37 37 37 37
Time: (min) 0 20 40 60 0 20 40 60 0 20 40 60
WT
HSF1c
WT
D
lane 1 2 3 4 5 6 7 8 9 10 11 12
HAC1u
ACT1
HAC1 mRNA, relative abundance
DTT: - - - - - + + + - + + +
Temp: (°C) 23 37 37 37 30 30 30 30 23 37 37 37
Time: (min) 0 20 40 60 0 20 40 60 0 20 40 60
Δire1

Figure 2-3: Activation of the *HAC1* Promoter Controls Increase in *HAC1* mRNA Abundance.

(A) Analysis of *HAC1* promoter activity during bipartite stress conditions. *Δhac1* cells containing either a construct restoring *HAC1* expression (lanes 1–4) or a construct expressing *GFP* driven by the *HAC1* promoter (lanes 5–8) were grown at 23 °C and shifted to 37 °C concurrent with addition of DTT as indicated.

(B) Determination of mRNA half-life during *HAC1*-mRNA-inducing conditions. polIIts cells were grown at 23 °C and were shifted to 37 °C either in the absence (open symbols) or presence (filled symbols) of DTT. *HAC1* mRNA abundance (squares) and *ACT1* mRNA abundance (circles) are normalized to the abundance of the PolIII transcript *SCR1*.

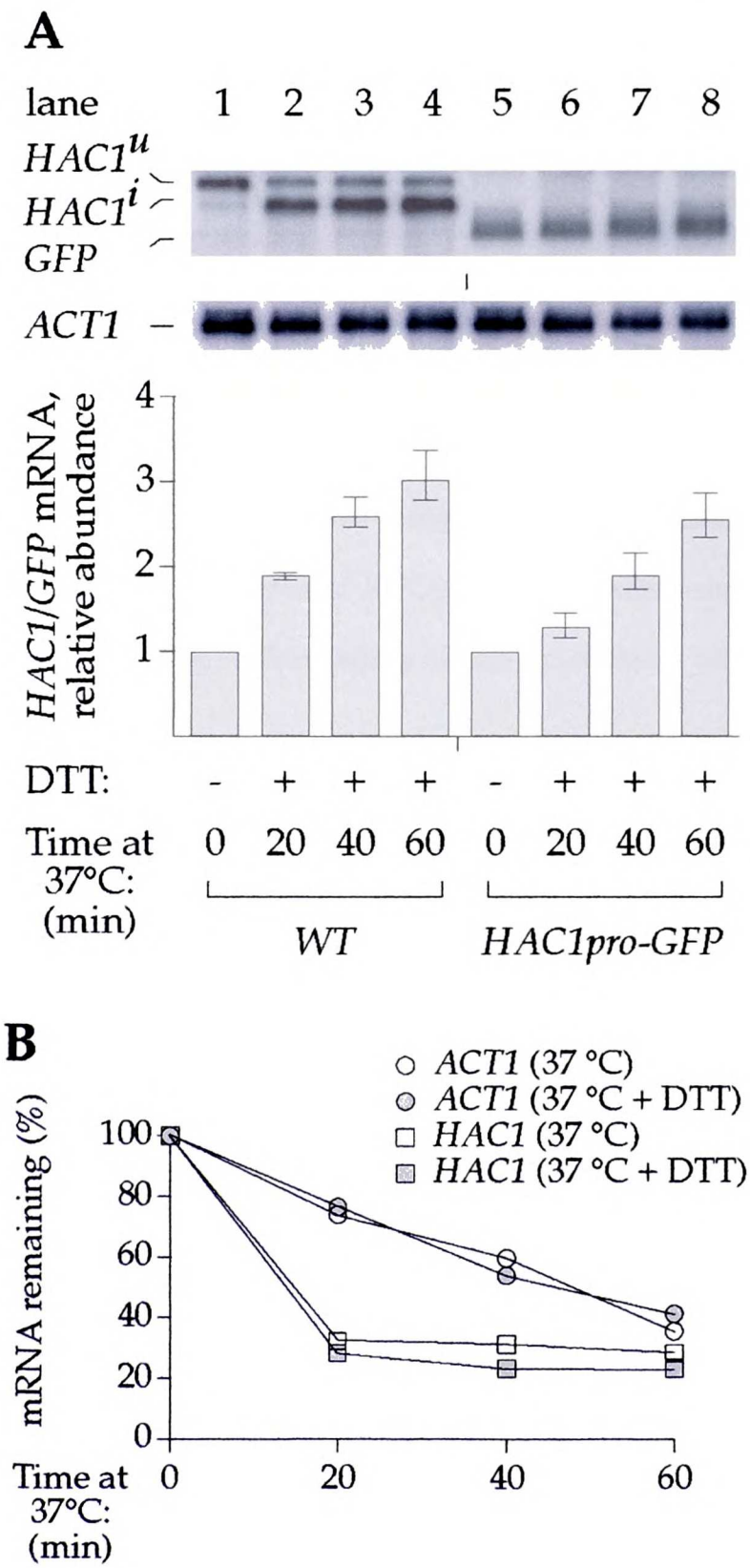
A
lane 1 2 3 4 5 6 7 8
HAC1u
HAC1i
GFP
ACT1
HAC1/GFP mRNA, relative abundance
4
3
2
1
DTT: - + + + - + + +
Time at 37°C: (min) 0 20 40 60 0 20 40 60
WT
HAC1pro-GFP
B
ACT1 (37 °C)
ACT1 (37 °C + DTT)
HAC1 (37 °C)
HAC1 (37 °C + DTT)
mRNA remaining (%)
100
80
60
40
20
0
Time at 37°C: (min) 0 20 40 60

Figure 2-4: *HAC1* Promoter Regulation Is Required to Survive Stress.

(A) Determination of Hac1p levels during either ER stress alone or during both ER stress and temperature shift. WT cells were either grown at 30 °C and treated with DTT (lanes 1–4) or grown at 23 °C and simultaneously shifted to 37 °C and treated with DTT (lanes 5–8). Protein lysates were prepared, and protein levels were analyzed by Western blot analysis. The relative Hac1p/Pgk1p ratio is normalized to the DTT-treated sample (lane 4).

(B) Characterization of *HAC1* expression in strain used to approximate basal *HAC1* expression. Cells expressing *HAC1* from the endogenous promoter (lanes 1–4) or the *ADH1* promoter (lanes 5–8) were grown at 30 °C in synthetic medium supplemented with inositol and shifted to synthetic medium lacking inositol simultaneous with the addition of tunicamycin.

(C) Reduced viability of strains unable to express *HAC1* at elevated levels. The strains described in (B) were plated in serial dilutions (left to right) on synthetic medium lacking inositol ("-ino") and synthetic medium lacking inositol and containing tunicamycin ("-ino +TM").

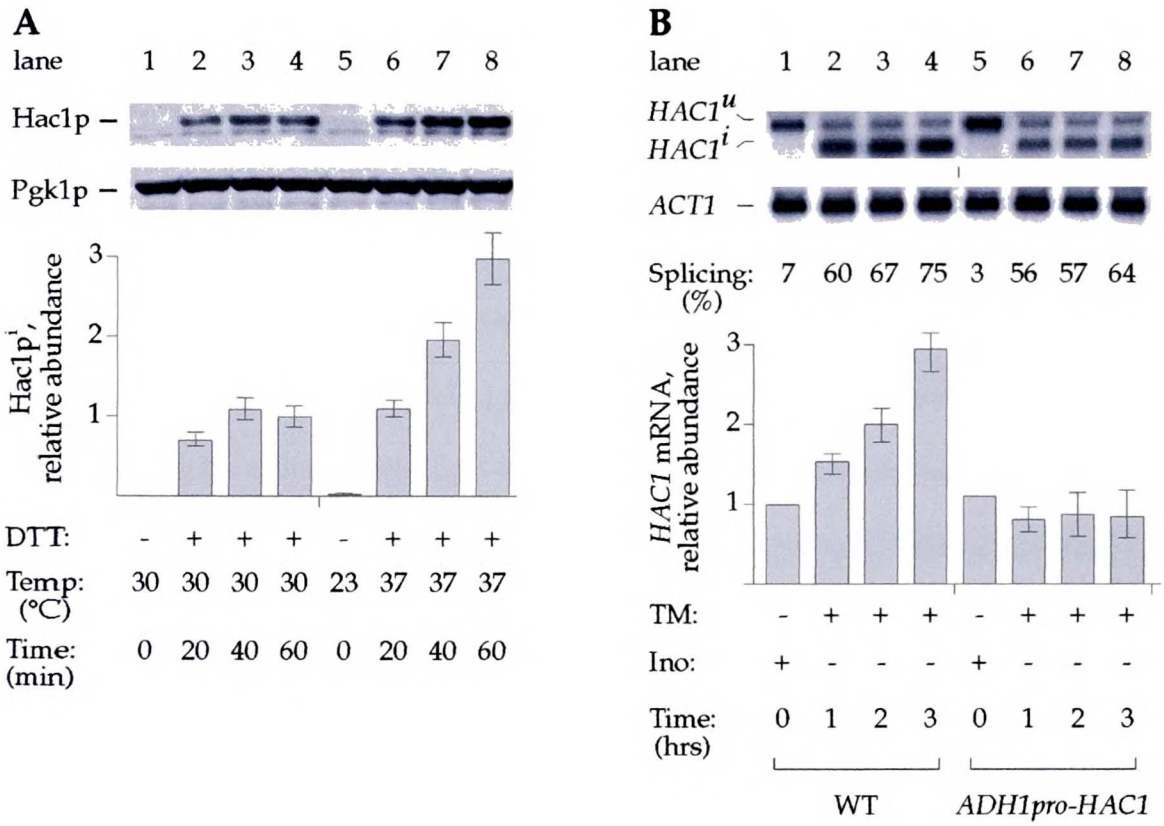
A
lane 1 2 3 4 5 6 7 8
Hac1p –
Pgk1p –
Hac1p^{i}, relative abundance
3
2
1
DTT: - + + + - + + +
Temp: (°C) 30 30 30 30 23 37 37 37
Time: (min) 0 20 40 60 0 20 40 60
B
lane 1 2 3 4 5 6 7 8
HAC1^{u}
HAC1^{i}
ACT1 –
Splicing: (%) 7 60 67 75 3 56 57 64
HAC1 mRNA, relative abundance
3
2
1
TM: - + + + - + + +
Ino: + - - - + - - -
Time: (hrs) 0 1 2 3 0 1 2 3
WT
ADH1pro-HAC1

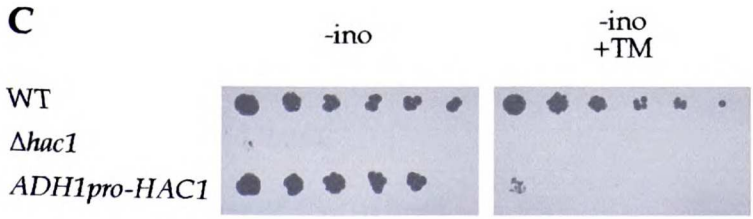
C
-ino
-ino +TM
WT
Δhac1
ADH1pro-HAC1

Figure 2-5: Differential UPR Target Gene Induction by Elevated Hac1p Levels.

(A) Comparison of UPR target gene induction under either UPR or S-UPR conditions. Whole-genome mRNA expression analysis was carried out on WT cells harvested after 60 min of treatment, either grown at 30 °C and treated with 6 mM DTT (x-axis), or grown at 23 °C and simultaneously shifted to 37 °C and treated with 6 mM DTT (y-axis). Fold changes in gene expression are in reference to the untreated (t = 0) samples. Shown are only those genes designated as targets of the UPR (see Materials and Methods). The dashed diagonal line represents equal induction under both conditions.

(B) Comparison of UPR target gene induction under either UPR or S-UPR conditions (alternate display). The data from (A) were analyzed to generate a ratio (x-axis) for each gene, dividing the induction during S-UPR-inducing conditions by the induction during UPR-inducing conditions, with target genes of similar ratio grouped together (y-axis).

(C) Characterization of *HAC1* expression in a strain constitutively expressing *HAC1* at high levels. Cells expressing *HAC1* from the endogenous promoter (WT; lanes 1 and 2), or a modified promoter constitutively expressing *HAC1* at high levels (*HAC1*proHI; lanes 3 and 4) were treated with 6 mM DTT for 60 min. Although the basal transcription of *HAC1*proHI is elevated, the promoter is still capable of further induction during the S-UPR (unpublished data).

(D) Determination of Hac1p level in a strain constitutively expressing *HAC1* at high levels. Protein lysates were prepared from the strains described in (C), and protein levels were analyzed by Western blot analysis. The relative Hac1p/Pgk1p ratio is normalized to the WT DTT-treated (t = 60) sample from Figure 4A.

(E) Transcriptional response of different classes of UPR targets to high levels of Hac1p. Whole-genome mRNA expression analysis was carried on *HAC1*proHI and WT cells treated with 6 mM DTT and harvested after 60 min. For the genes in each of the three classes of UPR targets defined in (B), a ratio (x-axis) is calculated by dividing the fold induction in DTT-treated *HAC1*proHI cells by the fold induction in DTT-treated WT cells. This ratio is plotted against the number of genes with a similar ratio (y-axis). The Class 2 target *YFR026C* (asterisk), which is DTT-induced approximately 10-fold more in *HAC1*proHI than in WT cells, is of unknown function. a, *DER1*; b, *INO1*; c, *YOR289W*; d, *YHR087W*.

(F) Transcriptional response of different classes of UPR targets to UMF. Whole-genome mRNA expression analysis was carried on *ADH1pro-HAC1* cells grown at 23 °C and simultaneously shifted to 37 °C and treated with 6 mM DTT, and WT cells treated with 6 mM DTT, both harvested after 60 min. For the genes in each of the three classes of UPR targets defined in (B), a ratio (x-axis) is calculated by dividing the fold induction in ADH1pro-*HAC1* cells under S-UPR-inducing conditions by the fold induction in WT cells under UPR-inducing conditions. This ratio is plotted against the number of genes with a similar ratio (y-axis). a, *DER1*; b, *INO1*; c, *YOR289W*; d, *YHR087W*.

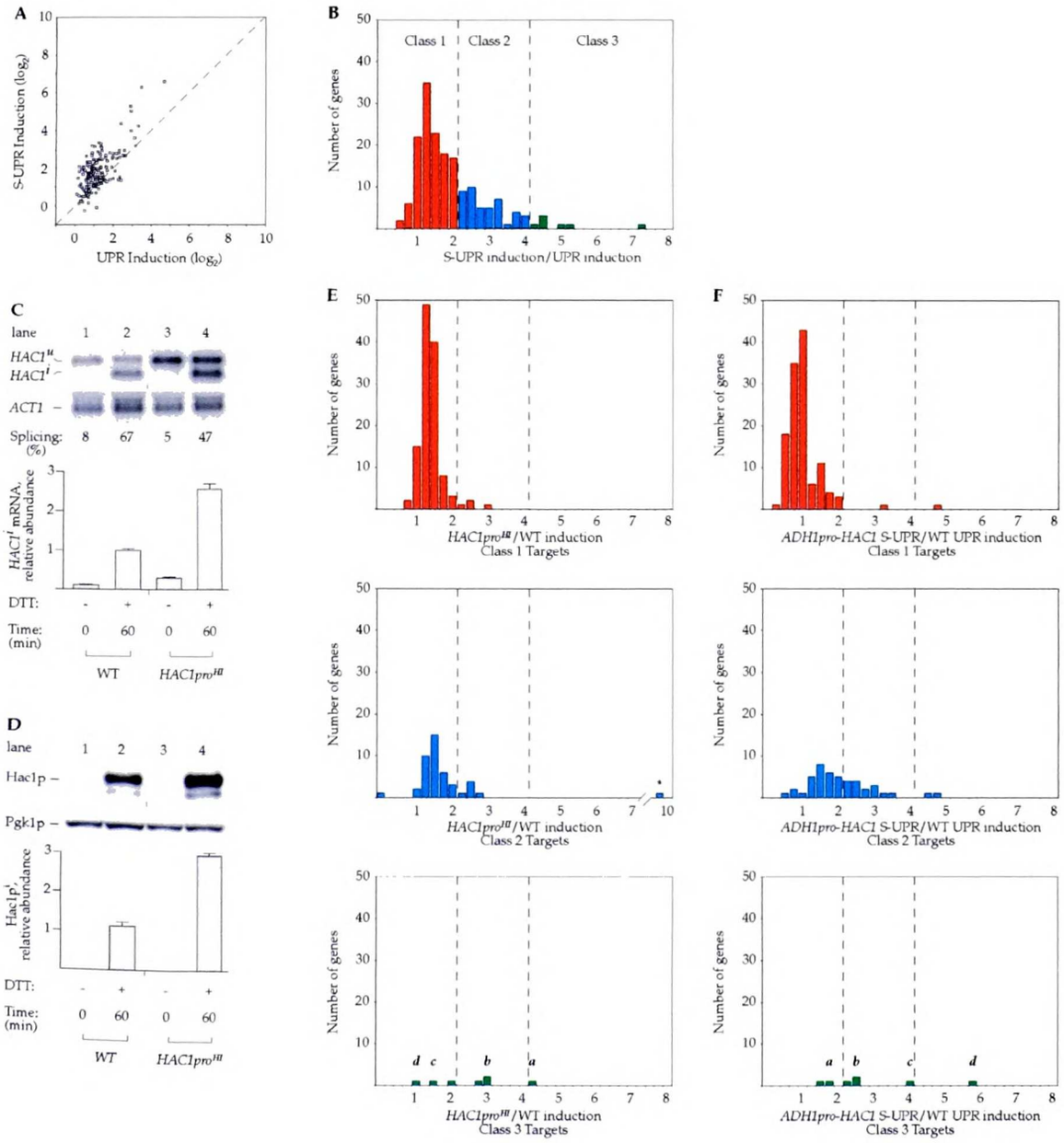
A
S-UPR Induction (log2)
UPR Induction (log2)
B
Class 1
Class 2
Class 3
Number of genes
S-UPR induction/UPR induction
C
lane 1 2 3 4
HAC1u
HAC1i
ACT1
Splicing: (%) 8 67 5 47
HAC1i mRNA, relative abundance
DTT: - + - +
Time: (min) 0 60 0 60
WT
HAC1proIR
D
lane 1 2 3 4
Hac1p
Pgk1p
Hac1p, relative abundance
DTT: - + - +
Time: (min) 0 60 0 60
WT
HAC1proIR
E
Number of genes
HAC1proIR/WT induction
Class 1 Targets
HAC1proIR/WT induction
Class 2 Targets
HAC1proIR/WT induction
Class 3 Targets
d c b a
F
Number of genes
ADH1pro-HAC1 S-UPR/WT UPR induction
Class 1 Targets
ADH1pro-HAC1 S-UPR/WT UPR induction
Class 2 Targets
ADH1pro-HAC1 S-UPR/WT UPR induction
Class 3 Targets
a b c d

Figure 2-6: A Schematic of the Circuitry of the UPR.

The model depicts the circuitry of the UPR (red) and the S-UPR (blue). Transcriptional control of *HAC1* is indicated by an icon representing a rheostat affording gain control of the UPR; Ire1p-dependent *HAC1u* mRNA splicing is indicated by an icon representing an on/off switch. The I/T and UP signals in the S-UPR are integrated by an AND gate (semicircle, top right), i.e., both conditions must be met to propagate the S-UPR signal. The putative UMF may collaborate with Hac1p to control transcription of UPR target genes (shown) and also be involved in regulating *HAC1* transcription (not shown); alternatively, different factors may be involved. The collaboration of Hac1p and UMF is indicated by the diamond-shaped icon, which integrates the information coming from both Hac1p and UMF concentration and activity.

Figure 2-6 *Leber et al. (2004)*

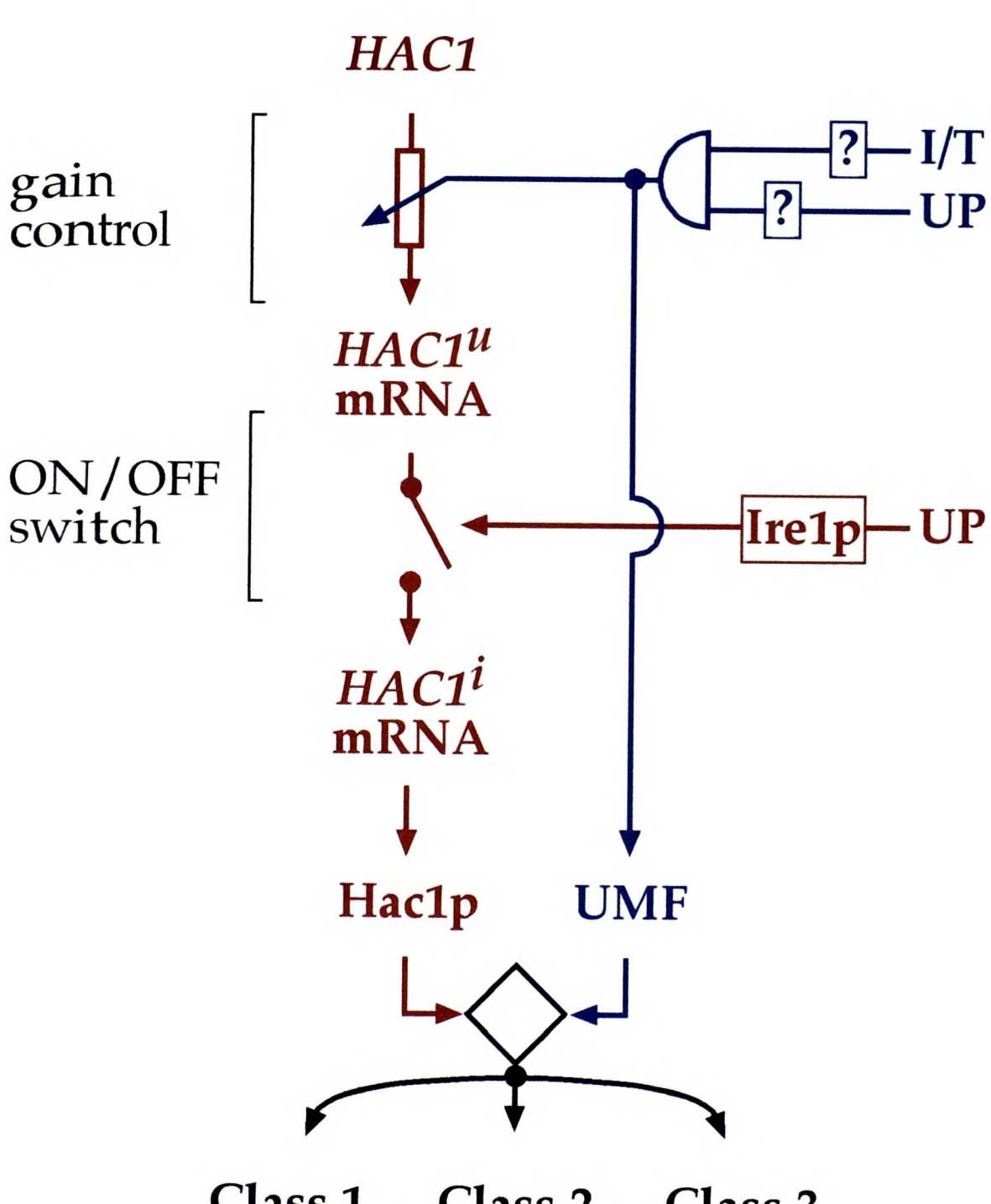

Chapter 3

Autophagy Counterbalances Endoplasmic Reticulum Expansion during the Unfolded Protein Response

Autophagy Counterbalances Endoplasmic Reticulum Expansion during the Unfolded Protein Response

Sebastián Bernales[1,2]*, Kent L. McDonald[3], Peter Walter[1,2]

[1]Howard Hughes Medical Institute, University of California San Francisco, San Francisco, California, United States of America, [2]Department of Biochemistry and Biophysics, School of Medicine, University of California San Francisco, San Francisco, California, United States of America, [3]Electron Microscope Laboratory, University of California Berkeley, California, United States of America

* Corresponding author

phone: (415) 476-5676

fax: (415) 476-5233

email: sebastian.bernales@ucsf.edu

SUMMARY

The protein folding capacity of the endoplasmic reticulum (ER) is regulated by the unfolded protein response (UPR). The UPR senses unfolded proteins in the ER lumen and transmits that information to the cell nucleus, where it drives a transcriptional program that is tailored to re-establish homeostasis. Using thin section electron microscopy, we found that yeast cells expand their ER volume at least 5-fold under UPR-inducing conditions. Surprisingly, we discovered that ER proliferation is accompanied by the formation of autophagosome-like structures that are densely and selectively packed with membrane stacks derived from the UPR-expanded ER. In analogy to pexophagy and mitophagy, which are autophagic processes that selectively sequester and degrade peroxisomes and mitochondria, the ER-specific autophagic process described utilizes several autophagy genes: they are induced by the UPR and are essential for the survival of cells subjected to severe ER stress. Intriguingly, cell survival does not require vacuolar proteases, indicating that ER sequestration into autophagosome-like structures, rather than their degradation, is the important step. Selective ER sequestration may help cells to maintain a new steady-state level of ER abundance even in the face of continuously accumulating unfolded proteins.

INTRODUCTION

Secretory proteins and most integral membrane proteins enter the secretory pathway at the endoplasmic reticulum (ER) [1], where they fold and, if appropriate, become covalently modified and assembled into higher order complexes. ER-resident chaperones and other modifying enzymes assist as proteins achieve their active, three-dimensional conformation. Only properly folded and assembled proteins are allowed to leave the ER, thus providing exquisite quality control to ensure fidelity of plasma membrane and secreted proteins through which cells communicate with their environment [2]. This process is regulated at multiple levels to ensure that ER folding capacity is sufficient and adjusted appropriately according to need, i.e., that ER homeostasis is maintained. Cells regulate, for example, the amount of protein translocated into the ER, the concentration of chaperones and other ER enzymes, the abundance of the ER membrane system, and the degradation of unfolded proteins [3–5].

At the center of this regulation is a phylogenetically conserved ER-to-nucleus signaling pathway–called the unfolded protein response (UPR)–that adjusts ER abundance in response to the accumulation of unfolded proteins [6]. Unfolded proteins result when protein folding demand exceeds the protein folding capacity of the ER. The ER-resident transmembrane kinase/endoribonuclease Ire1 is a primary sensor for unfolded proteins in the ER [7–9]. It transmits this information to the cytosol by activating its endoribonuclease domain, which initiates an unconventional mRNA splicing reaction [10–13]. Splicing removes a short intron from a single mRNA species, *HAC1*, allowing the production of an active transcription activator Hac1i [13,14] (or its

metazoan ortholog XBP1 [15–17]). Hac1i (or XBP1) then transcriptionally activates a vast set of UPR target genes that in yeast represents more than 5% of the genome [18]. Induction of the UPR target genes increases the biosynthesis of chaperones and modifying enzymes needed to fold proteins, as well as factors involved in transport through the secretory pathway, ER-associated protein degradation (ERAD), and phospholipids biosynthesis. The UPR therefore drives a comprehensive program that adjusts the cell's capacity to fold, process, and secrete proteins.

In metazoan cells, the regulation of the UPR is more complicated; at least three mechanistically distinct pathways (Ire1, ATF6, and Perk) operate in parallel to sense unfolded proteins in the ER. Each activates distinct transcription factors that collaborate to trigger a continuum of transcriptional programs in a tissue-specific manner [6]. Among other genes, the ATF6 pathway increases transcription of *XBP1* mRNA [19–23], therefore more of the transcription factor XBP1 is produced upon splicing of its mRNA by Ire1. A similar information network affording "gain control" to the UPR is observed in yeast: the concentration of the *HAC1* mRNA increases 3- to 4-fold when yeast cells are subjected to particularly severe ER stress conditions [24]. This new state, called Super-UPR (S-UPR), allows cells to synthesize more Hac1 protein, yielding a qualitatively different transcriptional output. The up-regulation of the *HAC1* mRNA during S-UPR conditions is necessary for cell survival. The molecular machinery that senses the S-UPR signal and transmits it across the ER membrane is not yet known, but it is clear that it does not require Ire1 [24].

The set of UPR targets includes key players in ERAD [25,26]. ERAD mediates the retro-translocation of unfolded proteins from the ER lumen into the cytosol for

degradation by the proteasome. In this way, ERAD complements other UPR targets—such as chaperones and protein-modifying enzymes, whose up-regulation positively facilitates protein folding—by removing hopelessly misfolded proteins from the ER. Proteins entering the ERAD pathway, however, have to traverse the membrane in reverse and presumably do so as an unfolded chain through a protein translocation channel in the membrane. Severely misfolded proteins and protein aggregates might be difficult to unravel and degrade by this mechanism.

An alternative pathway that targets proteins for degradation is autophagy. Autophagy describes a collection of pathways by which sections of the cytoplasm, including its organelles, can become sequestered into membrane-bounded compartments that then fuse with the vacuole (or lysosomes), where their content is degraded by acid hydrolases [27]. In this way, whole organelles can be degraded, regardless of their size or the folding state of their constituent proteins. Many of the components that mediate autophagy have been identified [28–31] and extensively characterized.

Autophagy pathways differ in their selectivity. Macro-autophagy, for example, is induced by starvation and serves to encapsulate and degrade non-selectively large portions of the cytosol [32] and organelles suspended in it, including mitochondria [33] and segments of the ER [34]. This provides cells with badly needed nutrients in the form of metabolites derived from digested proteins and macromolecular structures (auto-cannibalism) [35]. How particular regions of the cytoplasm are chosen to become enclosed in autophagosomes is unknown, as is the origin of the double membrane structure that sequesters them. However, it has been shown that the early secretory pathway contributes to the assembly of autophagosomes [36–38]. By contrast to macro-

autophagy, pexophagy and mitophagy are highly selective processes that degrade an excess of peroxisomes and mitochondria, respectively, under growth conditions that change the requirement for these organelles [39,40]. It has been proposed that marker proteins are selectively displayed on no longer needed or damaged organelles, and direct their sequestration. Most of the components that mediate degradative autophagy are also shared by the biosynthetic cytoplasm-to-vacuole targeting (Cvt) pathway [41–43], which operates constitutively to deliver a subset of content proteins to the vacuole during their biosynthesis [44]. The degradative autophagy and biosynthetic Cvt pathways are morphologically and topologically similar and share many components.

Here, we describe an unexpected link between the UPR and autophagy. We show that under UPR-inducing conditions, ER membranes become selectively sequestered in autophagosome-like structures, utilizing components shared with other autophagic processes. We discuss how this ER-selective branch of autophagy, or ER-phagy for short, and the UPR might be physiologically linked during UPR-induced ER proliferation.

RESULTS

The ER Expands during Induction of the UPR

To ask whether activation of the UPR alters ER structure or abundance, we examined cell thin sections by electron microscopy (EM). To this end, we collected exponentially growing wild-type cells treated with dithiothreitol (DTT) to induce the UPR, and compared them to untreated cells. As shown in Figure 1, the majority of the ER was found at the periphery of the cell (Figure 1A, ER, traced in magenta) or forming the nuclear envelope (Figure 1A, NE, traced in blue).

Even a cursory glance at the images revealed that a massive expansion of the ER occurred after UPR induction. To quantify this effect over time, we measured the cumulative length of the ER in individual EM sections and normalized the results to the area of the cell. As shown in Figure 1B (magenta bars), by this metric, the amount of ER increased more than 3-fold over a 3-h time course after addition of DTT. By contrast, the amount of NE remained constant (Figure 1B, blue bars), indicating that the nuclear volume remained unchanged—thereby serving as a convenient internal control. Proliferation of the ER was rapid, doubling 40 min after the addition of DTT.

To determine whether the observed morphological changes were a direct consequence of the induction of the UPR, we activated the UPR transcriptional program downstream of Ire1 without misfolding proteins in the ER. To this end, we expressed the spliced form of the *HAC1* mRNA (*HAC1i* mRNA, for induced) from a regulated glucocorticoid receptor-activated promoter. We induced *HAC1i* mRNA in *hac1* Δ cells

by addition of deoxycorticosterone (DOC), which binds to the glucocorticoid receptor expressed in these cells and activates it [18]. The amount of ER expansion during *HAC1i* mRNA expression was similar to the increase observed during DTT treatment, indicating that activation of the UPR by Hac1 is sufficient to induce the observed ER proliferation (Figure 1C).

In addition to ER proliferation during the UPR, we observed that the continuity of the ER membrane system increased significantly within a section (Figure 2A). In sequential 70 nm–thick serial sections, short stretches of ER appeared and disappeared in control cells, whereas we could trace a continuous ER over many sections in UPR-induced cells (Figure 2B). This observation suggests a change from predominantly tubules or very small sheets in control cells, to expansive sheets in UPR-induced cells. The expansion of the ER measured in Figure 1B, therefore, is likely an underestimation of both membrane area and organelle volume. Moreover, we observed that the spacing between ER membranes was significantly increased in the expanded UPR-induced ER (Figure 2C; ER membrane distance = 31 ± 5 nm in control cells versus 48 ± 6 nm in UPR-induced cells). We observed this effect qualitatively in fixed permanganate-stained sections, but performed a more accurate distance measurement between ER membranes in flash-frozen/freeze-substituted sections to minimize the chance of specimen distortion [45]. Thus, even without considering the altered geometry of a possible tubule-to-sheet transition, ER volume expands about 5-fold upon UPR induction (3.3-fold expansion of length × 1.5-fold expansion of width).

Autophagosome-Like Structures Form in a Subset of UPR-Induced Cells

Unexpectedly, we observed that a fraction of UPR-induced cells accumulated large amounts of double membrane–bounded, autophagosome-like structures packed with tightly stacked membrane cisternae (Figure 3A and 3B). We show below that, the content membranes are derived from the ER, and henceforth refer to these structures as ER-containing autophagosomes, or ERAs. ERAs were present in more than 20% of the cells 3 h after the UPR-induction. Significantly, none of the cells in the population containing ERAs had proliferated ER. ERAs show characteristic features of autophagosomes: they are surrounded by a double membrane (Figure 3C) and have similar sizes (300 to 700 nm) [46,47]. Frequently, the delimiting outer membranes connected to tubular or single sheet extensions (Figure 3A and 3D, arrow). To determine if ERAs are derived from the ER, we examined flash-frozen/freeze-substituted sections stained with osmium. In these samples, we found that the outer membrane of ERAs and the extensions were densely studded with ribosomes, suggesting that these membranes are indeed derived from ER (Figure 3E).

The common specimen preparation technique used in Figure 3E does not allow to visualize membranes adequately. While trying to optimize the procedure, we found that inclusion of 3% water during the osmium fixation/substitution step vastly improved membrane visualization in the images, as previously reported [48]. Representative images obtained with this improved technique are shown Figure 3F and 3G, which strongly reinforces the notion that the delimiting membrane of ERAs is continuous with ribosome-studded ER membranes. In the image shown, the continuity of the bilayer can be traced

neatly through the junction where the membrane extension meets up with an ERA. Figure 3G show a cross section through an ERA, with clearly visible content of membrane stacks. Note that the sequestered membranes are ribosome-free where they are tightly stacked, but contain membrane-bound ribosomes in regions where they are less tightly apposed.

Examination of the ER at a 3-h time point after UPR induction by fluorescent microscopy in cells expressing a Sec61-cherry fusion protein [49] revealed proliferated ER in 80% of the cells (Figure 4A, +DTT, bottom row), in agreement with the EM images shown in Figure 1. By contrast, 20% of the cells showed multiple distinct and intensely fluorescent cytoplasmic bodies (Figure 4B, arrows). Their abundance per cell, their appearance at late (3 h) but not early (90 min) time points after UPR induction, the penetrance of their appearance in 20% of the cells in the population, and their appearance in cells that lack expanded ER are each consistent with the notion that these structures correspond to the ERAs observed by electron microscopy.

To obtain further evidence that the membrane stacks observed in ERAs in the EM images are indeed derived from the ER, we prepared EM images for staining with immunogold, using antibodies directed against an epitope tag of an ER resident protein Sec63 (Figure 5). We obtained selective labeling of clearly identifiable ER structures (Figure 5A and 5B), as well as selective labeling of ERAs (Figure 5C). Quantitation of gold particles per area revealed a signal-to-noise ratio of approximately 7:1 when we compared ERA and nucleoplasm (Figure 5D; in cell sections, the nucleoplasm showed the highest density of background staining). In addition, we found that the density of gold particles over ERA regions closely matched the value predicted from the amount of ER

membrane packaged in them (Figure 5C). To reach this conclusion, we determined the density of ER membranes in ERAs from EM sections such as shown in Figure 3B (ER length per area) and the density of gold particles along stretches of cytoplasmic ER in immunogold-stained sections such as shown in Figure 5B.

Taken together, the data presented so far suggest that after UPR induction, the ER proliferates significantly. At later time points after induction, some cells in the population reduce their ER back to uninduced levels, and the striking images shown in Figure 3 suggest that this occurs by sequestering ER membranes into ERAs. Interestingly, Hac1i induction, described in Figure 1C, from the DOC-induced reporter construct led to ER proliferation, but by itself was insufficient to induce ERA formation. Since Hac1i is the only known component relaying Ire1 signaling in yeast [50,51], a Hac1- and Ire1-independent second signal must originate from the ER lumen and be required for ERA formation.

As ERAs structurally resemble autophagosomes, we next sought to determine if there is a functional connection between the UPR-induced ER proliferation and autophagy. To this end, we used Atg8, one of the early mediators of autophagosome formation, as a marker [52,53]. ATG8 is transcriptionally up-regulated when autophagy is induced, e.g., by nitrogen starvation. Atg8 is a cytosolic protein that becomes lipidated [54,55] and accumulates in pre-autophagosomal structures (PASs) that are in close proximity to the vacuole and can be visualized as dots by fluorescent microscopy in cells expressing green fluorescent protein (GFP)-Atg8 fusion proteins [56–58]. PASs are thought to act as nucleation sites for the formation of autophagosomes, which then fuse with the vacuole where its membranes and internal content are degraded. Because Atg8

(as well as GFP-Atg8) is incorporated into the autophagosomes and subsequently deposited into vacuoles when fusion occurs, GFP-Atg8 has been used as a marker for vacuolar processing: when autophagosomes are delivered to the vacuole, proteolytic cleavage leads to the release of the GFP moiety, which is relatively long lived and hence can be detected as a discrete fragment [59,60]. The data in Figure 6A show that macroautophagy induced by nitrogen starvation leads to a large induction of GFP-Atg8 (compare lanes 1 and 4), about half of which was proteolyzed to GFP at the time point analyzed (Figure 1, lane 4). Proteolysis was no longer observed in *vps4 Δ pep4 Δ* cells lacking vacuolar proteases (Figure 6D, lane 8). Under nitrogen starvation, no Hac1 was produced (Figure 6A, lower panel), consistent with previous observations that these conditions do not induce the UPR [61].

Similarly, when cells were treated with the UPR-inducing agents DTT or tunicamycin, GFP-Atg8 was strongly induced (Figure 6A). By contrast to Atg8 induction by nitrogen starvation, however, we observed no cleavage of the GFP domain (Figure 6A), even after prolonged incubation of the exponentially growing cells in the presence of the drugs (unpublished data). These surprising results show that the fate of GFP-Atg8—and by inference that of Atg8—is different in UPR-induced and nitrogen-starved cells. When we compared GFP-Atg8 in UPR-induced and nitrogen-starved cells by fluorescence microscopy, we detected a significantly larger number of PASs in UPR-induced cells (Figure 6B).

Expression of *HAC1i* mRNA from the glucocorticoid-induced promoter was sufficient to up-regulate GFP-Atg8 (Figure 6C), indicating that DTT and tunicamycin can exert their effects on Atg8 transcription through classical UPR signaling mediated by Ire1

and Hac1. This result was surprising because previous profiling of the total transcriptional scope of the UPR did not identify ATG8 as a UPR target gene [18]. The paradox is resolved by the data shown in Figure 6D, which demonstrate that, although Hac1i is sufficient to induce Atg8, it is not necessary: Atg8 is strongly induced by DTT and tunicamycin even in *hac1 Δ* and *ire1 Δ* cells. Our previous study [18] applied stringent filters that required that transcriptional activation of any gene classified as a UPR target gene be Hac1 and Ire1 dependent. *ATG8*, as well as other DTT- and tunicamycin-induced autophagy genes, *ATG5, ATG7*, and *ATG19* [18], were therefore not included in the definition as UPR target genes.

GFP-Atg8 Localizes in Proximity to ERAs and Facilitates Cell Survival under ER Stress

To determine if ERAs co-localize with GFP-Atg8-staining structures (PASs), we double-labeled cells by co-expressing GFP-Atg8 and Sec61-cherry. Consistent with previous reports [62], we found only a few PASs in uninduced cells (approximately one spot in every 3–4 cells), presumably reflecting a low constitutive rate of autophagy in normally growing cells or the role of PASs in the Cvt pathway. This picture was unchanged at early time points after UPR induction. By contrast, 3 h after UPR-induction, we observed a vast proliferation of PASs (6 ± 2 spots per cell). PASs seemed to be randomly localized in most cells, but upon staining of internal cell membranes with the lipophilic dye FM4–64, were always seen in close juxtaposition to vacuoles or other FM4–64–staining structures (unpublished data), as well as to ERAs in the population of cells that have them

(Figure 7). The juxtaposition suggests that PASs may be involved in nucleating ERAs, although they do not co-localize with them. Importantly and in strong support of the notion that Atg8 has a role in ERA formation, we detected no ERAs by EM or by fluorescence microscopy in *atg8 Δ* cells.

Given the possible link between autophagy and the UPR, we next asked whether the ability to induce autophagy would give cells a growth advantage under conditions of ER stress. We found that *ATG8* as well as five other autophagy genes tested (*ATG1*, *ATG9, ATG16, ATG20* (Figure 8), and *ATG19* [unpublished data] [63–66]) are each required for cell growth under strong UPR-inducing conditions: similar to *hac1 Δ* cells, atg8 Δ cells did not grow when plated on media containing 1-mg/ml tunicamycin (Figure 8, right panel). In contrast to *hac1 Δ* cells, the autophagy mutants showed no growth defect under less stringent conditions (0.2-mg/ml tunicamycin; Figure 8, middle panel). These results demonstrate a physiologically important relationship between the UPR and autophagy: autophagy augments the UPR to help cells deal with life-threatening consequences of ER stress.

Intriguingly, cell survival under stringent UPR conditions is not dependent on vacuolar proteases: a *vps4 Δ pep4 Δ* strain showed significant growth even on 1-mg/ml tunicamycin plates (Figure 8, right panel, bottom row). This result is particularly remarkable as this strain is already growth impaired even under normal growth conditions (Figure 8, left panel, bottom row).

DISCUSSION

The vast scope of the transcriptional profile of UPR target genes previously suggested that the UPR leads to a comprehensive remodeling of the secretory pathway, allowing cells to adjust their ER protein folding and secretory activities according to need. The transcription factor XBP1, the metozoan ortholog of Hac1, was shown in mammalian cells to induce an expansion of the ER [67,68]. Here we show that in yeast, a similar organelle expansion occurs, with the volume of the ER increasing at least 5-fold upon UPR induction. It seems logical for a cell to expand both the machinery and the space dedicated to protein folding to meet the needs of a new physiological state in which proteins stay longer in the ER until they are properly folded or committed to degradation. Proliferating the ER reduces the concentration of unfolded protein, thereby preventing aggregation and giving more time to properly fold proteins or to degrade folding failures. To our surprise, we discovered that an ER-selective UPR-induced form of autophagy, ER-phagy, is activated and is required for cells to survive under conditions of severe ER stress, thus establishing the existence of a physiologically important link between the UPR and autophagy.

Because execution of the UPR transcriptional program leads to ER expansion, it is plausible to assume that ER-phagy serves to provide the opposite effect of reducing the volume of the ER and with it, unfolded ER proteins that have accumulated there. For example, it has been recently shown that the Z variant of human α-1 proteinase inhibitor (A1PiZ) encounters different degradation pathways depending on its expression and aggregation level [69]. Normally, A1PiZ is a substrate of ERAD. However, when A1PiZ

is overexpressed, it is sent to the vacuole via the secretory pathway, and any excess of A1PiZ that aggregates inside the ER is targeted to the vacuole via an autophagy pathway, suggesting that ER-phagy may be induced under these conditions. In liver cells, reduction by autophagy of barbiturate-induced expansion of smooth ER was previously observed when the drug was removed [70]; similarly, in UT-1 cells, the expanded ER induced by HMG-CoA reductase (an ER membrane protein) overexpression is reduced by autophagy when the expression of the enzyme is tuned down [71,72]. Thus the UPR may function in conjunction with ER-phagy to balance ER synthesis with ER degradation as part of the homeostatic control network that adjusts ER abundance up and down. Similarly, pexophagy degrades excess peroxisomes when cells switch carbon sources from using fatty acids to other food stuffs [39,73], and mitophagy reduces mitochondrial abundance, e.g., under starvation conditions or under respiring conditions when mitochondria become easily damaged by oxygen radicals [40,74]. For pexophagy, Pex14 has been proposed to have a role in the selective targeting of peroxisomes for degradation [75], but how autophagy targets other organelles for selective sequestration remains an open question.

The ERAD pathway is thought to continually remove unfolded proteins from the ER and channel them to degradation by the proteasome. We have previously shown that ERAD is intimately linked to the UPR; either pathway is necessary for cell survival if the other one is impaired [18,76]. Many ERAD genes are UPR targets, and it was their up-regulation during UPR-inducing conditions that let to the discovery of this connection. By contrast to ERAD genes, autophagy genes were not defined as UPR targets in this study, and the connection between the UPR and autophagy escaped attention. Autophagy

genes were excluded from the set of UPR target genes because they are subject to dual control: in response to protein misfolding in the ER, they are induced by Hac1i in the Ire1-dependent UPR pathway, but also by a parallel pathway that can operate in the absence of Ire1 and Hac1. It is likely that this parallel signaling pathway originating from the ER lumen corresponds to the S-UPR previously described to control the expression level of *HAC1* mRNA [24]. Studying the regulation of autophagy genes therefore provides a powerful new experimental angle on deciphering the molecular mechanism of Ire1-independent ER-to-nucleus signaling in yeast. Because Hac1i expression from the glucocorticoid receptor-activated promoter is not sufficient to induce ERA formation, another signal from the ER lumen beyond activating Ire1 must be required. This signal could (directly or indirectly) establish a marker on the ER surface, labeling the organelle as "damaged" for sequestration into ERAs, and it may utilize the same pathway that confers Ire1-independent regulation of ATG8 transcription and, possibly, of other genes encoding components of the autophagy machinery.

The ERAs observed in this study show several remarkable features. First, they have a strikingly homogenous appearance and are largely filled with tightly stacked membrane cisternae. Second, the Sec61-cherry staining and the Sec63-myc immunogold staining show that the cisternae are derived from the ER. This notion is supported by the observation that cells containing ERAs lack expanded ER, which appears to be consumed during ERA formation. Third, the outer membrane of the delimiting double membrane of ERAs is densely studded with ribosomes and thus also derives—at least in part—from the ER. It has been a longstanding and still unresolved question where the delimiting membrane of conventional starvation-induced autophagosomes comes from [77]. Our

finding thus represents a first identification of the origin of the delimiting membrane of an autophagosomal structure by showing that the ER can serve as the membrane source to generate autophagosomal double membranes. Finally, the inner envelope membrane and the membrane of the stacked cisternae for the most part lack bound ribosomes (Figure 3E). The tight packing of the cisternae is consistent with the absence of ribosomes, which could not be accommodated in the approximately 16-nm space between them (a ribosome is approximately 30 nm in diameter). Taken together, these observations suggest that a sophisticated mechanism must exist that peels ER from the cell cortex, strips off most bound ribosomes, compacts the membrane into tight stacks, and packages the stacks selectively and with exclusion of most of the surrounding cytosol into ERAs by enclosing them in an envelope that is also derived—at least in part—from ER membranes. Hence, ERA formation involves a controlled "self-eating" of the ER.

No ERAs are formed in cells lacking Atg8, which is required for early steps in the biogenesis of autophagosomes. We found that during the UPR, Atg8 is first diffusely distributed throughout the cytosol. At later time points, Atg8 coalesces into discrete foci (PASs). This phenomenon occurred in the vast majority of cells (6 ± 2 PASs per cell at 3 h after UPR induction). At the same time point, ERAs formed in 20% of the cells in apparent juxtaposition to PASs. Notably, there is no overlap in staining. Moreover, and in contrast to nitrogen starvation–induced macroautophagy, no Atg8 is delivered to the vacuole (as indicated by the lack of proteolytic cleavage of GFP-Atg8). In principle, two distinct but not mutually exclusive explanations could account for this observation. First, ERA biogenesis selectively excludes co-packaging of Atg8. Although Atg8-containing PASs may nucleate ERA formation, the fluorescence microscopy images show that their

localization remains distinct. If a similar process occurred during formation of classical autophagosomes induced by nitrogen starvation, the less-selective sequestrations of surrounding cytosol might non-selectively co-package Atg8 in proximity. Second, ERAs do not fuse with vacuoles when UPR-inducing conditions are maintained. The role of ERAs in the face of ongoing folding stress would therefore primarily be one of sequestration rather than degradation. Consistent with this idea, *vps4 Δ pep4 Δ* cells lacking vacuolar proteases can live in UPR-inducing conditions despite the fact that they are already sick under normal growth conditions. Cells that are unable to form autophagosomes, however, die upon exposure to folding stress. This is in contrast to macroautophagy during nitrogen starvation, which has the primary purpose to cannibalize portions of the cytoplasm to provide recycled metabolites to the starving cells. *vps4 Δ pep4 Δ* cells cannot degrade autophagocytosed material and therefore die under these conditions [78]. Either of these two possibilities further supports the notion that ERAs have distinct properties and/or have a distinct fate from classical starvation-induced autophagosomes.

If the main function of ER-phagy is to counteract UPR-induced ER expansion, why do some cells already form ERAs despite ongoing folding stress? We can speculate that an expanded ER could allow cells to isolate potentially toxic unfolded proteins or aggregates into distinct regions of the ER; their preferential packaging into ERAs might serve to make this segregation complete, allow their eventual degradation in bulk, or prevent passing them on to daughter cells. ER-phagy may therefore not only be a homeostatic mechanism to control ER size, but could also serve a detoxification function

under certain conditions. The existence of such an additional role of ERAs is supported by the observation that ERAs are not generated in cells expressing Hac1i, arguing that ERA formation under UPR-inducing conditions is not triggered by an expanded ER, but requires the actual presence of unfolded proteins. This idea may also explain why ERAs are found only in a fraction of the cells exposed to folding stress. ERA formation under UPR-inducing conditions might only set in when a large load of unfolded proteins has accumulated, and this may be the case only in some cells. UPR activation may induce almost all cells to eventually downsize their ER through ER-phagy, as judged by the widespread generation of extra PASs. However, only some cells may be challenged by unfolded proteins to such an extent that they trigger ER-phagy despite continuing ER stress. The activation of the Ire1-independent arm of the UPR, leading to S-UPR induction, might increase the fraction of cells that form ERAs during folding stress. It will be interesting to determine whether the fraction of cells containing ERAs increases once the folding stress ceases, as the homeostatic function of ER-phagy may then dominate over its detoxification function. In support of such a switch, we have seen in preliminary experiments that ERAs can fuse with vacuoles after UPR-inducing agents have been washed out and the cells recover from stress (S. Bernales and P. Walter, unpublished data). Thus the delivery of ERAs to the vacuole may be a controlled process that can be turned on and off. In summary, many questions about the molecular mechanisms and the cellular functions of ERAs formation remain, but it seems clear that ER-phagy serves as a countermeasure to ER expansion and helps to bring organelle abundance back into balance.

While this work was under review, Yorimitsu et al. [79] independently reported that ER stress triggers autophagy. Their results confirm the transcriptional up-regulation of ATG8 and GFP-ATG8 foci formation reported here. Moreover, the authors show that ER stress–induced Atg8 is activated by lipid modification, and that the formation of GFP-ATG8 foci depends on *ATG12*, indicating that these structures correspond to PASs seen during starvation-induced macroautophagy. One significant difference is that Yorimitsu et al. report that GFP-Atg8 is degraded, whereas we do not see degradation (Figure 6). This difference is likely due to growth conditions, as they allow cells to go into stationary phase in which starvation-induced macroautophagy is turned on.

After our work was accepted for publication, Ogata et al. [80] reported that autophagy is activated and promotes cell survival upon ER stress in mammalian cells.

MATERIALS AND METHODS

Yeast strains and plasmids.

Strains used in this study were derived from the wild-type strain W303. The *ire1* Δ and *hac1* Δ strains are as described [7,13]. All the *ATG* deletions, the *PEP4/VPS4* double deletion, and the Sec61-cherry strain were derived from the W303 strain by using PCR-based knock-out strategies [49,81]. Strains expressing GFP-Atg8 were transformed with the plasmid pRS316-GFPAtg8p (kindly provided by Yoshinori Ohsumi, National Institute for Basic Biology, Japan). Strains used in Figures 1C and 6C are as previously described [18].

Cell culture and plates.

Yeast cells were grown in YPD (Figures 1, 2, and 3) or in defined synthetic medium (Figures 4–7) at 30 °C to log phase. For nitrogen starvation experiments, cultures were grown as described [32]. To induce the UPR in liquid medium, cells were treated with 8 mM dithiothreitol (DTT) or 0.2 μg/ml tunicamycin (TM).

Serial dilution experiments (Figure 8) were performed by growing cells at 30 °C to midlog phase. Cells were diluted 5-fold between consecutive positions and then plated on YPD plates, either in the absence or in the presence of 0.2-μg/ml or 1.0-μg/ml TM. Plates were incubated at 37 °C. Induction of Hac1i using the glucocorticoid system was performed as described [18].

Isolation and detection of protein.

For each condition, total yeast proteins were extracted from 5–10 optical densities (ODs) of exponentially growing cells. To this end, cells were first collected by centrifugation at 5,000 rpm for 5 min. The cell pellets were frozen in liquid nitrogen. The pellets were then resuspended in 200 μl of a solution containing 8 M urea, 50 mM HEPES (pH 7.4), and vortexed with 100 μl of glass beads for 5 min at maximum intensity. Cells extracts were then incubated at 100 °C with 20 μl of 25% SDS. Then, to separate the glass beads from the cell lysate, the bottom of the tube was pierced, placed inside a new 1.5-ml tube, and centrifuged at 1,000 rpm for 30 s. Flow through was collected and centrifuged at maximum speed for 5 min. The supernatant was collected, and protein concentrations were determined by the BCA assay (Bio-Rad Protein Assay, Hercules, California, United States).

For protein detection, 20 μg of total protein were loaded per lane in NuPAGE 10% Bis-Tris Gels (Invitrogen, Carlsbad, California, United States) and separated by electrophoresis. Proteins were then transferred to Protran BA83 nitrocellulose membranes (Whatman Schleicher & Schuell BioScience, Keene, New Hampshire, United States) and analyzed by Western blotting techniques. GFP-Atg8 (Figure 6) was detected using a mouse anti-GFP monoclonal antibody (Molecular Probes, Eugene, Oregon, United States); Hac1 was detected using a polyclonal antibody raised against the carboxy-terminus (Figure 6A) [13].

EM.

Two different techniques were used to analyze the ultrastructure of cells. First, we used paraformaldehyde fixation followed by KMnO4 staining to best visualize membrane structures (Figures 1A, 2A, 2B, 3A, 3B, 3C, and 3E) [82]. To this end, 10 OD units of exponentially growing cells were collected by centrifugation, and the cell pellet was then resuspended in 1 ml of fixative media (1% glutaraldehyde [EMS, Hatfield, Pennsylvania, United States], 0.2% paraformaldehyde [EMS], and 40 mM potassium phosphate [pH 7.0]) for 5 min at room temperature. Cells were then spun down and resuspended in 1 ml of fresh fixative media for 50 min on ice. After the incubation, cells were washed twice with 1 ml of 0.9% NaCl and once with 1 ml of water. Cells were next resuspended in 2% KMnO4 for 5 min at room temperature, centrifuged, and resuspended again in fresh 2% KMnO4 for 45 min at room temperature. Then we dehydrated the cells by consecutive 15-min washes with graded ethanol (50%, 70%, 80%, 90%, 95%, and 100%). For embedding, we used the Low Viscosity Embedding Media Spurr's Kit (EMS). Cells were infiltrated by 2-h incubations with a 3:1, 1:1, 1:3 dehydrating agent/embedding medium. Then, cells were resuspended in pure embedding medium and incubated at room temperature overnight. The next day, cells were resuspended in fresh embedding medium and cured for 24–48 h at 70 °C.

In addition, we used a high-pressure freezing/freeze substitutions technique known to be less prone to fixation artifacts and dimensional distortions (Figures 2C and 3D). We fixed cells using the Leica EM PACT2 High Pressure Freezer and freeze-substituted them in 2% OsO4 plus 0.1% uranyl acetate in the Leica EM AFS2 (Leica, Wetzlar, Germany). Fixed cells were then washed three times with pure acetone and embedded as described above. In the images shown in Figure 3F and 3G, the

OsO4/uranyl acetate freeze-substitution solution contained 3% water [48]. For the immunogold labeling, we freeze-substituted the samples in 0.1% glutaraldehyde, 0.25% uranyl acetate, and 0.01% OsO4, and we embedded them using the LR white resin system [45].

Blocks from these preparations were next sectioned and post-stained with 2% uranyl acetate in 50% methanol for 5 min and Reynold's lead citrate for 2 min. The final material was visualized on a FEI Tecnai 20 electron microscope (FEI, Hillsboro, Oregon, United States). Images were processed and analyzed using ImageJ (W. S. Rasband: http://rsb.info.nih.gov/ij/).

Light microscopy.

To analyze cells by fluorescence microscopy, we first treated microscope cover glasses with concanavalin A for 30 min. We then deposited 10 to 20 μl of cell culture on a microscope slide and covered it with the treated cover glass. Prepared cells were visualized on a Zeiss Axiovert 200M fluorescence microscope (Zeiss), and images were processed using ImageJ.

SUPPORTING INFORMATION

Acknowledgments. We thank Pablo Aguilar, Tomás Aragon, Niels Bradshaw, Graeme Davis, Alex Engel, Carol Gross, Jonathan Lin, Hiten Madhani, Saskia Neher, María Paz Ramos, Sebastian Schuck, Marco de Shumanos, Eelco van Anken, Mark von Zastrow, and Tobias Walther for valuable discussions and comments on the manuscript. We also thank Michael Braunfeld, Lucy Collinson, Mark Marsh, and Mei Lie Wong for their expert assistance and invaluable help with the EM techniques and the high-pressure freezing procedures; Pablo Valenzuela and "Fundación Ciencia para la Vida" for their encouragement and guidance; and Yoshinori Ohsumi for sending us the plasmid pRS316-GFPAtg8p. We dedicate this paper to Dr. Günter Blobel in honor of his 70th birthday.

Author contributions. SB and PW conceived and designed the experiments. SB and KLM performed the experiments. SB and PW analyzed the data. SB and KLM contributed reagents/materials/analysis tools. SB and PW wrote the paper.

REFERENCES

1. Wickner W, Schekman R (2005) Protein translocation across biological membranes. Science 310: 1452–1456.

2. Ellgaard L, Helenius A (2003) Quality control in the endoplasmic reticulum. Nat Rev Mol Cell Biol 4: 181–191.

3. McCracken AA, Brodsky JL (2005) Recognition and delivery of ERAD substrates to the proteasome and alternative paths for cell survival. Curr Top Microbiol Immunol 300: 17–40.

4. Ron D (2002) Translational control in the endoplasmic reticulum stress response. J Clin Invest 110: 1383–1388.

5. van Anken E, Braakman I (2005) Versatility of the endoplasmic reticulum protein folding factory. Crit Rev Biochem Mol Biol 40: 191–228.

6. Bernales S, Papa FR, Walter P (2006) Intracellular signaling by the unfolded protein response. Annu Rev Cell Dev Biol 22 : 487–508.

7. Cox JS, Shamu CE, Walter P (1993) Transcriptional induction of genes encoding endoplasmic reticulum resident proteins requires a transmembrane protein kinase. Cell 73: 1197–1206.

8. Mori K, Ma W, Gething MJ, Sambrook J (1993) A transmembrane protein with a cdc2+/CDC28-related kinase activity is required for signaling from the ER to the nucleus. Cell 74: 743–756.

9. Credle JJ, Finer-Moore JS, Papa FR, Stroud RM, Walter P (2005) On the mechanism of sensing unfolded protein in the endoplasmic reticulum. Proc Natl Acad Sci U S A 102: 18773–18784.

10. Shamu CE, Walter P (1996) Oligomerization and phosphorylation of the Ire1p kinase during intracellular signaling from the endoplasmic reticulum to the nucleus. EMBO J 15: 3028–3039.

11. Sidrauski C, Walter P (1997) The transmembrane kinase Ire1p is a site-specific endonuclease that initiates mRNA splicing in the unfolded protein response. Cell 90: 1031–1039.

12. Kawahara T, Yanagi H, Yura T, Mori K (1997) Endoplasmic reticulum stress-induced mRNA splicing permits synthesis of transcription factor Hac1p/Ern4p that activates the unfolded protein response. Mol Biol Cell 8: 1845–1862.

13. Cox JS, Walter P (1996) A novel mechanism for regulating activity of a transcription factor that controls the unfolded protein response. Cell 87: 391–404.

14. Mori K, Kawahara T, Yoshida H, Yanagi H, Yura T (1996) Signalling from endoplasmic reticulum to nucleus: Transcription factor with a basic-leucine zipper motif is required for the unfolded protein-response pathway. Genes Cells 1: 803–817.

15. Shen X, Ellis RE, Lee K, Liu CY, Yang K, et al. (2001) Complementary signaling pathways regulate the unfolded protein response and are required for *C. elegans* development. Cell 107: 893–903.

16. Yoshida H, Matsui T, Yamamoto A, Okada T, Mori K (2001) *XBP1* mRNA is induced by ATF6 and spliced by IRE1 in response to ER stress to produce a highly active transcription factor. Cell 107: 881–891.

17. Calfon M, Zeng H, Urano F, Till JH, Hubbard SR, et al. (2002) IRE1 couples endoplasmic reticulum load to secretory capacity by processing the XBP-1 mRNA. Nature 415: 92–96.

18. Travers KJ, Patil CK, Wodicka L, Lockhart DJ, Weissman JS, et al. (2000) Functional and genomic analyses reveal an essential coordination between the unfolded protein response and ER-associated degradation. Cell 101: 249–258.

19. Ye J, Rawson RB, Komuro R, Chen X, Dave UP, et al. (2000) ER stress induces cleavage of membrane-bound ATF6 by the same proteases that process SREBPs. Mol Cell 6: 1355–1364.

20. Yoshida H, Haze K, Yanagi H, Yura T, Mori K (1998) Identification of the cis-acting endoplasmic reticulum stress response element responsible for transcriptional induction of mammalian glucose-regulated proteins. Involvement of basic leucine zipper transcription factors. J Biol Chem 273: 33741–33749.

21. Li M, Baumeister P, Roy B, Phan T, Foti D, et al. (2000) ATF6 as a transcription activator of the endoplasmic reticulum stress element: Thapsigargin stress-induced changes and synergistic interactions with NF-Y and YY1. Mol Cell Biol 20: 5096–5106.

22. Kokame K, Kato H, Miyata T (2001) Identification of ERSE-II, a new cis-acting element responsible for the ATF6-dependent mammalian unfolded protein response. J Biol Chem 276: 9199–9205.

23. Okada T, Yoshida H, Akazawa R, Negishi M, Mori K (2002) Distinct roles of activating transcription factor 6 (ATF6) and double-stranded RNA-activated protein kinase-like endoplasmic reticulum kinase (PERK) in transcription during the mammalian unfolded protein response. Biochem J 366: 585–594.

24. Leber JH, Bernales S, Walter P (2004) IRE1-independent gain control of the unfolded protein response. PLoS Biol 2: E235. DOI: 10.1371/journal.pbio.0020235.

25. Meusser B, Hirsch C, Jarosch E, Sommer T (2005) ERAD: The long road to destruction. Nat Cell Biol 7: 766–772.

26. Romisch K (2005) Endoplasmic reticulum-associated degradation. Annu Rev Cell Dev Biol 21: 435–456.

27. Yorimitsu T, Klionsky DJ (2005) Autophagy: Molecular machinery for self-eating. Cell Death Differ 12(Suppl 2): 1542–1552.

28. Tsukada M, Ohsumi Y (1993) Isolation and characterization of autophagy-defective mutants of Saccharomyces cerevisiae. FEBS Lett 333: 169–174.

29. Thumm M, Egner R, Koch B, Schlumpberger M, Straub M, et al. (1994) Isolation of autophagocytosis mutants of Saccharomyces cerevisiae. FEBS Lett 349: 275–280.

30. Harding TM, Morano KA, Scott SV, Klionsky DJ (1995) Isolation and characterization of yeast mutants in the cytoplasm to vacuole protein targeting pathway. J Cell Biol 131: 591–602.

31. Yuan W, Tuttle DL, Shi YJ, Ralph GS, Dunn WA Jr. (1997) Glucose-induced microautophagy in Pichia pastoris requires the alpha-subunit of phosphofructokinase. J Cell Sci 110. (Pt 16): 1935–1945.

32. Takeshige K, Baba M, Tsuboi S, Noda T, Ohsumi Y (1992) Autophagy in yeast demonstrated with proteinase-deficient mutants and conditions for its induction. J Cell Biol 119: 301–311.

33. Leao-Helder AN, Krikken AM, Gellissen G, van der Klei IJ, Veenhuis M, et al. (2004) Atg21p is essential for macropexophagy and microautophagy in the yeast Hansenula polymorpha. FEBS Lett 577: 491–495.

34. Hamasaki M, Noda T, Baba M, Ohsumi Y (2005) Starvation triggers the delivery of the endoplasmic reticulum to the vacuole via autophagy in yeast. Traffic 6: 56–65.

35. Cuervo AM (2004) Autophagy: In sickness and in health. Trends Cell Biol 14: 70–77.

36. Hamasaki M, Noda T, Ohsumi Y (2003) The early secretory pathway contributes to autophagy in yeast. Cell Struct Funct 28: 49–54.

37. Ishihara N, Hamasaki M, Yokota S, Suzuki K, Kamada Y, et al. (2001) Autophagosome requires specific early Sec proteins for its formation and NSF/SNARE for vacuolar fusion. Mol Biol Cell 12: 3690–3702.

38. Reggiori F, Wang CW, Nair U, Shintani T, Abeliovich H, et al. (2004) Early stages of the secretory pathway, but not endosomes, are required for Cvt vesicle and autophagosome assembly in Saccharomyces cerevisiae. Mol Biol Cell 15: 2189–2204.

39. Dunn WA Jr., Cregg JM, Kiel JA, van der Klei IJ, Oku M, et al. (2005) Pexophagy: The selective autophagy of peroxisomes. Autophagy 1: 75–83.

40. Kundu M, Thompson CB (2005) Macroautophagy versus mitochondrial autophagy: A question of fate? Cell Death Differ 12(Suppl 2): 1484–1489.

41. Harding TM, Hefner-Gravink A, Thumm M, Klionsky DJ (1996) Genetic and phenotypic overlap between autophagy and the cytoplasm to vacuole protein targeting pathway. J Biol Chem 271: 17621–17624.

42. Scott SV, Hefner-Gravink A, Morano KA, Noda T, Ohsumi Y, et al. (1996) Cytoplasm-to-vacuole targeting and autophagy employ the same machinery to deliver proteins to the yeast vacuole. Proc Natl Acad Sci U S A 93: 12304–12308.

43. Baba M, Osumi M, Scott SV, Klionsky DJ, Ohsumi Y (1997) Two distinct pathways for targeting proteins from the cytoplasm to the vacuole/lysosome. J Cell Biol 139: 1687–1695.

44. Scott SV, Baba M, Ohsumi Y, Klionsky DJ (1997) Aminopeptidase I is targeted to the vacuole by a nonclassical vesicular mechanism. J Cell Biol 138: 37–44.

45. McDonald K (1999) High-pressure freezing for preservation of high resolution fine structure and antigenicity for immunolabeling. Methods Mol Biol 117: 77–97.

46. Baba M, Osumi M, Ohsumi Y (1995) Analysis of the membrane structures involved in autophagy in yeast by freeze-replica method. Cell Struct Funct 20: 465–471.

47. Baba M, Takeshige K, Baba N, Ohsumi Y (1994) Ultrastructural analysis of the autophagic process in yeast: detection of autophagosomes and their characterization. J Cell Biol 124: 903–913.

48. Walther P, Ziegler A (2002) Freeze substitution of high-pressure frozen samples: The visibility of biological membranes is improved when the substitution medium contains water. J Microsc 208: 3–10.

49. Shaner NC, Campbell RE, Steinbach PA, Giepmans BN, Palmer AE, et al. (2004) Improved monomeric red, orange and yellow fluorescent proteins derived from Discosoma sp. red fluorescent protein. Nat Biotechnol 22: 1567–1572.

50. Niwa M, Patil CK, DeRisi J, Walter P (2005) Genome-scale approaches for discovering novel nonconventional splicing substrates of the Ire1 nuclease. Genome Biol 6: R3.

51. Papa FR, Zhang C, Shokat K, Walter P (2003) Bypassing a kinase activity with an ATP-competitive drug. Science 302: 1533–1537.

52. Huang WP, Scott SV, Kim J, Klionsky DJ (2000) The itinerary of a vesicle component, Aut7p/Cvt5p, terminates in the yeast vacuole via the autophagy/Cvt pathways. J Biol Chem 275: 5845–5851.

53. Kirisako T, Baba M, Ishihara N, Miyazawa K, Ohsumi M, et al. (1999) Formation process of autophagosome is traced with Apg8/Aut7p in yeast. J Cell Biol 147: 435–446.

54. Ichimura Y, Kirisako T, Takao T, Satomi Y, Shimonishi Y, et al. (2000) A ubiquitin-like system mediates protein lipidation. Nature 408: 488–492.

55. Kirisako T, Ichimura Y, Okada H, Kabeya Y, Mizushima N, et al. (2000) The reversible modification regulates the membrane-binding state of Apg8/Aut7 essential for autophagy and the cytoplasm to vacuole targeting pathway. J Cell Biol 151: 263–276.

56. Reggiori F, Tucker KA, Stromhaug PE, Klionsky DJ (2004) The Atg1-Atg13 complex regulates Atg9 and Atg23 retrieval transport from the pre-autophagosomal structure. Dev Cell 6: 79–90.

57. Suzuki K, Kamada Y, Ohsumi Y (2002) Studies of cargo delivery to the vacuole mediated by autophagosomes in Saccharomyces cerevisiae. Dev Cell 3: 815–824.

58. Suzuki K, Kirisako T, Kamada Y, Mizushima N, Noda T, et al. (2001) The pre-autophagosomal structure organized by concerted functions of APG genes is essential for autophagosome formation. EMBO J 20: 5971–5981.

59. Kim J, Huang WP, Klionsky DJ (2001) Membrane recruitment of Aut7p in the autophagy and cytoplasm to vacuole targeting pathways requires Aut1p, Aut2p, and the autophagy conjugation complex. J Cell Biol 152: 51–64.

60. Shintani T, Klionsky DJ (2004) Cargo proteins facilitate the formation of transport vesicles in the cytoplasm to vacuole targeting pathway. J Biol Chem 279: 29889–29894.

61. Schroder M, Chang JS, Kaufman RJ (2000) The unfolded protein response represses nitrogen-starvation induced developmental differentiation in yeast. Genes Dev 14: 2962–2975.

62. Suzuki K, Noda T, Ohsumi Y (2004) Interrelationships among Atg proteins during autophagy in Saccharomyces cerevisiae. Yeast 21: 1057–1065.

63. Kamada Y, Funakoshi T, Shintani T, Nagano K, Ohsumi M, et al. (2000) Tor-mediated induction of autophagy via an Apg1 protein kinase complex. J Cell Biol 150: 1507–1513.

64. Lang T, Reiche S, Straub M, Bredschneider M, Thumm M (2000) Autophagy and the cvt pathway both depend on AUT9. J Bacteriol 182: 2125–2133.

65. Mizushima N, Noda T, Ohsumi Y (1999) Apg16p is required for the function of the Apg12p-Apg5p conjugate in the yeast autophagy pathway. EMBO J 18: 3888–3896.

66. Yorimitsu T, Klionsky DJ (2005) Atg11 links cargo to the vesicle-forming machinery in the cytoplasm to vacuole targeting pathway. Mol Biol Cell 16: 1593–1605.

67. Shaffer AL, Shapiro-Shelef M, Iwakoshi NN, Lee AH, Qian SB, et al. (2004) XBP1, downstream of Blimp-1, expands the secretory apparatus and other organelles, and increases protein synthesis in plasma cell differentiation. Immunity 21: 81–93.

68. Sriburi R, Jackowski S, Mori K, Brewer JW (2004) XBP1: A link between the unfolded protein response, lipid biosynthesis, and biogenesis of the endoplasmic reticulum. J Cell Biol 167: 35–41.

69. Kruse KB, Brodsky JL, McCracken AA (2006) Characterization of an ERAD gene as VPS30/ATG6 reveals two alternative and functionally distinct protein quality control pathways: One for soluble Z variant of human alpha-1 proteinase inhibitor (A1PiZ) and another for aggregates of A1PiZ. Mol Biol Cell 17: 203–212.

70. Feldman D, Swarm RL, Becker J (1980) Elimination of excess smooth endoplasmic reticulum after phenobarbital administration. J Histochem Cytochem 28: 997–1006.

71. Chin DJ, Luskey KL, Anderson RG, Faust JR, Goldstein JL, et al. (1982) Appearance of crystalloid endoplasmic reticulum in compactin-resistant Chinese hamster cells with a 500-fold increase in 3-hydroxy-3-methylglutaryl-coenzyme A reductase. Proc Natl Acad Sci U S A 79: 1185–1189.

72. Orci L, Brown MS, Goldstein JL, Garcia-Segura LM, Anderson RG (1984) Increase in membrane cholesterol: A possible trigger for degradation of HMG CoA reductase and crystalloid endoplasmic reticulum in UT-1 cells. Cell 36: 835–845.

73. Farre JC, Subramani S (2004) Peroxisome turnover by micropexophagy: An autophagy-related process. Trends Cell Biol 14: 515–523.

74. Mijaljica D, Prescott M, Devenish RJ (2007) Different fates of mitochondria: Alternative ways for degradation? Autophagy 3. Online ISSN: 1554–8635.

75. Bellu AR, Kiel JA (2003) Selective degradation of peroxisomes in yeasts. Microsc Res Tech 61: 161–170.

76. Ng DT, Spear ED, Walter P (2000) The unfolded protein response regulates multiple aspects of secretory and membrane protein biogenesis and endoplasmic reticulum quality control. J Cell Biol 150: 77–88.

77. Juhasz G, Neufeld TP (2006) Autophagy: A forty-year search for a missing membrane source. PLoS Biol 4: e36. DOI: 10.1371/journal.pbio.0040036.

78. Teichert U, Mechler B, Muller H, Wolf DH (1989) Lysosomal (vacuolar) proteinases of yeast are essential catalysts for protein degradation, differentiation, and cell survival. J Biol Chem 264: 16037–16045.

79. Yorimitsu T, Nair U, Yang Z, Klionsky DJ (2006) Endoplasmic Reticulum stress triggers autophagy. J Biol Chem 281: 30299–30304.

80. Ogata M, Hino SI, Saito A, Morikawa K, Kondo S, et al. (2006) Autophagy is activated for cell survival after ER stress. Mol Cell Biol E-pub 9 October 2006.

81. Longtine MS, McKenzie A 3rd, Demarini DJ, Shah NG, Wach A, et al. (1998) Additional modules for versatile and economical PCR-based gene deletion and modification in Saccharomyces cerevisiae. Yeast 14: 953–961.

82. Heiman MG, Walter P (2000) Prm1p, a pheromone-regulated multispanning membrane protein, facilitates plasma membrane fusion during yeast mating. J Cell Biol 151: 719–730.

Figure 3-1: ER Proliferation under UPR-Inducing Conditions

(A) Determination of ER abundance in control and UPR-induced cells. Representative cells are shown. The UPR was induced in wild-type cells by addition of DTT. Ultrastructure of control cells and UPR-induced cells was analyzed using ImageJ. The lower images show traces of cortical ER (represented in magenta) and the nuclear envelope (NE, in blue). Vacuoles, nuclei, and mitochondria are indicated as V, N, and M, respectively.

(B) Quantification of the ER proliferation during the UPR. UPR was induced and cells were collected for EM at the indicated time points. Length of the ER (as traced in [A]) was measured and divided by the area of the section. Data are plotted relative to time 0. Measurements for each time point correspond to the mean of 25 independent cell images.

(C) Expression of *HAC1i* was induced by addition of 100 μM DOC for 3 h. ER was quantified as described above in (B).

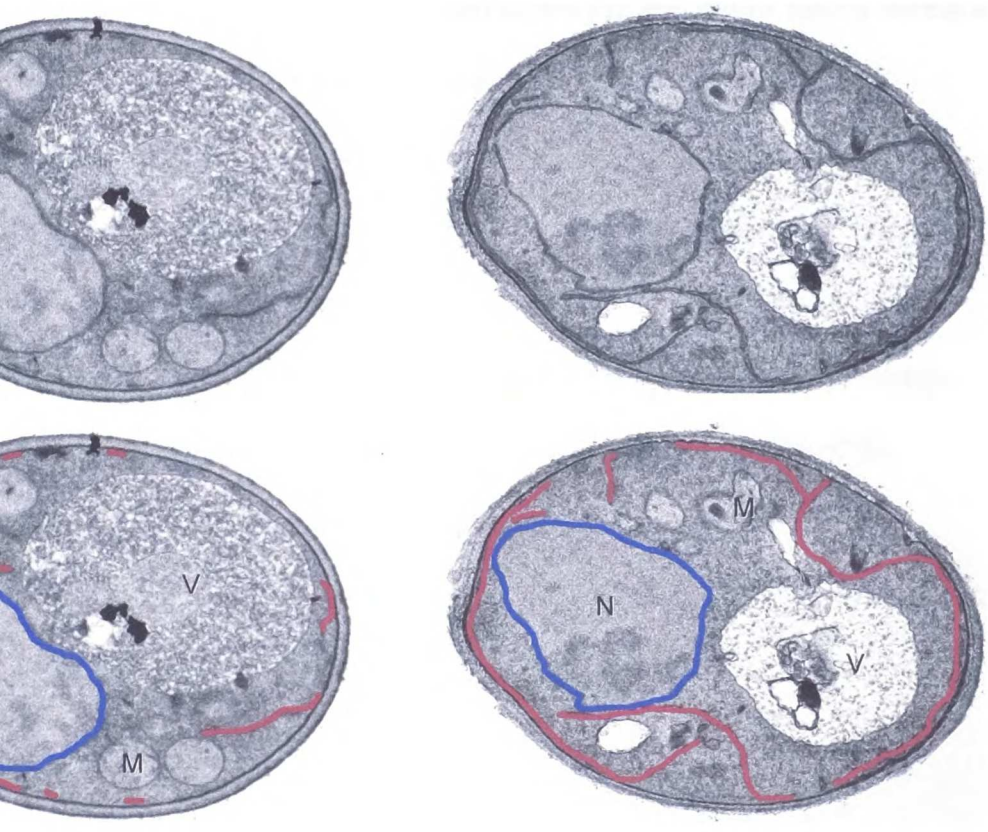

control

UPR-induced

C

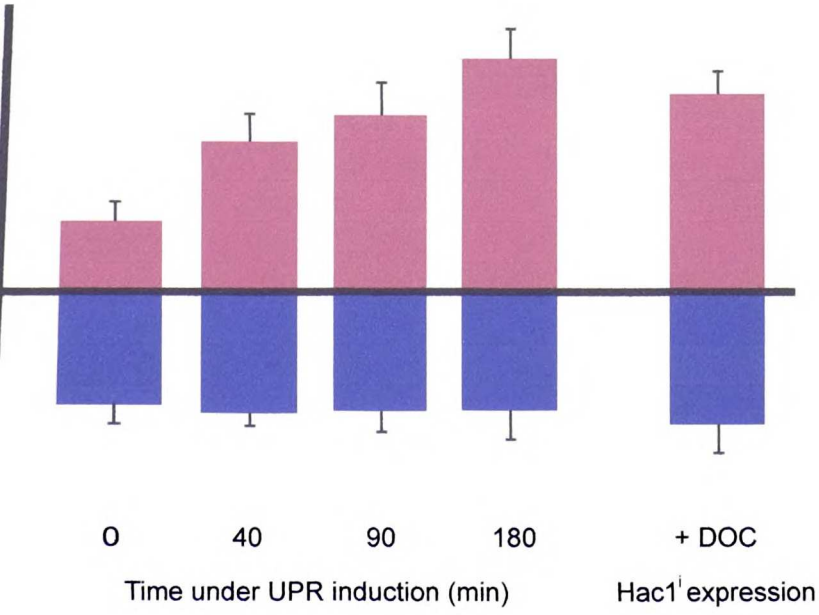

ure 3-2: The ER Morphologically Changes during the UPR

Control cells and UPR-induced cells were used to analyze and follow the ER within a
le cell using EM. Boxes indicate the areas magnified in (B). Cells shown here
espond to the full section of the images labeled "+140 nm" in (B).

Serial section of control and UPR-induced cells. Sections are separated by 70 nm on
z-axis. ER is represented in magenta and NE in blue.

Electro micrographs from control and UPR-induced cells showing that the distance
ween ER membranes increases during the UPR. For a better preservation of the
structure, samples for this experiment were prepared using high-pressure
zing/freeze substitution techniques (see Material and Methods).

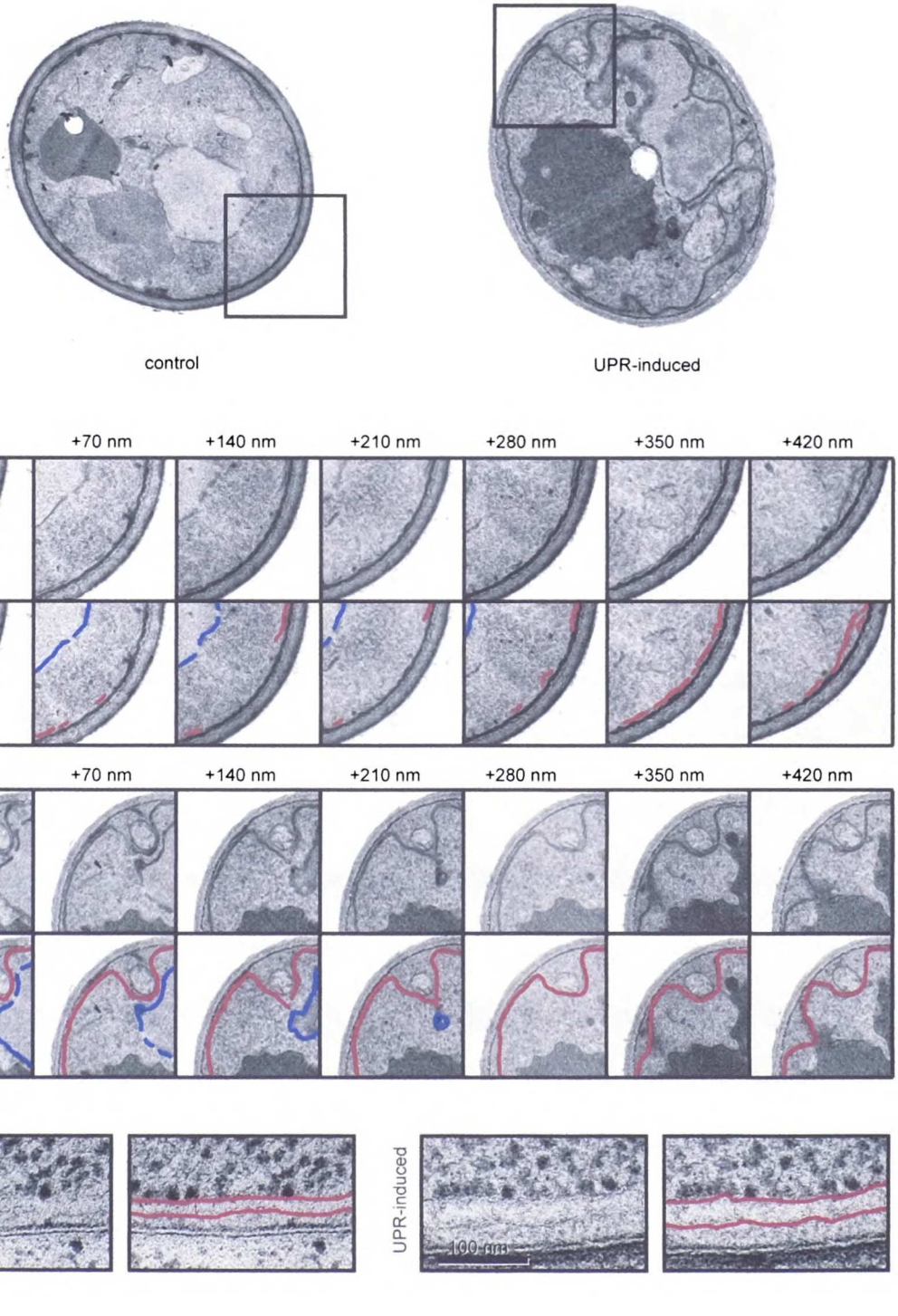
control
UPR-induced
0 nm
+70 nm
+140 nm
+210 nm
+280 nm
+350 nm
+420 nm
0 nm
+70 nm
+140 nm
+210 nm
+280 nm
+350 nm
+420 nm
100 nm
UPR-induced
100 nm

igure 3-3: Characterization of ER-Containing Autophagosomes (ERAs) during the PR

A) Images of representative DTT-treated wild-type cells that contain ERAs. Nuclei and toplasm are indicated as N and C, respectively.

B) Enlargement of representative images of ERAs from different cells. The bottom right age is likely to show a section through a cup-shaped ERA. Note that there are no nnections between the stacked cisternae and the envelope.

C) High magnification of the ERA double membrane envelope.

D) Some ERAs are found attached to or are in close proximity to ER tubules/sheets dicated by the arrow). Note that the section in (A) includes two such junctions.

E) High-pressure freezing/freeze substitution image of an ERA linked to an ER ule/sheet. The osmium/lead staining used in this technique visualizes ribosomes and monstrates that the outer ERA envelope membrane, but not the stacked internal ternae, are tightly studded with ribosomes, indicating that they originate from ER mbranes.

F) High-pressure freezing/freeze substitution image of an ER-ERA junction using an proved protocol to visualize membranes.

G) Using the same technique as in (F), we visualized the internal membrane content of ERA. Note that both portions of the internal membranes and of the sequestering uble membrane envelope contain bound ribosomes, and hence are likely derived from ER.

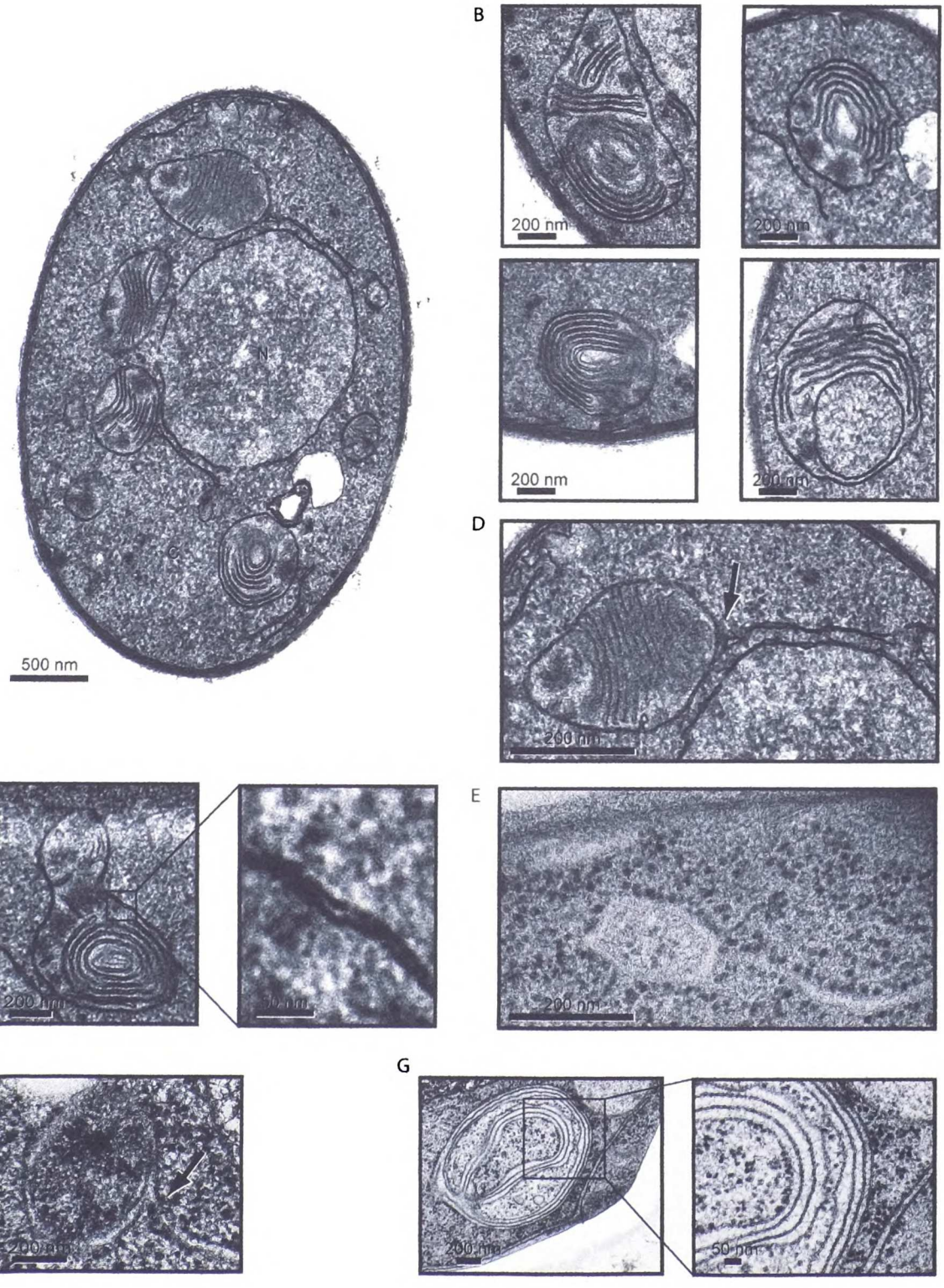
B
200 nm
200 nm
200 nm
200 nm
N
C
500 nm
D
200 nm
E
200 nm
200 nm
50 nm
200 nm
G
200 nm
50 nm

gure 3-4. Fluorescence Visualization of an ER Marker after UPR Induction.

.) Cells treated with the UPR-inducing drug DTT (+DTT) or with no drug were sualized using a fusion protein between the translocon component Sec61 and the red- uorescent protein "cherry." Top panels show untreated cells, and bottom panels show presentative UPR-induced cells.

) Representative images showing UPR-induced cells that contain ERAs (indicated by rows).

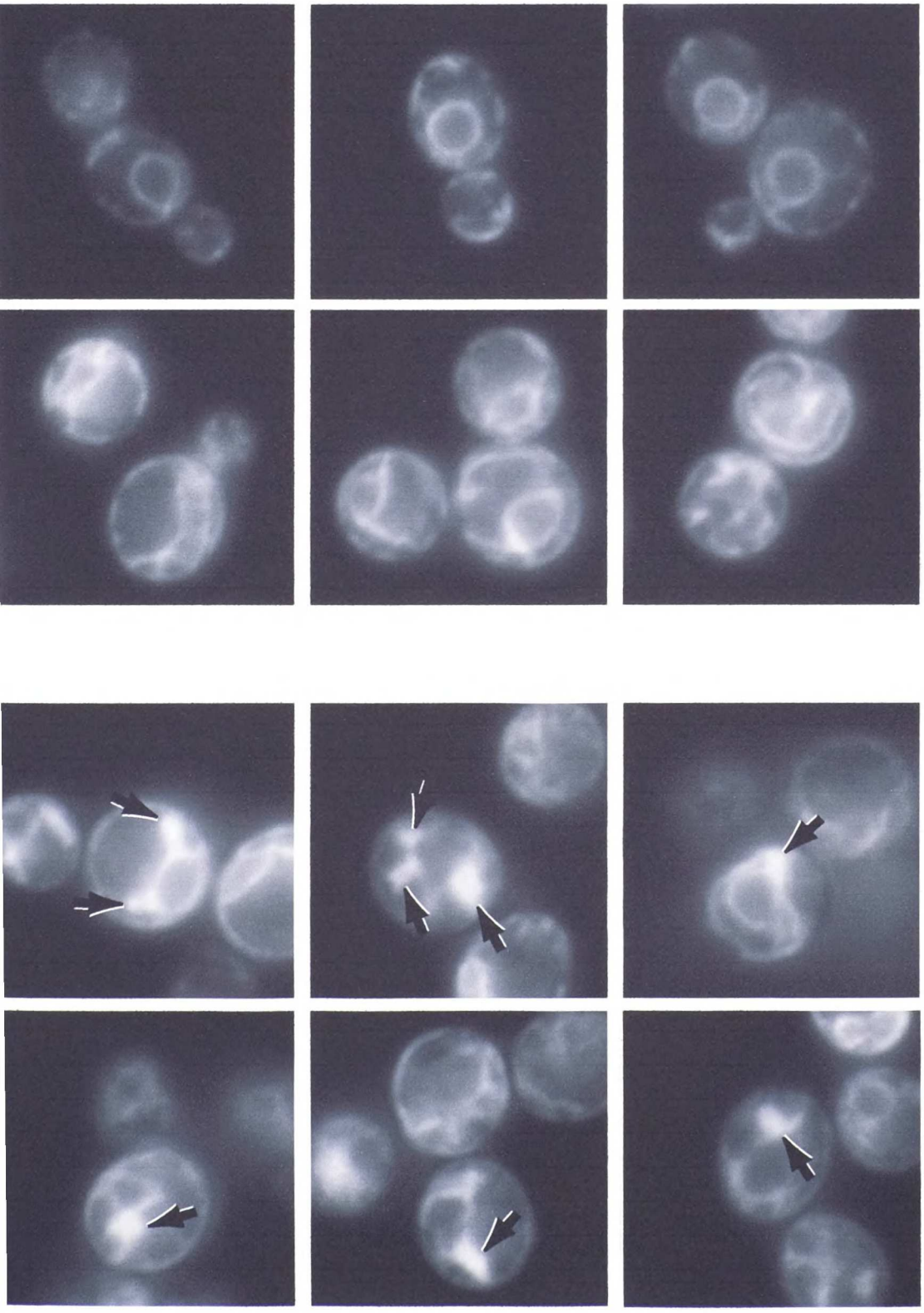
Sec61-cherry

igure 3-5. Immunogold Labeling of ERAs with an Antibody Directed against an R Membrane Marker.

A) Representative section of a cell immunolabeled against a myc-tagged Sec63, an tegral ER membrane protein. As a primary antibody, we used a rabbit polyclonal anti-yc and, as a secondary, we used 15-nm gold particles–conjugated anti-rabbit antibody. ucleus, nuclear envelope, ER, and ERA are indicated as N, NE, ER, and ERA, spectively.

) High magnification of an electron micrograph of a section of ER. Quantification owed that there are 5 ± 2 gold particles per linear micrometer of ER.

) High magnification of ERAs. To predict how many gold particles one should expect a particular ERA, we first calculated and averaged the amount of ER (expressed as gth in linear micrometers) present in an ERA (similar to the ones shown in Figure 3B), d normalized the value for its area. These calculations determined that there are 20.8 ± μm of ER per μm2 inside the ERAs. These values allowed us to predict how many d particles would be expected over a section of an ERA if it were packed with ER mbranes. Two representative ERAs are shown. The ERA shown in the middle picture uld hold 2.4 μm of ER inside and, therefore, should have 12 gold particles. We nted 12 gold particles. The ERA on the right could contain 2.7 μm of ER and should tain14 gold particles; we counted 16 gold particles. The image on the right shows a resentative view of a nucleoplasmic region.

Quantification of gold-labeling density per area. To assess the signal-to-noise ratio of immunogold-labeling procedure, we assessed background labeling by counting the

umber of gold particles over an areas of nucleoplasm (N) and over ERAs, and

ormalized the counts to the respective areas.

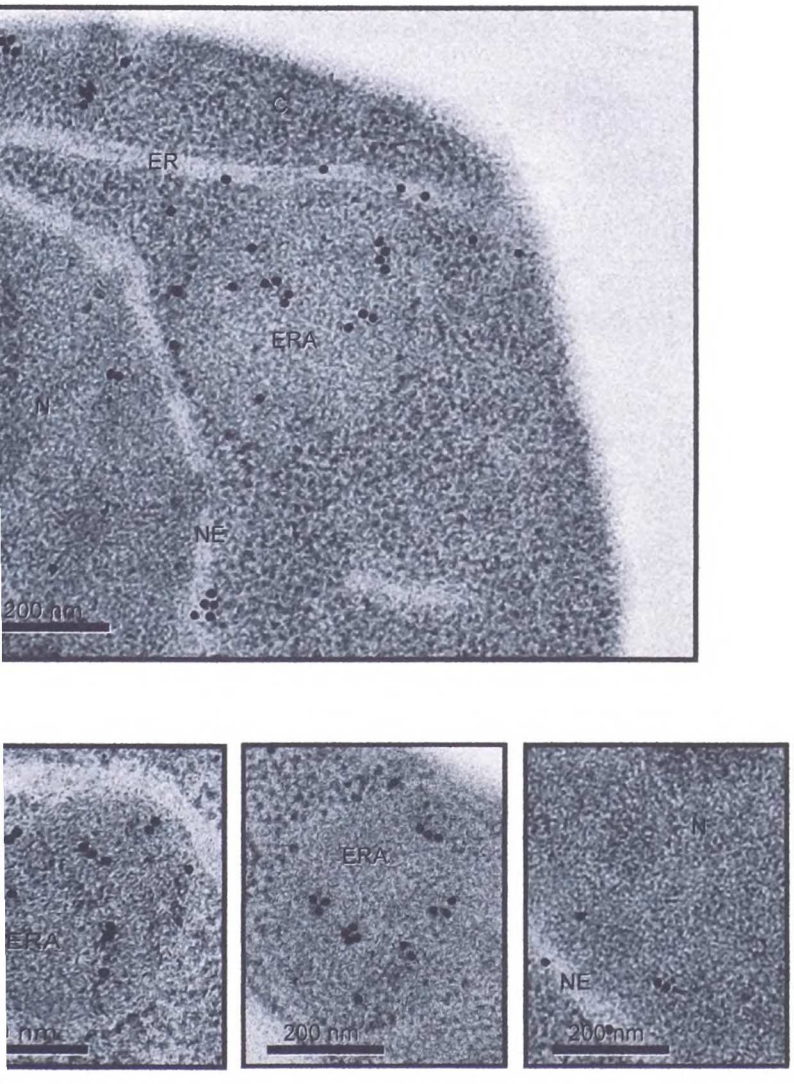
C
ER
ERA
N
NE
200 nm


B
ER
200 nm

ERA
nm

ERA
200 nm

N
NE
200 nm

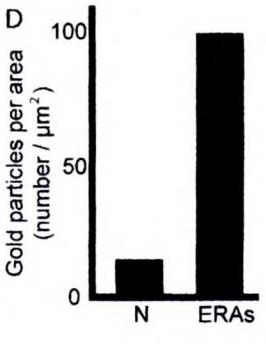
D
Gold particles per area
(number / μm²)
100
50
0
N
ERAs

Figure 3-6: UPR-Induction of the Autophagy Marker GFP-Atg8.

(A) Wild-type cells transformed with a plasmid containing GFP-Atg8 were grown for 4 h in synthetic media with no drug, with UPR-inducing conditions (+DTT and +TM), or under nitrogen starvation conditions (N starv), and then harvested for protein preparation. Protein extracts were analyzed by Western blotting using antibodies against GFP (top panel) or Hac1 (bottom panel). Total protein concentration was measured by BCA protein assay. Same concentration of protein was loaded in each lane, and transfer efficiency was checked by Ponceau staining. The identities of the different bands are indicated.

(B) Wild-type cells expressing GFP-Atg8 grown under the conditions described above were visualized by fluorescence microscopy.

(C) GFP-Atg8 was detected in extracts from untreated *hac1 Δ* cells or cells expressing *ire1i* (+DOC) by Western blotting using antibodies against GFP.

(D) Western blot using antibodies against GFP of extracts from *hac1 Δ*, *ire1 Δ*, or *vps4 Δ* cells expressing GFP-Atg8. Mutant cells were grown under regular conditions, UPR-inducing conditions (+DTT), or nitrogen starvation conditions (N starv).

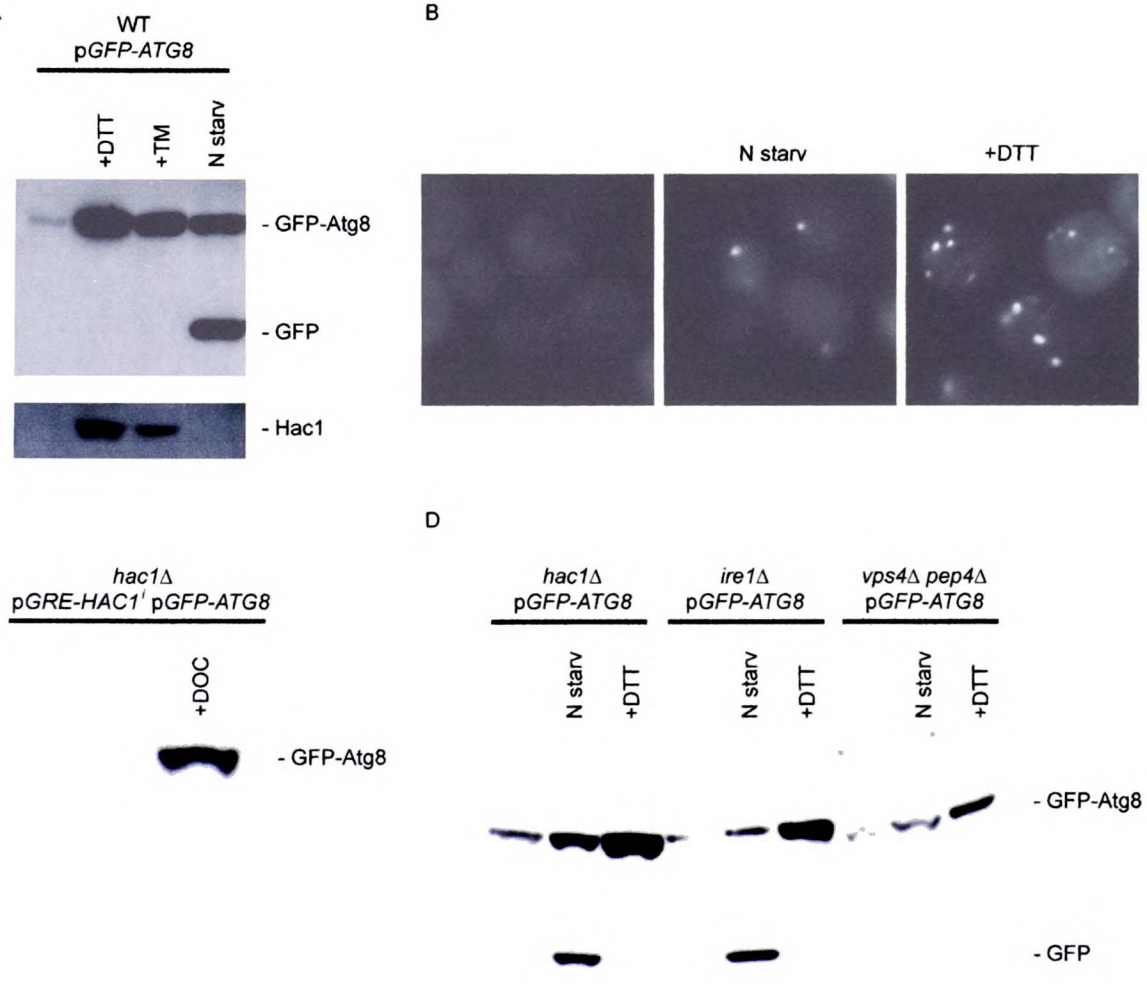
WT
pGFP-ATG8
+DTT
+TM
N starv
- GFP-Atg8
- GFP
- Hac1
B
N starv
+DTT
hac1Δ
pGRE-HAC1i pGFP-ATG8
+DOC
- GFP-Atg8
D
hac1Δ
pGFP-ATG8
ire1Δ
pGFP-ATG8
vps4Δ pep4Δ
pGFP-ATG8
N starv
+DTT
N starv
+DTT
N starv
+DTT
- GFP-Atg8
- GFP

'igure 3-7: Localization of GFP-Atg8 during UPR Induction.

ome of the DTT-treated cells shown in Figure 4B expressing GFP-Atg8 and Sec61-herry (as an ER marker) were visualized using fluorescence microscopy. GFP-Atg8 ocalizes in close proximity to the ERAs detected by the ER marker.

Figure 3-7 *Bernales et al. (2006)*

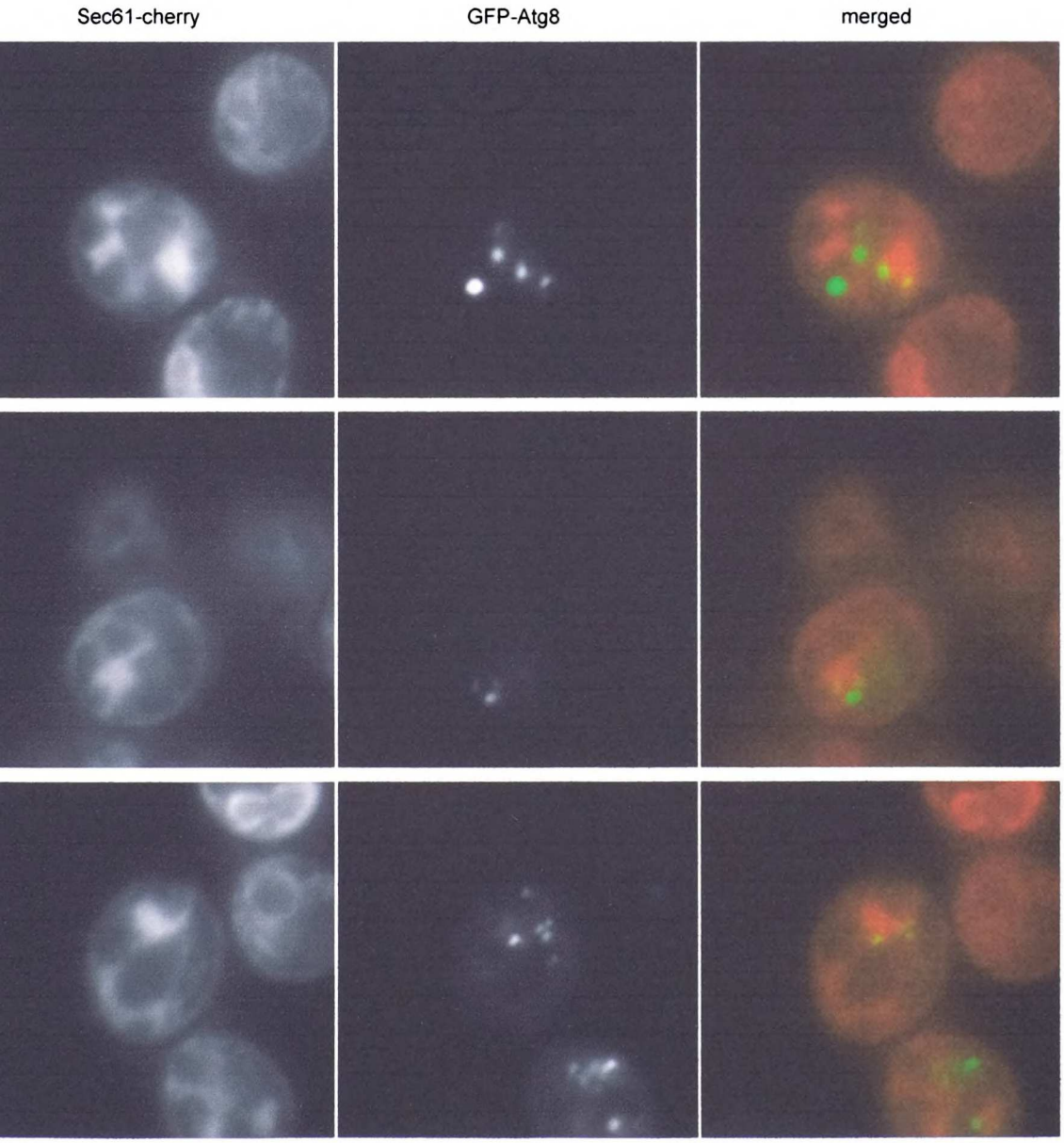

igure 3-8: Atg8 and Other ATG Genes Are Necessary during UPR Induction.

erial dilutions for wild-type, *hac1 Δ*, *atg1 Δ*, *atg8 Δ*, *atg9 Δ*, *atg16 Δ*, and *atg20 Δ*

eletion cells and *vps4 Δ pep4 Δ* double deletion cells were grown on rich-media plates

ith no drug (YPD) or with different concentrations of tunicamycin (TM; 0.2 or 1.0

g/ml). *atg19 Δ* gave an identical result to the other autophagy genes shown here

npublished data).

Figure 3-8 *Bernales et al. (2006)*

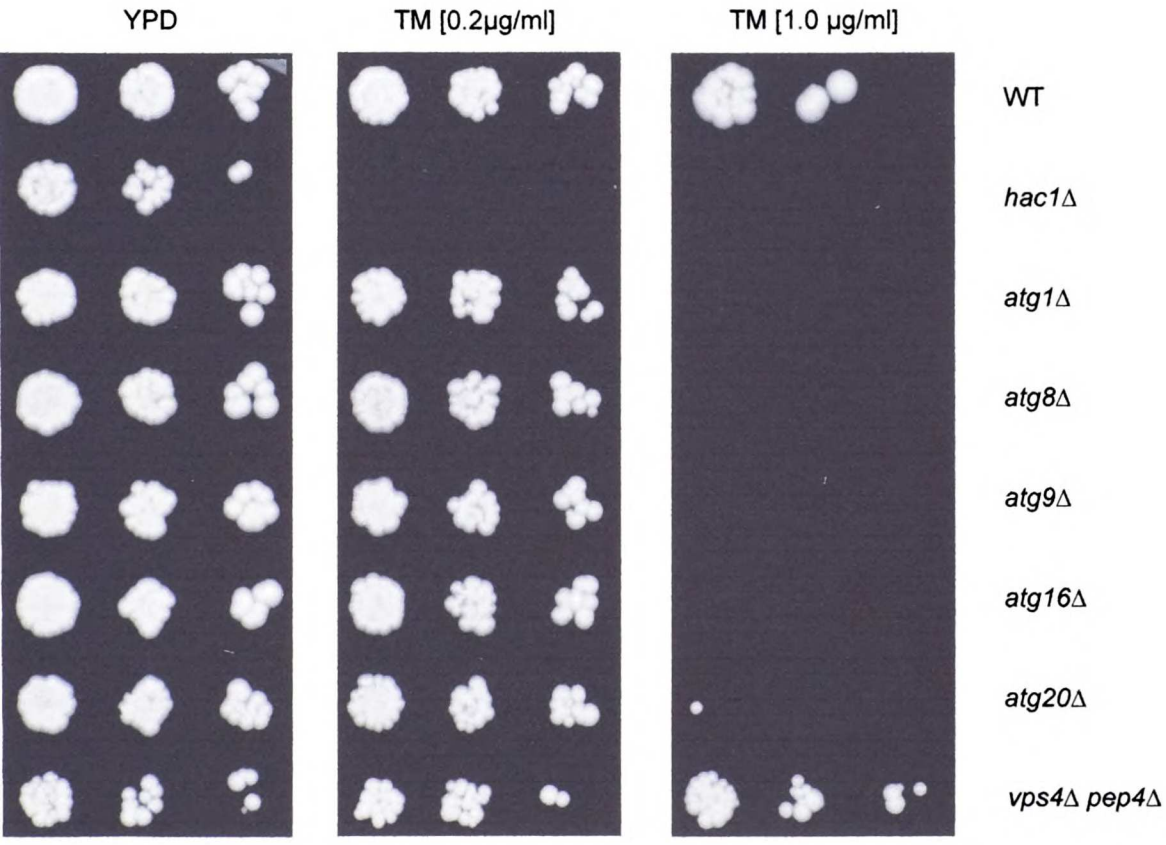

Appendix A

Transcriptional control of the *HAC1* mRNA during the S-UPR

To understand the transcriptional upregulation of the *HAC1* mRNA during the S-UPR, we used a battery of approaches to specifically look for the upstream activating sequence(s) (UAS) in the *HAC1* promoter and for the transcription factor(s) or molecules involved in this response.

To this end, we first subcloned 1000 base pairs (bps) upstream of the initiation codon of the *HAC1* open reading frame (ORF) in front of a cripple *CYC* promoter driving the expression of the reporter gene *lacZ.* We then used serial deletion mutants from the 5'-end of the *HAC1* promoter to identify important motifs. We found that the full *HAC1* promoter did not provide considerable *LACZ* expression under S-UPR-inducing (23°C to 37°C + 8 mM DTT for 2.5 hrs) conditions by measuring the hydrolysis of ONPG in the colorimetric beta galactosidase assay. Nonetheless, we observed that shortening of the 3' end of the *HAC1* promoter in two of the constructs resulted in an increased signal. Specifically, the segments containing sequences from -1000 bps to -143 bps (construct A) and from -1000 bps to -263 bps (construct B) of the *HAC1* promoter provided the best fields, ~2- and ~3-fold inductions over background after, respectively.

Using construct B, we applied a similar approach to the 5' end of the promoter. The minimal segment that gave us the same intensity as the full construct B contained the sequence from –450 bps to –263 bps of the *HAC1* promoter (construct C).
When comparing the results of this assay between N-UPR- and S-UPR-inducing conditions for construct C, we noticed a similar upregulation of the reporter gene. For this reason, we did not pursue this approach. However, we believe that critical information for the S-UPR regulation could be contained in this segment of the promoter. Additional analyses of construct C might give clues about the regulatory process that governs *HAC1*

ranscription. For example, we noticed that deleting a 15-nucleotide segment (from –406 ops to –392 bps) that is present in construct C in the wild-type promoter gave a 5-fold nduction of the *HAC1* mRNA (Figure 1A). However, this deletion is not important for he S-UPR because the *HAC1* mRNA is still upregulated 3-fold during S-UPR inducing onditions. An even more surprising result was obtained with a 45-nucleotide deletion from –406 to –361) that included the 15-nucleotide segment mentioned above. Cells vith this deletion have a normal amount of the *HAC1* mRNA and the upregulation during ne S-UPR is unaffected. This experiment was only done once, so confirmation is ecessary.

In a parallel approach, we performed PCR random mutagenesis on the *HAC1* romoter to identify elements that, when mutated, did not result in upregulation of the *AC1* mRNA. Viability of these cells in S-UPR-inducing conditions was used a nctional screen (Figure 1B). More than 20 candidates were sequenced and aligned to e if mutations were clustered in specific areas of the *HAC1* promoter. We observed that the mutants had some single or double point mutations in two defined nucleotide quences. We termed these sequences motif I and motif II (Figure 1C). Motif I did not ntain a binding site for any known protein but its deletion severely reduced *HAC1* RNA levels to 30% of its basal level. However, S-UPR-inducing conditions still duced the *HAC1* mRNA ~2.5 fold.

Motif II contained the sequence for a known transcription factor, Rlm1: $TA(T/A)_4TAG$. However, this motif is also very similar to a standard TATA-box. Basal *1C1* mRNA levels are also much lower in these cells and can still be up-regulated ring the S-UPR. Interestingly, *rlm1*Δ cells cannot survive in S-UPR inducing plates.

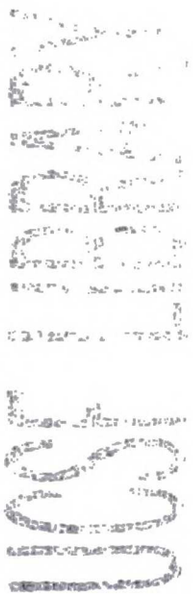

Nonetheless, these cells still up-regulate *HAC1* mRNA during the S-UPR. Overexpression of the *HAC1* mRNA in the *rlm1*Δ background does not rescue this ethality. Rlm1 is a MADS-box transcription factor and a component of the protein kinase C-mediated MAP kinase pathway. Many components of this signaling pathway are pregulated during the N-UPR and S-UPR and some of them are required for cell iability during the UPR. In particular, we noticed that Mpk1 was necessary for survival uring both N-UPR- and S-UPR-inducing conditions. One interesting possibility that was ever explored was the potential redundancy between Rlm1 and Smp1, a putative anscription factor involved in regulating the response to osmotic stress, and also is a ember of the MADS-box family of transcription factors. A double knockout between lm1 and Smp1 might provide new information about the regulation of the *HAC1* mRNA d the relation between the UPR and this MAP kinase pathway.

We also used site-directed mutagenesis to test and confirm the importance of otif I and II for the transcription of the *HAC1* mRNA (Figure 2).

identify transcription factors or other components that might be involved in the S-PR, we also performed an EMS-mutagenesis. To this end, we mutagenized cells to ~ % lethality and plated the mutant cells on YPD, N-UPR- and S-UPR-inducing plates. 5 candidates were unable to survive in S-UPR plates. As a secondary screen, we nsformed each mutant with a plasmid that expressed *HAC1* constitutively to determine ver-expression was able to rescue the lethality on S-UPR plates. Candidates 73 and were rescued by this method. Unfortunately, we did not observe any effect on *HAC1* NA induction during the S-UPR.

In collaboration with Dale Webster in Hao Li's laboratory, we also used

:omputational analyses to find putative S-UPR motifs. The first method used was
:lustering. In this case, ratios of gene expressions that are specific for the S-UPR-
lependent transcription factor were used (see Leber et al. 2004, Fig. 5F). In particular,
he ratios were calculated by dividing the fold induction in *ADH1pro-HAC1* cells under
;-UPR-inducing conditions by the fold induction in wild-type cells under N-UPR-
nducing conditions, and by dividing the fold induction in wild-type cells under S-UPR-
ıducing conditions by the fold induction in DTT-treated *HAC1*proHI cells. Promoters
:om genes in which both of these ratios were increased at least 1.5-fold were analyzed.
.s a complementary method, we used fReduce analyses (for more information visit
ttp://bussemaker.bio.columbia.edu:8080/reduce/). In this case, we used the same ratios
ıentioned above to determine whether there were correlations between expression levels
ıd the frequency of these motifs. We obtained similar results from both clustering and
Reduce analyses. By far the strongest motif was HARGGG. Two additional motifs that
ere very similar to HARGGG were found, also, ATHARG and ATAVGK. The
ARGGG motif was found three times in the *HAC1* promoter of *Saccharomyces*
revisiae. Two of these three sites are conserved between other yeast species. Using a
ol that searches for correlations between motifs and transcription factors in chIP-chip
ta, we found a strong correlation with Skn7. *skn7*Δ cells have a mild growth phenotype
S-UPR plates but otherwise behave like wild-type cells during the N-UPR or S-UPR.
ese computational analyses were performed by Dale Webster.

Figure A-1: Analyses of the *HAC1* promoter

A) (*top*) Quantification of normalized total *HAC1* mRNA levels for a S-UPR-induced wildtype strain (black bars), a strain lacking 15 nucleotides from -406 bps to -392 bps in the *HAC1* promoter (grey bars), and a strain lacking 45 nucleotides from -406 bps to -361 bps in the *HAC1* promoter (white bars). (*bottom*) Northen blots for the indicated bars.

B) N-UPR and S-UPR plate phenotypes for four strains mutagenized in the *HAC1* promoter. Note that all strains are viable under N-UPR-inducing conditions but only PCR1 and PCR3 can survive in S-UPR-inducing conditions.

C) Sequence analysis and alignment of strains mutagenized in the *HAC1* promoter that have a viability defect in S-UPR-inducing plates but not in N-UPR-inducing plates. Point mutations are indicated in red. Cluster of mutations allowed the discovery of motif I and motif II.

Figure A-1

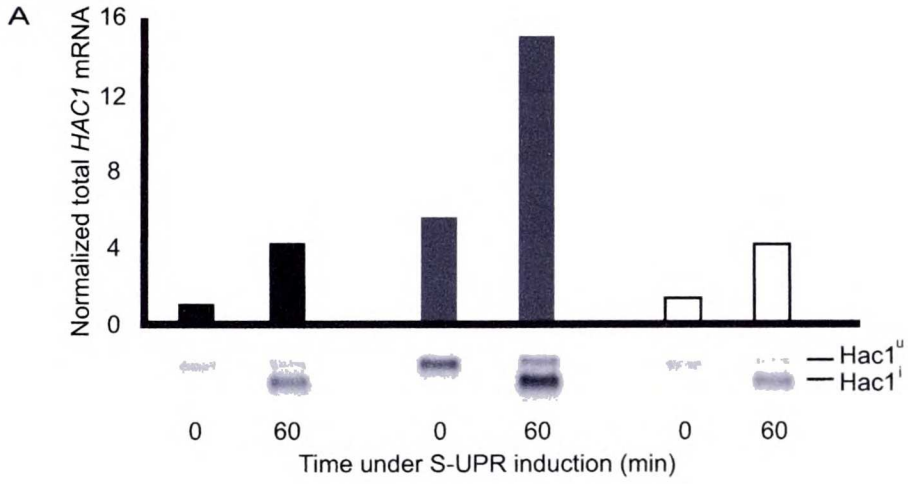

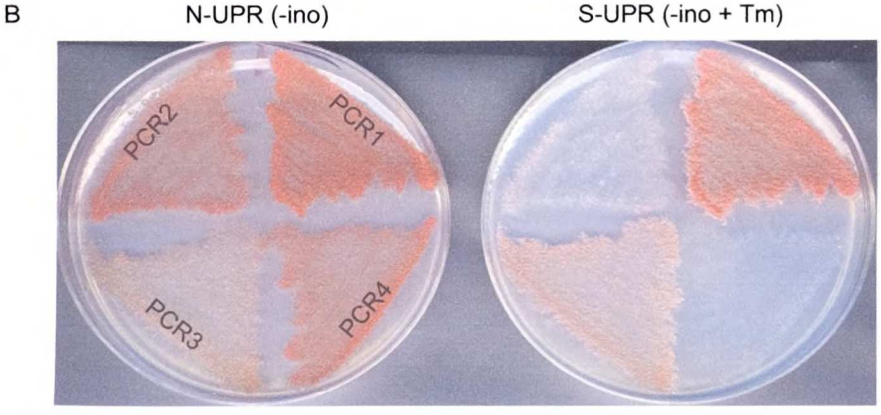

C

```
          -218                                                  -167
           |                                                     |
PCR21 GAACACCTTGTTCTCTTTTGTTCACGCTCCCTACATTCACTATATACTGGAA
PCR20 GAGCACCTTGTTCTCTTTTGTTCTCGCTCCCTACATTCACGATATATTAGAA
PCR19 GAACACCTTGTTCACTTTTGTTCTCGCCCCCTACATTCTCTATATATTAGAA
PCR17 GAACACCTTGTTCTCTTTTGTTCACGCTCCCTACATTCACTATATACTGGAA
PCR10 GAACACCTTGTTCTCTTTCGTTCTCGCTCCCTACATTCACTATATGTTAGAA
 PCR4 GAACGCCTTGTTCTCTTTTGTTCTCGCTCCCTACATTCACTATGTATTAGAA
 PCR2 GAACACCTTGCTCTCTTTTGTTCTCGCCCCCTACATTCTCTATATATTAGAA
wildtype GAACACCTTGTTCTCTTTTGTTCTCGCTCCCTACATTCACTATATATTAGAA
          ---------------------                 ----------
          Motif I                               Motif II
```

igure A-2: Motif I and II affect viability in S-UPR inducing plates.

A) Plate phenotype of a strain lacking motif II in the *HAC1* promoter ("Δmotif II"). his deletion affects cell viability in S-UPR-inducing plates but not in N-UPR-inducing ates. Controls include a wildtype strain, a strain where the *HAC1* ORF is driven by the *DH1* promoter to set *HAC1* levels to those observed during the N-UPR, and a Δ*hac1* ain.

Plate phenotype of a strain lacking motif I in the *HAC1* promoter ("Δmotif I"). This in is also not viable in S-UPR-inducing conditions.

Plate phenotype of a strain lacking both motif I and II in the *HAC1* promoter motif I & II"). This strain is also unviable under S-UPR-inducing conditions.

Plate phenotype of a strain with three point mutations in motif II ("AT***ggg***TT" ead of ATATATT). This triple-point mutation also affects viability of these cells ng the S-UPR.

igure A-2

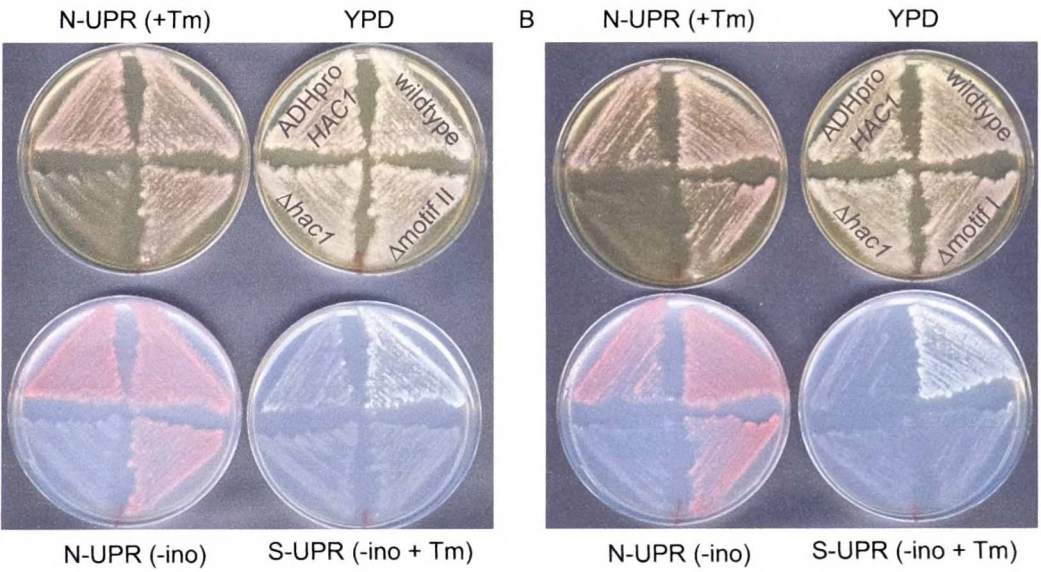

Figure A-1

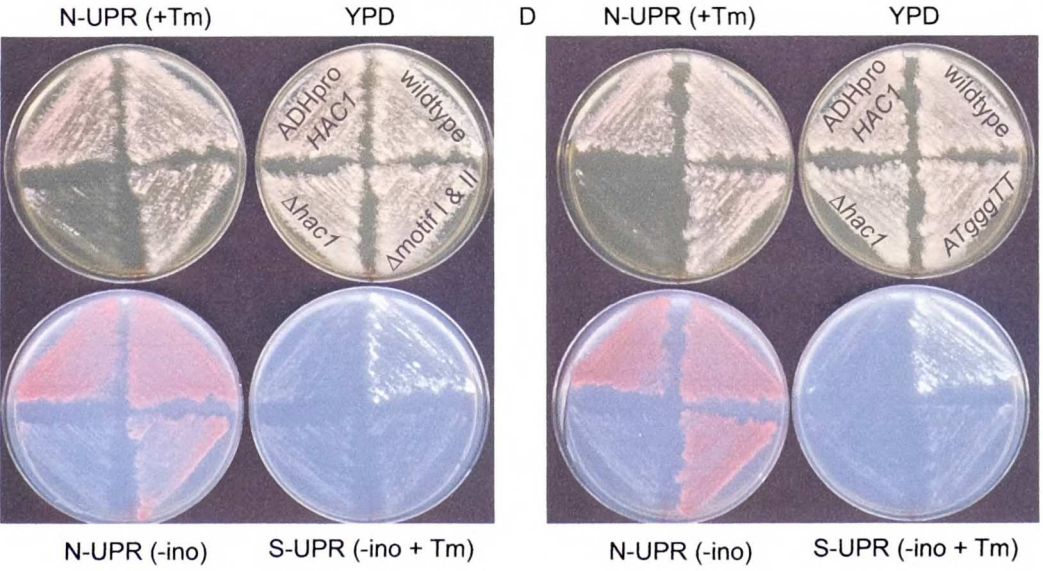

Appendix B

Viability during UPR-inducing conditions

dy the role of specific genes might have during the N-UPR and S-UPR, we took age of the yeast knockout strain collection and analyzed their growth phenotype on ete synthetic media plates, N-UPR-inducing plates and S-UPR-inducing plates. of the most significant phenotypes are summarized in Table 1.

The main goal of this screen was to identify candidates that might be important the S-UPR in general and for *HAC1* mRNA upregulation. We found 22 deletion that were specifically and markedly affected under S-UPR-inducing conditions. unately, all of the top candidates that are specific for S-UPR-inducing plates , *hal1*Δ, *yjl152w*Δ, *mac1*Δ, *hof1*Δ, *lip5*Δ, *sia1*Δ, *lyp1*Δ, *and est3*Δ) behaved like d-type strain when tested for induction of the *HAC1* mRNA during the S-UPR Northern blot hybridization.

It became clear from this screen that many pathways are essential during the UPR. ample, many genes important for vacuolar function, calcium homeostasis, and cell aintenance were unable to survive during UPR-inducing conditions. Components MAP kinase pathway were again picked in this screen (see Appendix A), including and *BCK1*.

B-1: Viability of yeast deletion strains during UPR-inducing conditions.

of the most significant phenotypes are shown here. This is a qualitative analysis of growth phenotype under N-UPR-inducing plates (+Tunicamycin ("+Tm") OR tol ("-ino")) and under S-UPR-inducing plates (+Tunicamycin –inositol ("-ino)). None of the strains had a growth defect in YPD plates. Column on the left shows l strains (top group), strains specifically affected on plates lacking inositol (middle) inositol, and strains affected under S-UPR-inducing conditions (bottom group). nn on the right shows strains affected in tunicamycin-treated plates. Colony size is ted by the black circles. Nomenclature is at the bottom of the table. Absence of a represents lack of growth under those conditions.

igure B-1

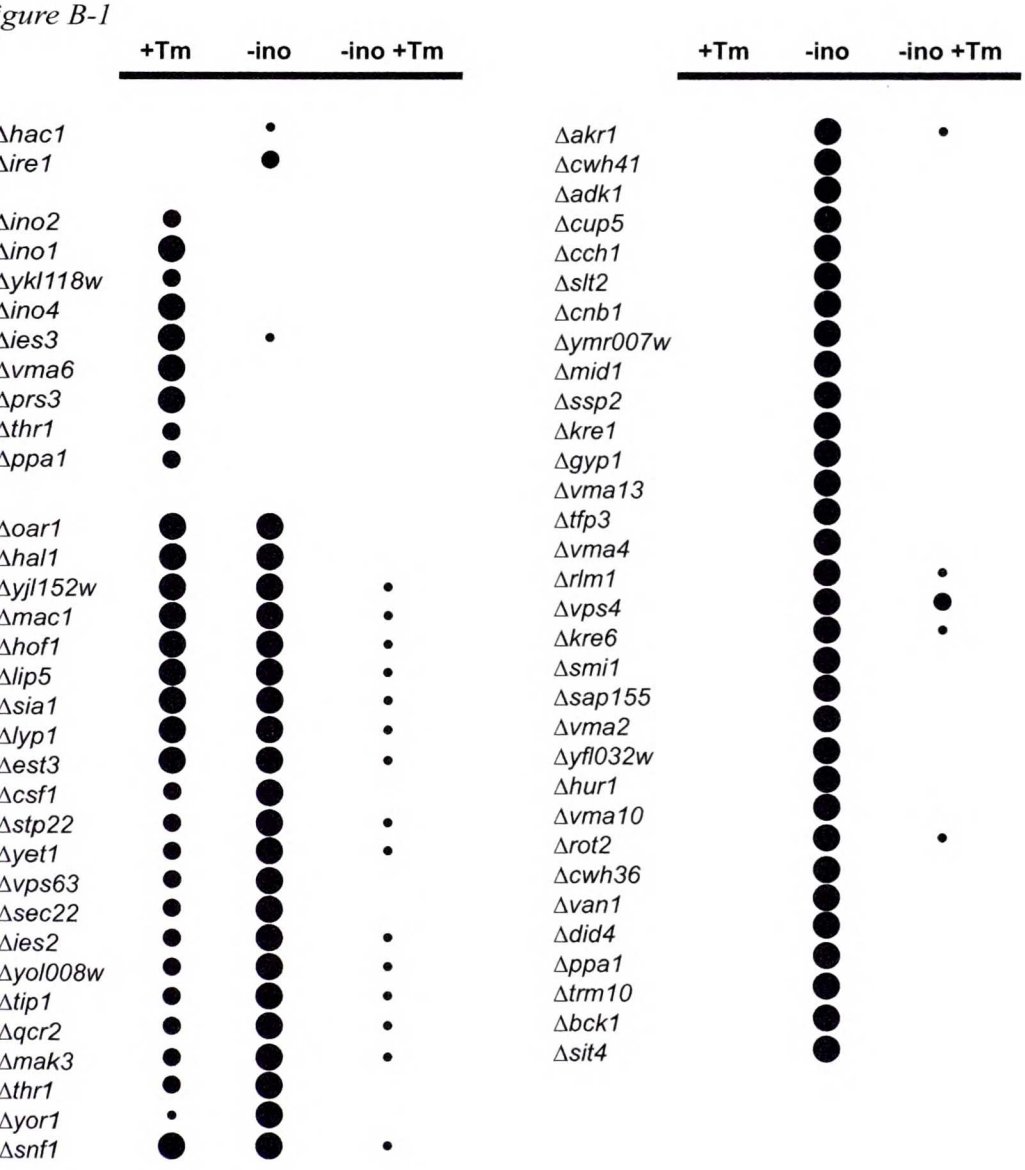
+Tm
-ino
-ino +Tm
Δhac1
Δire1
Δino2
Δino1
Δykl118w
Δino4
Δies3
Δvma6
Δprs3
Δthr1
Δppa1
Δoar1
Δhal1
Δyjl152w
Δmac1
Δhof1
Δlip5
Δsia1
Δlyp1
Δest3
Δcsf1
Δstp22
Δyet1
Δvps63
Δsec22
Δies2
Δyol008w
Δtip1
Δqcr2
Δmak3
Δthr1
Δyor1
Δsnf1
+Tm
-ino
-ino +Tm
Δakr1
Δcwh41
Δadk1
Δcup5
Δcch1
Δslt2
Δcnb1
Δymr007w
Δmid1
Δssp2
Δkre1
Δgyp1
Δvma13
Δtfp3
Δvma4
Δrlm1
Δvps4
Δkre6
Δsmi1
Δsap155
Δvma2
Δyfl032w
Δhur1
Δvma10
Δrot2
Δcwh36
Δvan1
Δdid4
Δppa1
Δtrm10
Δbck1
Δsit4
100% to 80% of wildtype
40% to 80% of wildtype
1% to 40% of wildtype

Appendix C

ATG8 transcriptional regulation

nd positive transcriptional regulators of *ATG8*, we transformed a pGFP-ATG8
Δ strain (Figure 1A) with a 2μ library and looked for increased fluorescence by
S. We used a *hac1*Δ strain based on our knowledge that Hac1 is sufficient to
gulate *ATG8*. We used this approach to avoid candidates that activate the UPR,
uce Hac1, and, therefore, up-regulate *ATG8*.

We sorted and plated the GFP-positive candidates to allow formation of colonies.
a secondary screen, we looked for GFP-positive colonies by analysing the plates with
uorescence microscope. We obtained 61 candidates. We then re-screened them for
reased fluorescence by FACS, and observed that 24 candidates had not only increased
orescence but also a normal Gaussian distribution (Figure 1B, C, and D). Interestingly,
se candidates were able to survive in plates without inositol, a condition known to be
hal to *hac1*Δ cells. We concluded that pGFP-ATG8 improved survival of *hac1*Δ cells
plates without inositol. Therefore, upregulation of *ATG8* by the candidate genes from
e 2μ library was beneficial for survival of the cells under these conditions.

We rescued and sequenced the 2μ plasmids from the strains with higher
uorescence. The top three sequenced candidates contained the information for the first
20 amino acids of Spt7, for Spo75, and for Hap2.

Spt7 is a subunit of the SAGA transcriptional regulatory complex, involved in
roper assembly of the complex. Spo75 is an uncharacterized, conserved transmembrane
protein. Hap2 is a transcriptional activator and is the yeast homologue of NF-Y, a protein
that interacts with Atf6 to activate specific UPR-target genes.

To investigate the role that Spo75 and Hap2 might have during the UPR, we
knocked these genes out. We observed that while *hap2*Δ cells were not affected in UPR-

ditions, *spo75*Δ cells were. In particular, the *spo75*Δ cells were not able to
tes with 1 μg/ml of tunicamycin. Spo75 has three additional homologues in
Rsn1, and YLR241W) and is conserved in mammalian cells. There is little
this family, but, interestingly, *rsn1*Δ had been previously shown to be
e to tunicamycin in a haploinsufficiency assay. However, the quadruple
able to survive under UPR-inducing conditions.

roject was done in collaboration with Alex Engel and Maria Paz Ramos.

1: FACS analyses of *ATG8*-inducing genes.

GFP intensity of Δ*hac1* pGFP-ATG8 strains. Mean intensity of the population

ntensity of a Δ*hac1* pGFP-ATG8 strain containing a 2μ plasmid that encodes

-1560 bps (520 amino acids) of *SPT7*. Mean intensity of the population is 751.

intensity of a Δ*hac1* pGFP-ATG8 strain containing a 2μ plasmid that encodes

Mean intensity of the population is 775.

P intensity of a Δ*hac1* pGFP-ATG8 strain containing a 2μ plasmid that encodes

Mean intensity of the population is 1402.

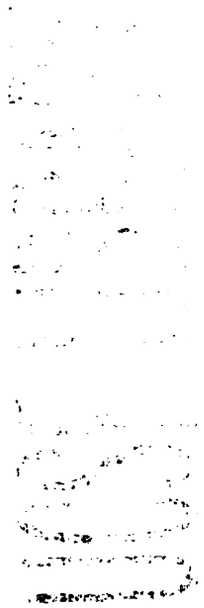

Figure C-1

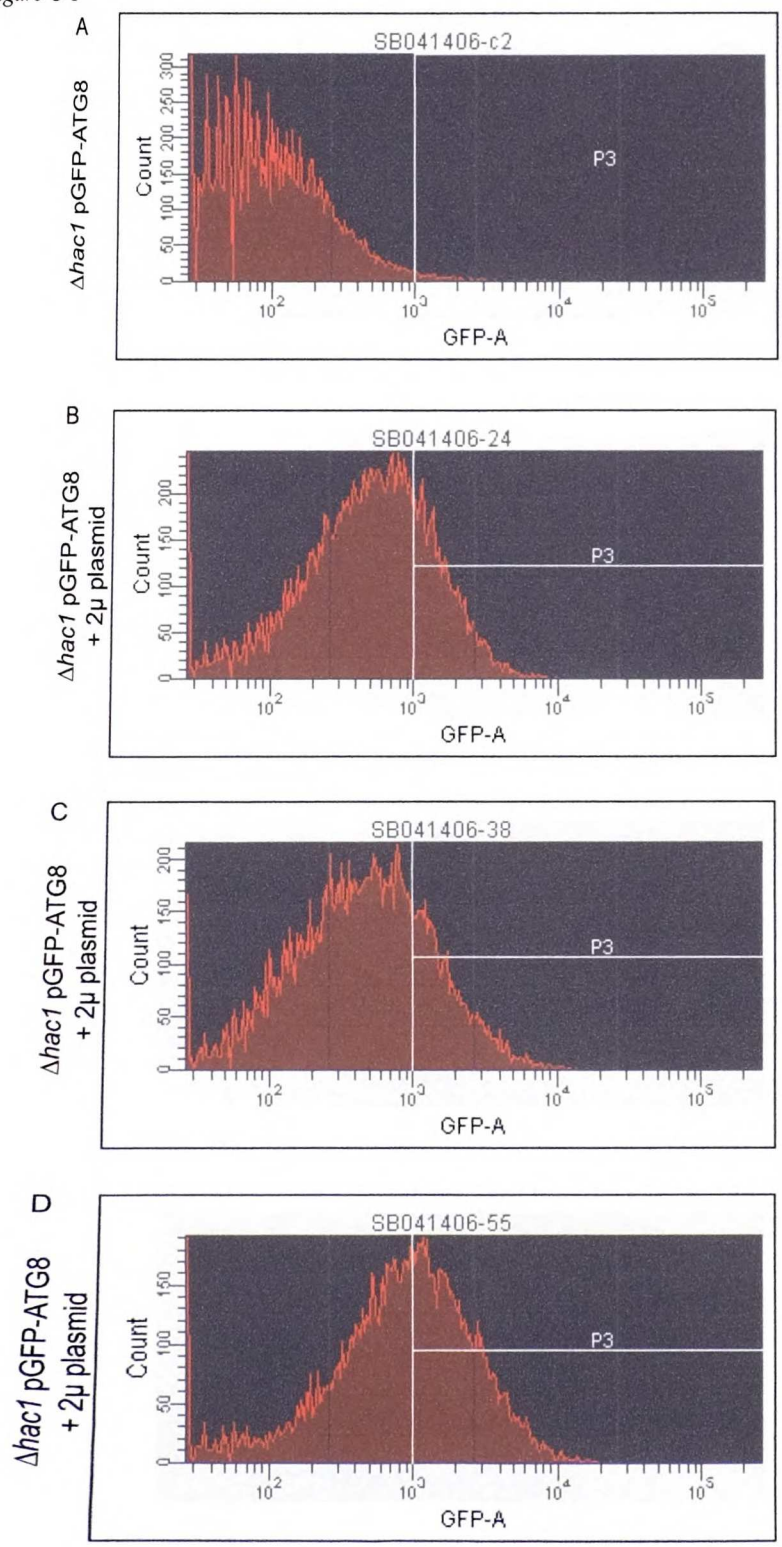
A
Δhac1 pGFP-ATG8
SB041406-c2
Count
P3
GFP-A
B
Δhac1 pGFP-ATG8 + 2μ plasmid
SB041406-24
Count
P3
GFP-A
C
Δhac1 pGFP-ATG8 + 2μ plasmid
SB041406-38
Count
P3
GFP-A
D
Δhac1 pGFP-ATG8 + 2μ plasmid
SB041406-55
Count
P3
GFP-A

Appendix D

Yeast Electron Microscopy

this section, I have included some of the electron micrographs I have taken during my
ıduate career at the University of California, San Francisco, at the University of
lifornia, Berkeley, and at the University College of London. Many thanks to my EM
ntor, Kent McDonald, and to all the people who helped me on the way: Pablo Aguilar,
chael Braunfeld, Lucy Collinson, Mark Marsh, and Mei Lie Wong.

gure D-1: Yeast electron micrographs.

.) High pressure freezing (HPF). ER-Containing Autophagosome (ERA) in DTT-
:ated cell. As it is clear from this picture, ERAs are ribosome-studded. This is a strong
dication that both content and isolation membranes are ER-derived.

) HPF. ERA's degradation inside the vacuole after DTT-washout. After the UPR-
ducing drug is removed, ERAs delimiting membrane fuses to the vacuole and their
ntent is deposit inside this organelle.

:) HPF. Endocytosis. This picture shows a coated invagination of the plasma
embrane.

) HPF. Golgi Apparatus (GA). In yeast, the GA localizes as dots all over the
toplasm. However, occasionally–like in this picture–a Golgi stack can be observed.

) HPF. Endocytosis. This invagination of the plasma membrane is flanked two dark
uctures one on each side of the invagination. We hypothesize represent eisosomes.

) HPF. Yeast cell wall is formed by mannoproteins, ß-glucans, and chitins.
annoproteins can be observed as filaments at the edge of the cell wall.

) KMnO4. Cytokinesis is achieved by the coordinated actions of the actomyosin
ntractile ring and targeted membrane and cell wall deposition. In this picture, an
termediate of this process can be observed.

I) KMnO4. Abnormal cytokinesis.

) HPF. ERA in DTT-treated cell. This micrograph shows the continuity between the
RA's delimiting membrane and a segment of ER.

) HPF. Abnormal endocytosis in DTT-treated cells. We observed that endocytic events
crease during the UPR.

K) HPF. ERA in DTT-treated cell. In this image, it appears that a portion of the ER is eing internalized into an ERA.

L) HPF. Endocytic event where the plasma membrane is clearly observed.

M) HPF. ERA in DTT-treated cell. Here, it is possible to see ER membranes that are orming the ERA..

N) HPF. Another endocytic event where the plasma membrane is clearly observed.

igure D-1

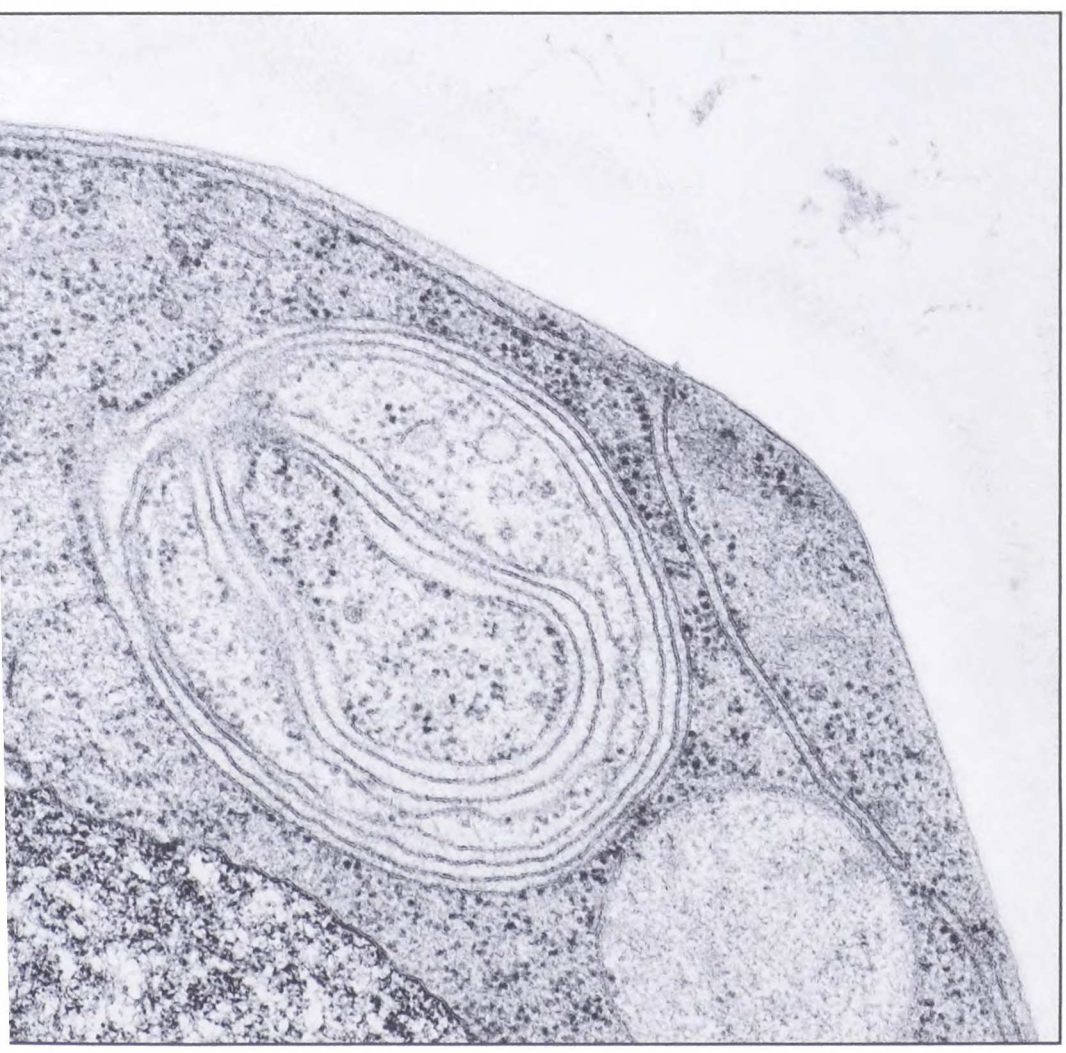

gure D-1

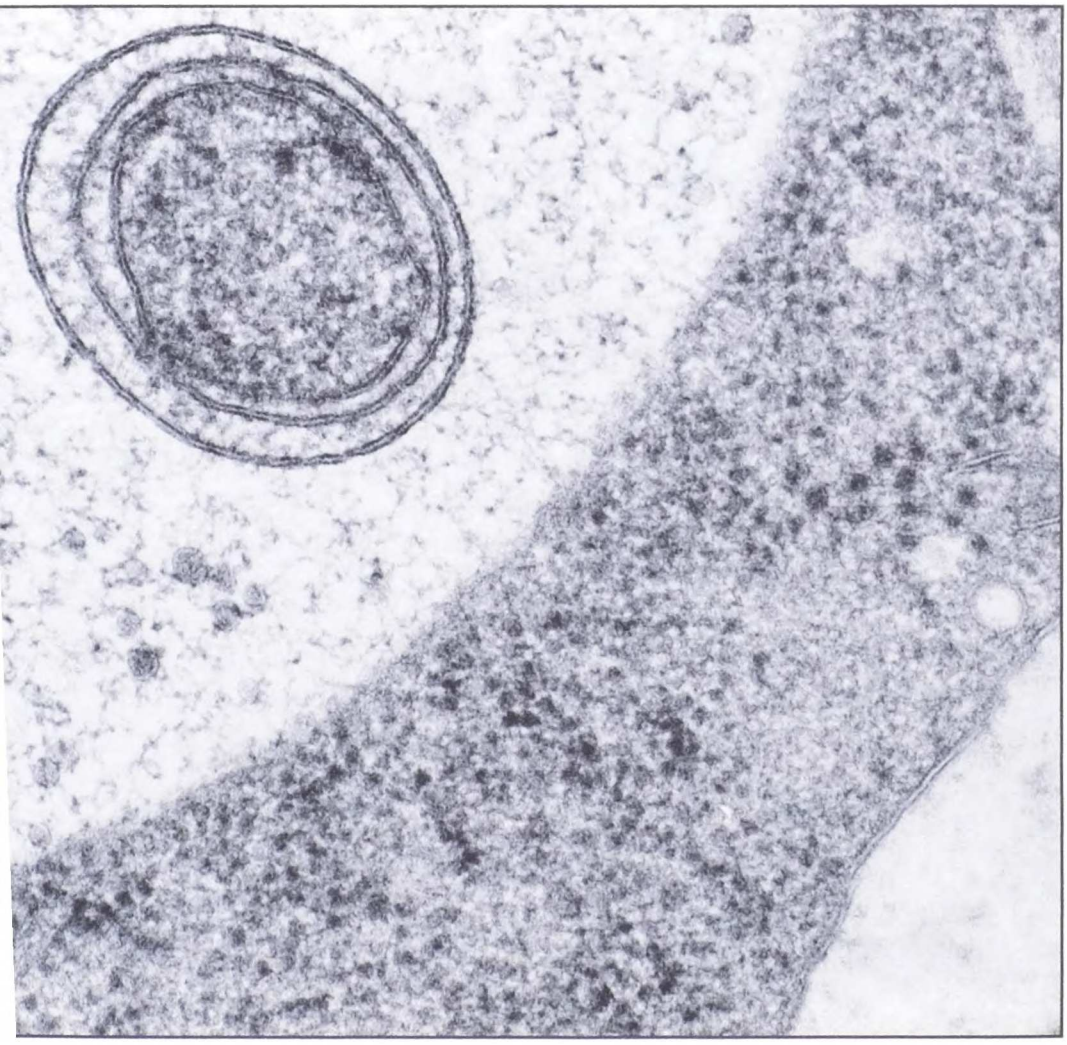

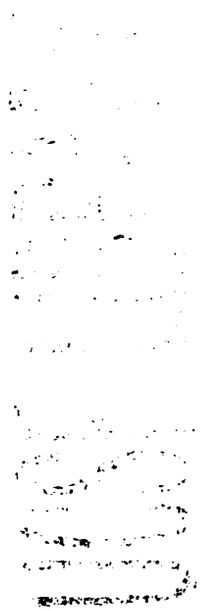

Figure D-1

C

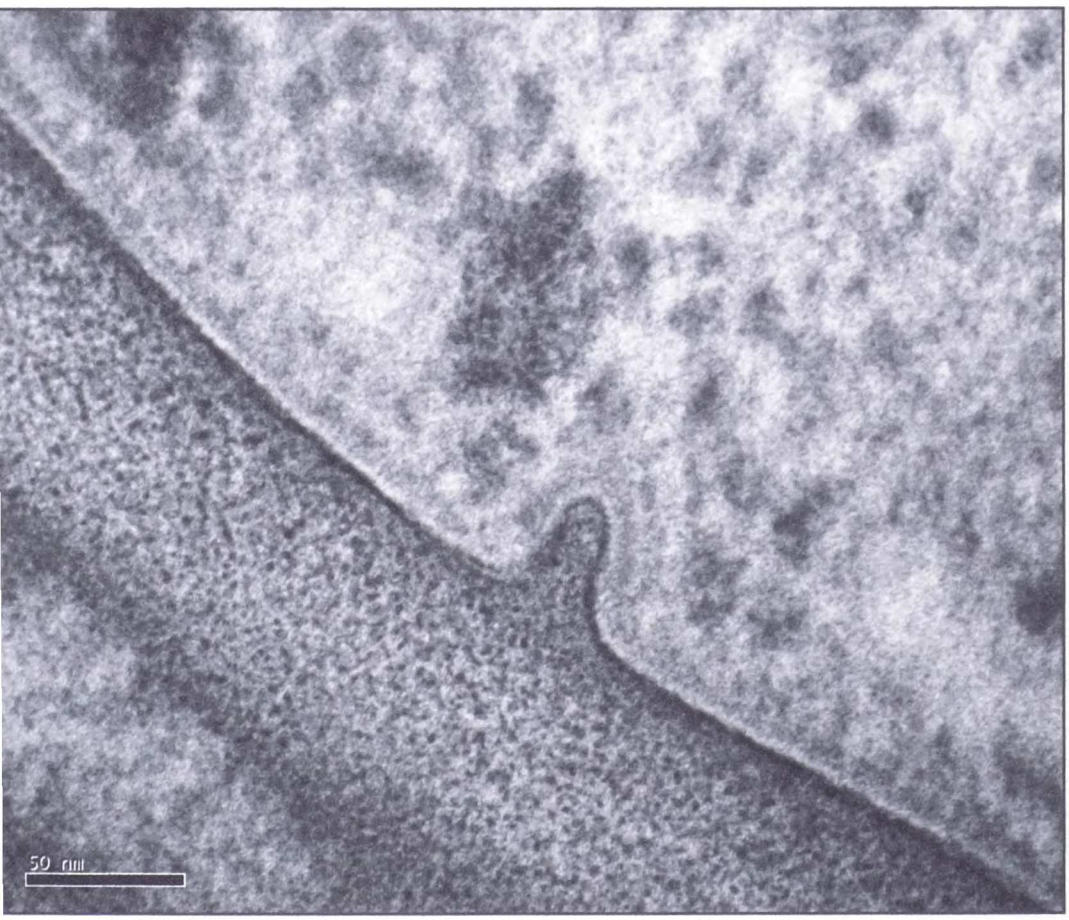

Figure D-1

D

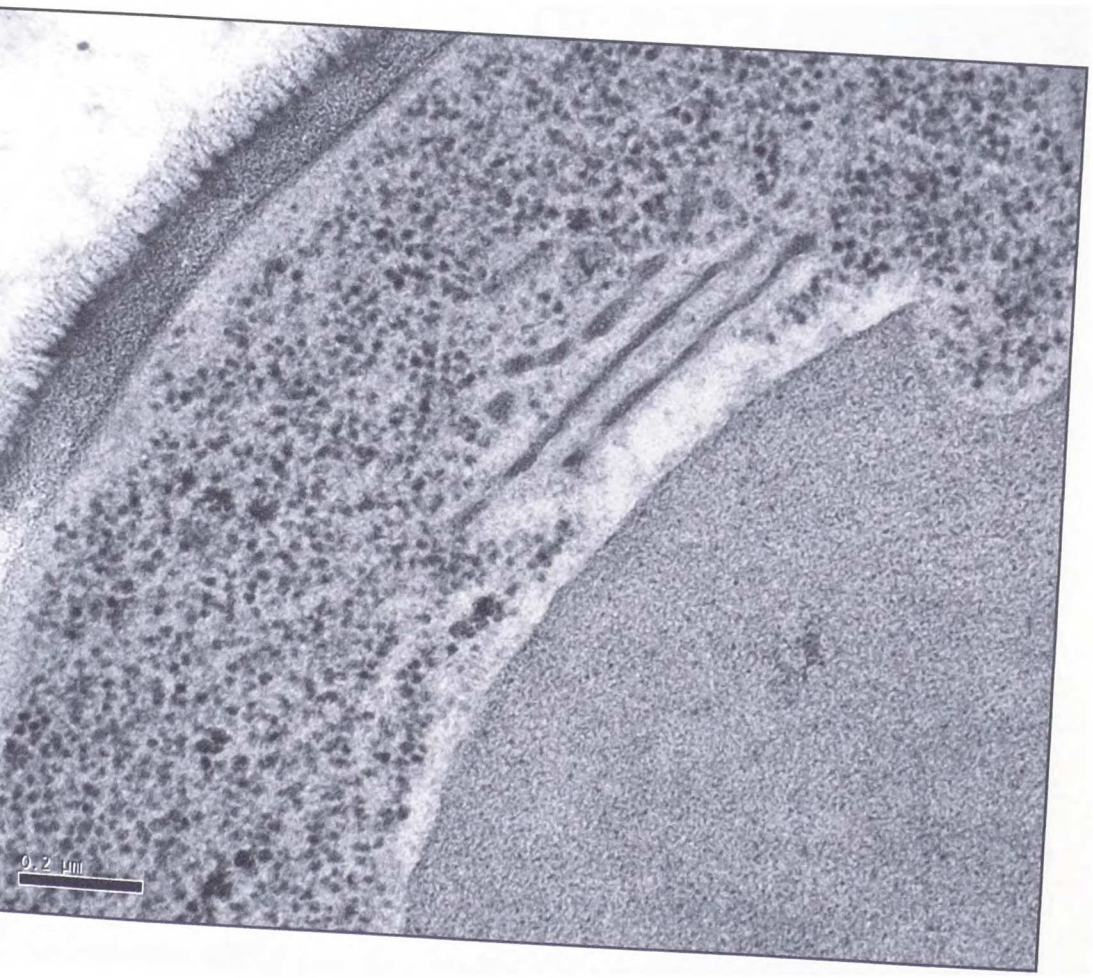

igure D-1

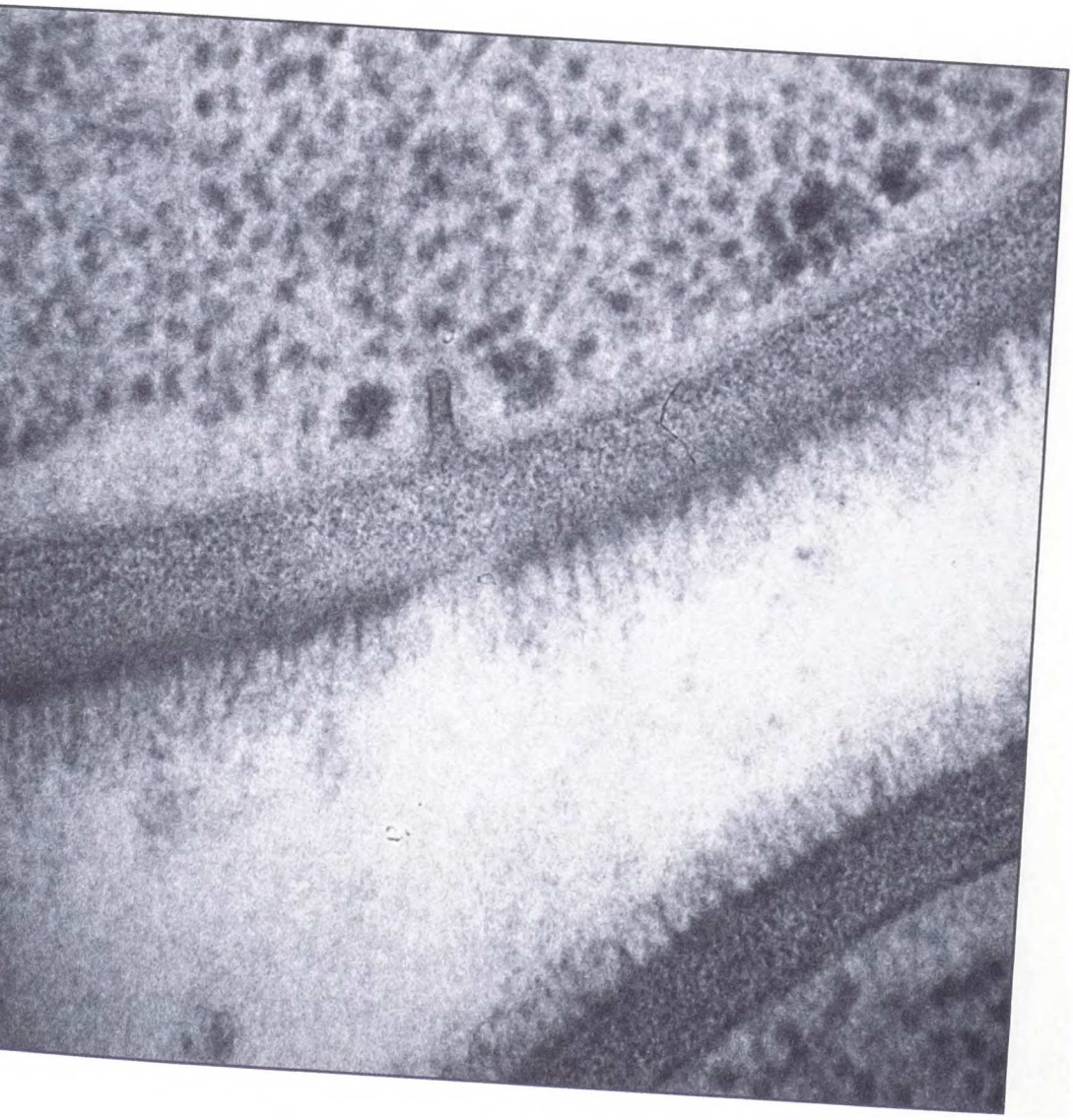

Figure D-1

Figure D-1

G

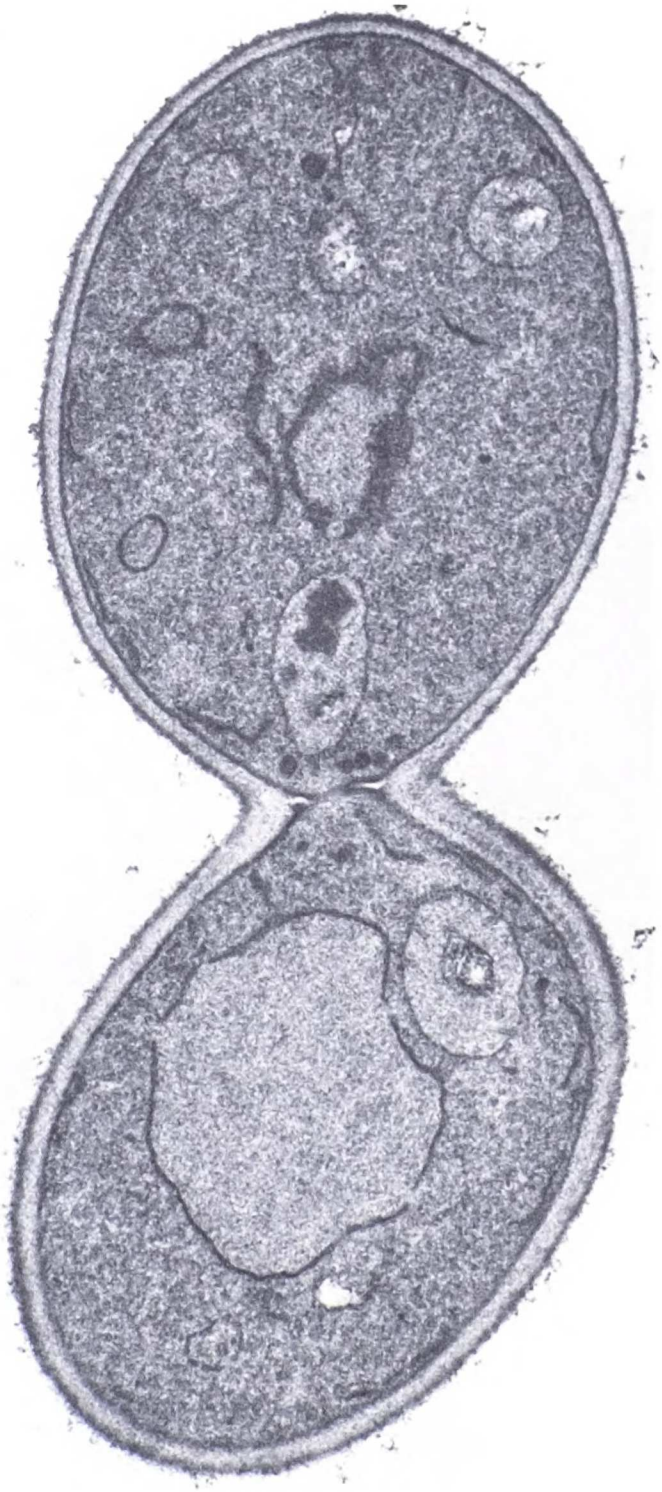

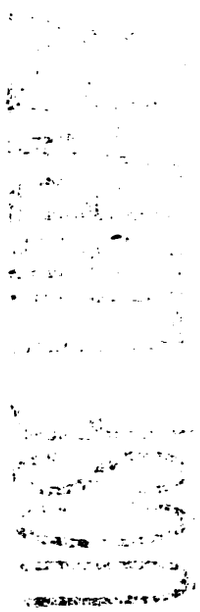

Figure D-1

H

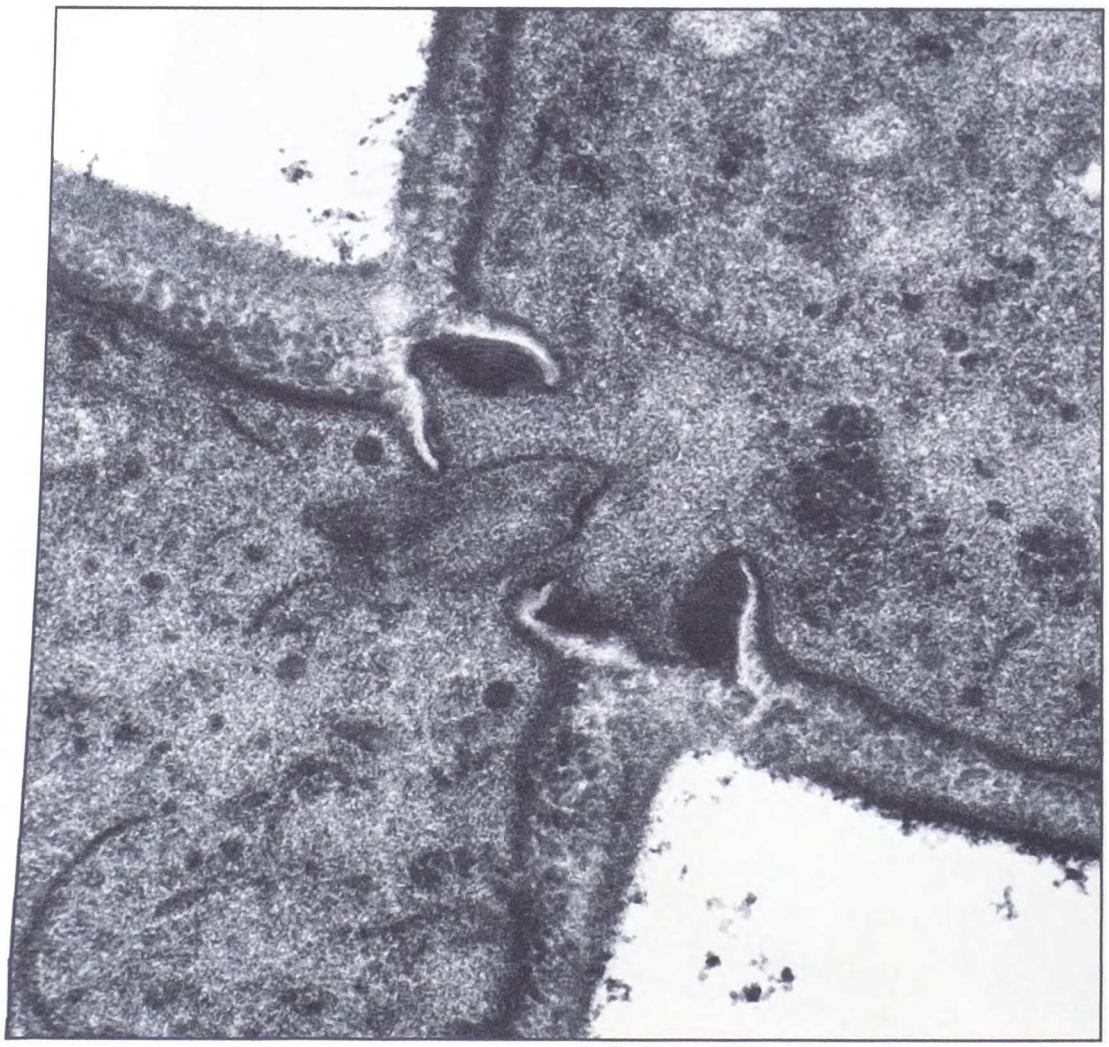

Figure D-1

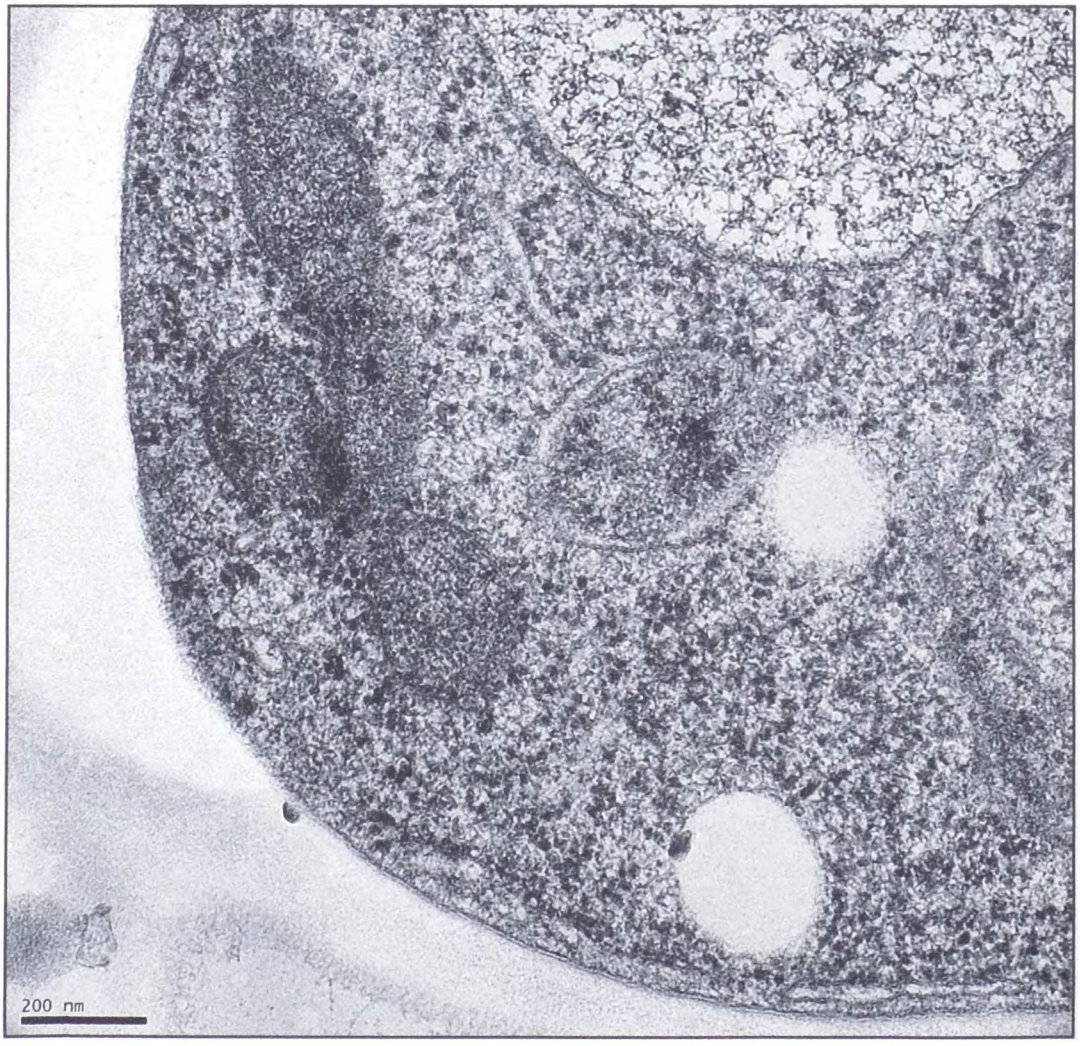

Figure D-1

J

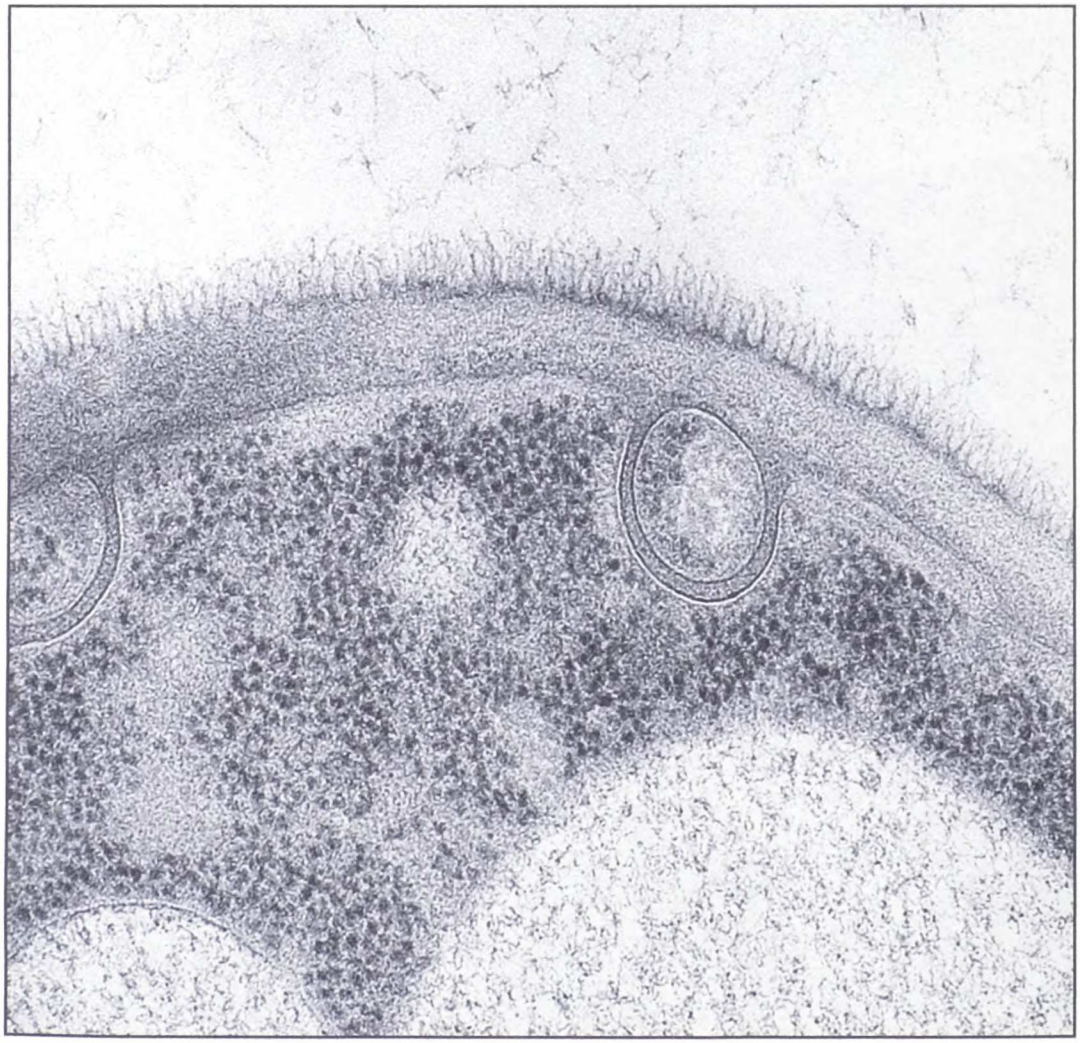

Figure D-1

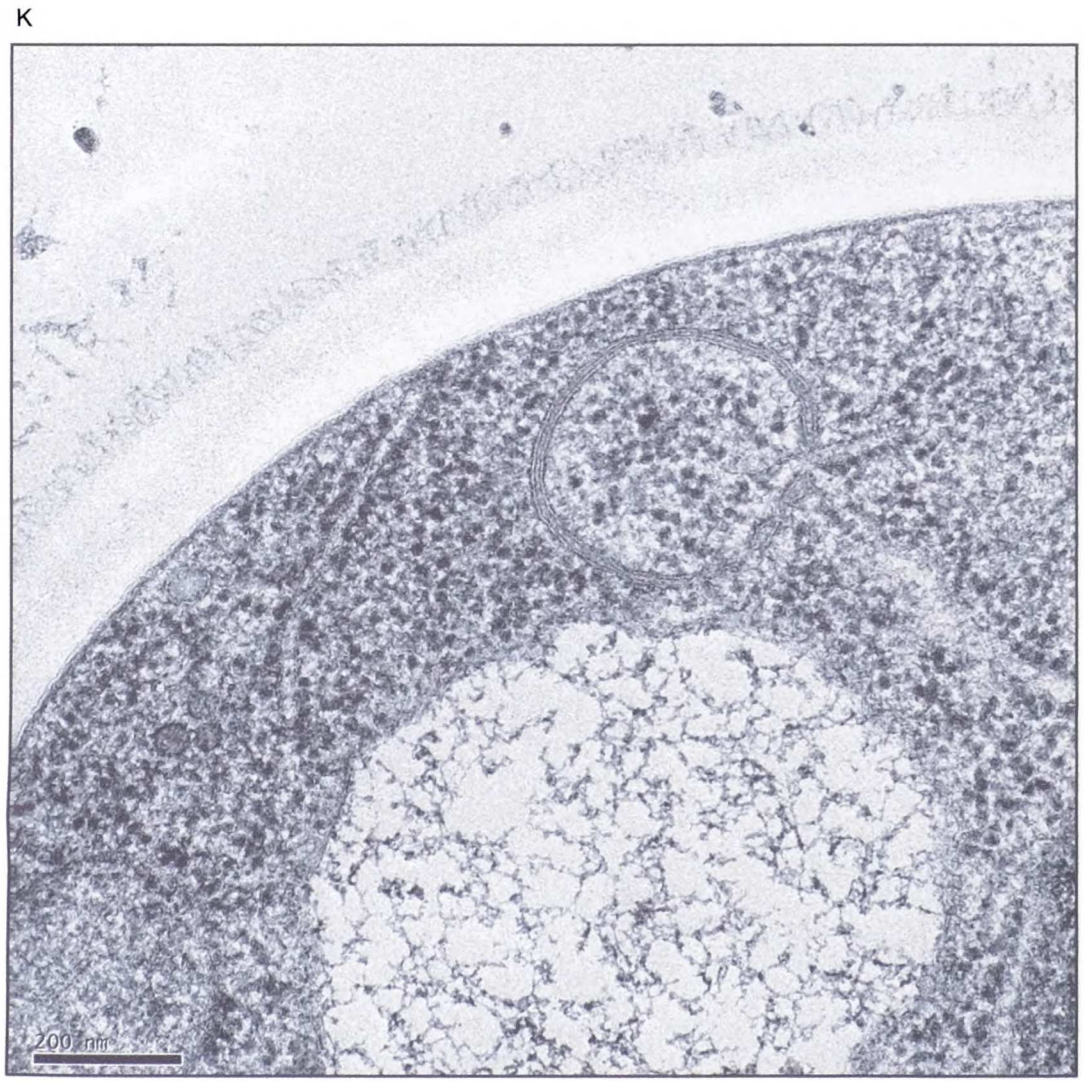

Figure D-1

L

Figure D-1

M

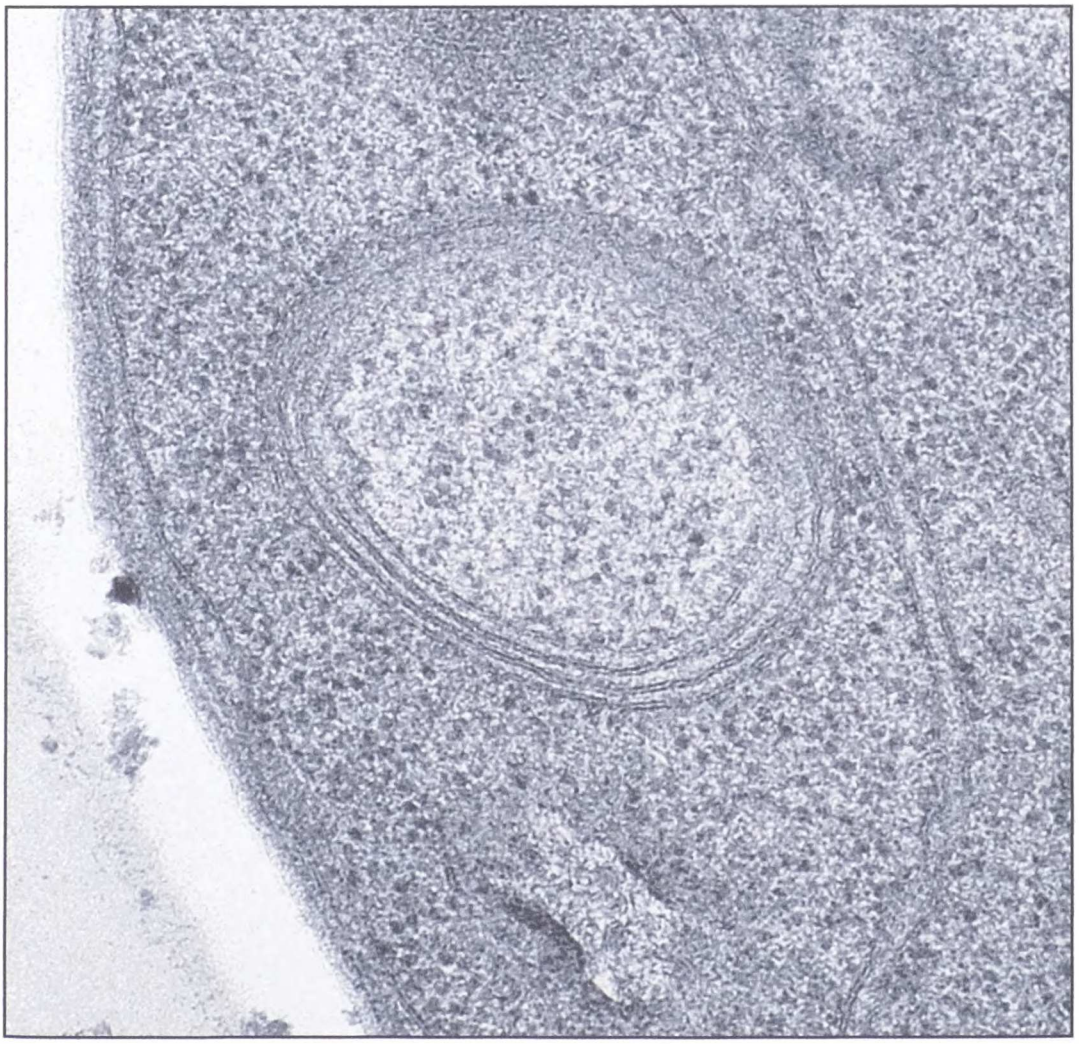

Figure D-1

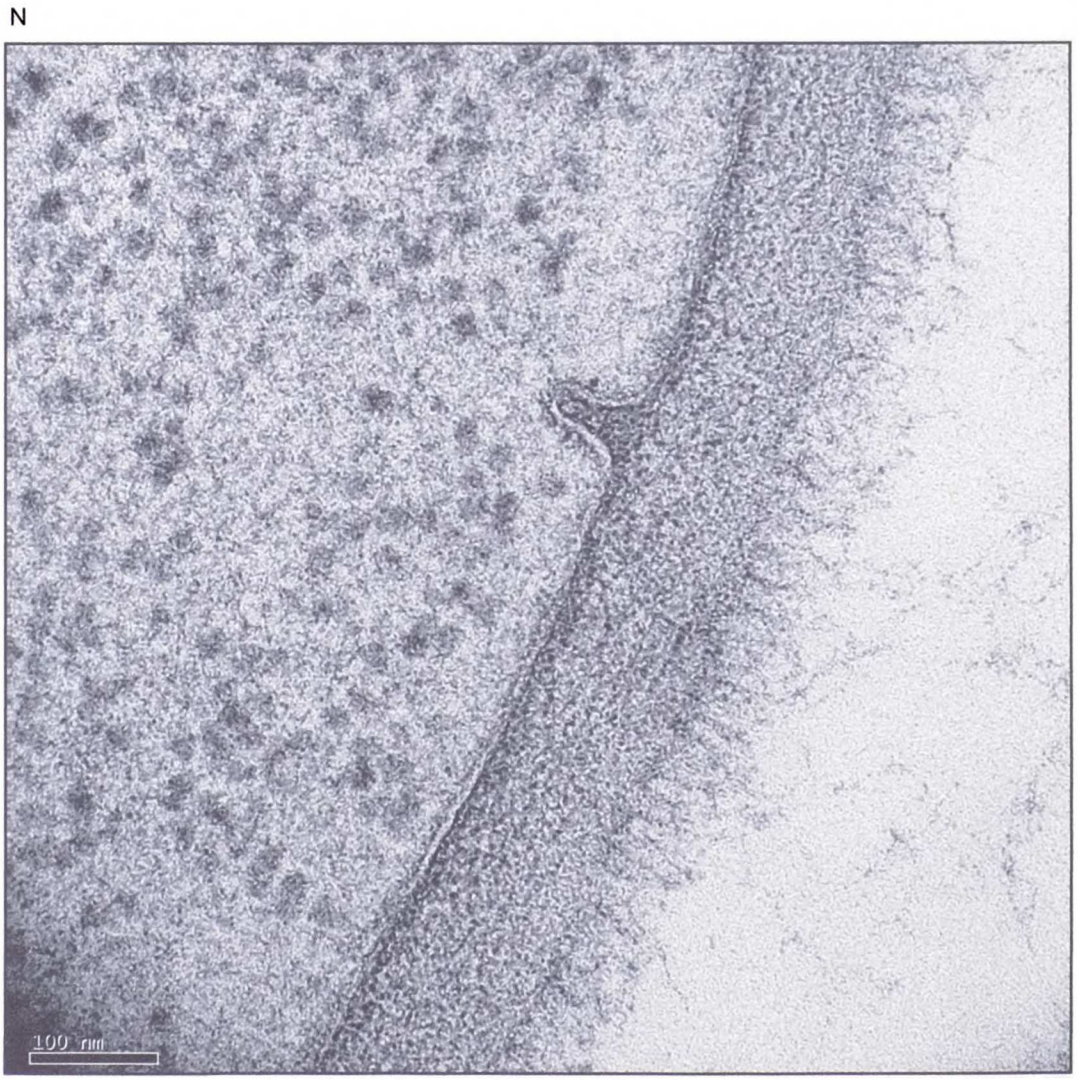

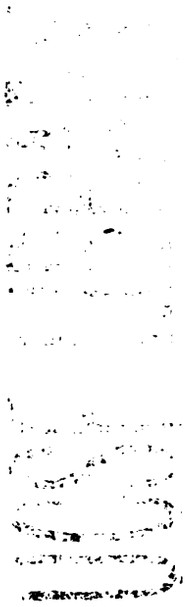

For reference

Not to be taken from the room.